

# Hybrid Generation Solution for Mining Site

Gustavo Andrés Castro, Marta Irena Murkowska, Pedro Zulaica Rey

Energy Technology, EPSH4-1032, 29-05-2019

Master's Thesis







**AALBORG UNIVERSITY**  
STUDENT REPORT

**Electronics and IT**  
Aalborg University  
<http://www.aau.dk>

**Title:**

Hybrid Generation Solution for Mining Site

**Theme:**

Engineering Theme

**Project Period:**

Spring Semester 2020

**Project Group:**

EPSH4-1032

**Participant(s):**

Gustavo Andrés Castro  
Marta Irena Murkowska  
Pedro Zulaica Rey

**Supervisor(s):**

Amjad Anvari-Moghaddam  
Gabriel Leite

**Copies:** 1

**Page Numbers:** 97

**Date of Completion:**

May 28, 2020

**Abstract:**

One of the difficulties of mining worldwide is that it must be carried out in remote places without grid connection. Therefore it is important to choose the most profitable and reliable combination of energy sources for electrification. In this paper, different technologies to meet the demand of a mine located in Western Australia are studied. Using HOMER Pro, several viable systems, for the resources considered, are obtained. Using analytic hierarchy process (AHP), the most suitable case is selected for further study. Using Monte-Carlo simulations several scenarios are developed for the study of uncertainties, and a risk-constrained optimization algorithm is implemented to obtain the optimal scheduling, the expected cost and conditional value at risk (CVaR). Numerical results demonstrate that the variations of operation cost and CVaR with the increase in risk aversion factor are not of high magnitude, due to rather low variable operation costs of renewable energy sources. It is shown that the proposed hybrid electrification plan, based on WT, PVs and battery, could not only provide a reliable power generation, but also very low daily operating cost.

*The content of this report is freely available, but publication (with reference) may only be pursued due to agreement with the author.*



# Preface

The dissertation is the final work of our Master study at the Energy Department at Aalborg University. As energy engineering students we are looking to work on projects related to renewable energy generation. We consider renewable technology to be the future of power systems. Therefore, the topic of mine electrification with use of renewables is interesting for us. The topic focuses on the important aspect of reducing the cost of the investment, by introducing the renewable energy sources, emissions are also reduced. Economical approach, but with consideration of the environmental aspect is what is particularly interesting for us.

We would like to express our gratitude to Amjad Anvari Moghaddam, our Aalborg University supervisor, for all his support and help in the project development. The input from the academia was of crucial importance to represent high academic level in the project. We would also like to thank our industrial partner supervisor, Gabriel Leite, for providing valuable input to the project.

Finally, we would like to thank our families and friends for the support during project work, which was especially difficult during the COVID-19 epidemic.

Aalborg University, May 28, 2020



---

Gustavo Andrés Castro  
<gcastr18@student.aau.dk>



---

Marta Irena Murkowska  
<mmurko18@student.aau.dk>



---

Pedro Zulaica Rey  
<pzulai18@student.aau.dk>

# Contents

<b>List of Figures</b>	<b>ix</b>
<b>List of Tables</b>	<b>xi</b>
<b>Nomenclature</b>	<b>xvii</b>
<b>1 Introduction</b>	<b>1</b>
1.1 State of Art . . . . .	2
1.1.1 Hybridization in Mines Energy Production . . . . .	2
1.1.2 HOMER Pro Used in Planning of Mines and Microgrid . . . . .	3
1.1.3 Decision Analysis . . . . .	4
1.1.4 Risk Analysis . . . . .	4
1.2 Problem Statement . . . . .	5
1.3 Objectives . . . . .	5
1.4 Assumptions . . . . .	6
1.5 Limitations . . . . .	6
<b>2 Methodology</b>	<b>7</b>
2.1 Mine Data . . . . .	7
2.2 Resource Assessment . . . . .	7
2.3 Planning and Operation of the Mine . . . . .	8
2.3.1 Planning . . . . .	8
2.3.2 Scheduling and Risk Assessment . . . . .	10
<b>3 Resource Assessment</b>	<b>11</b>
3.1 Solar Irradiance . . . . .	11
3.2 Wind Speed . . . . .	15
<b>4 HOMER Calculations</b>	<b>21</b>
4.1 Generator . . . . .	21
4.2 Idealized Battery . . . . .	22
4.3 Photovoltaic Panel . . . . .	23
4.4 Wind Turbine . . . . .	24

4.4.1	Calculation of Wind Speed at the Hub Height . . . . .	24
4.4.2	Calculation of Wind Turbine Power Output at the Standard Air Density . . . . .	25
4.4.3	Applying Density Correction . . . . .	25
4.5	Emissions . . . . .	26
4.6	Techno-Economic Indicators . . . . .	27
4.6.1	Renewable Fraction . . . . .	27
4.6.2	Net Present Cost . . . . .	27
4.6.3	Levelized Cost of Electricity . . . . .	27
4.6.4	Initial Capital Cost . . . . .	28
4.6.5	Operating Cost . . . . .	28
4.7	Dispatch Algorithm . . . . .	28
<b>5</b>	<b>Input Data</b>	<b>31</b>
5.1	Load . . . . .	31
5.2	Economics . . . . .	32
5.2.1	Inflation . . . . .	32
5.2.2	Discount Rate . . . . .	32
5.2.3	Project Lifetime . . . . .	32
5.3	Wind Speed Data . . . . .	33
5.4	Diesel Generator . . . . .	33
5.5	PV . . . . .	34
5.6	Battery Storage . . . . .	35
5.6.1	Economics . . . . .	35
5.6.2	Lifetime . . . . .	35
5.7	Wind Turbine . . . . .	36
<b>6</b>	<b>HOMER Pro Results and Plan Selection</b>	<b>39</b>
6.1	Results from HOMER Pro . . . . .	39
6.2	Description of AHP . . . . .	42
6.3	Criteria . . . . .	44
6.3.1	Robustness Assessment . . . . .	45
6.4	Profit Oriented . . . . .	45
6.5	Environmentally Friendly . . . . .	46
6.6	Verification of AHP . . . . .	47
<b>7</b>	<b>Optimization of Operation</b>	<b>49</b>
7.1	Evaluation of Uncertainties . . . . .	51
7.2	Diesel Prediction . . . . .	56
7.3	Incorporating Risk Management . . . . .	58
7.4	Formulation of Optimization . . . . .	59
7.4.1	Variables . . . . .	59

7.4.2	Constraints . . . . .	61
7.4.3	Objective Function . . . . .	63
<b>8</b>	<b>Results</b>	<b>67</b>
8.1	Results of Optimization - Plan 2 . . . . .	67
8.1.1	Risk Assessment in Plan 2 . . . . .	68
8.1.2	Hourly Operation of Plan 2 . . . . .	71
8.2	Results of Optimization - Plan 7 . . . . .	73
8.2.1	Risk Assessment in Plan 7 . . . . .	74
8.2.2	Hourly Operation in Plan 7 . . . . .	75
8.2.3	Influence of Changing Diesel Prices in Plan 7 . . . . .	77
<b>9</b>	<b>Conclusions and Future Work</b>	<b>81</b>
9.1	Conclusions . . . . .	81
9.2	Future Work . . . . .	83
	<b>Bibliography</b>	<b>85</b>
<b>A</b>	<b>Decision Making (AHP) - Results</b>	<b>91</b>
A.1	Subattributes Priority . . . . .	91
A.2	Profit Oriented Results . . . . .	92
A.3	Environmentally Friendly Results . . . . .	93
A.4	Consistency Ratio . . . . .	94
<b>B</b>	<b>Distribution Functions</b>	<b>95</b>
B.1	Empirical CDF . . . . .	95
B.2	Normal Distribution . . . . .	95
B.3	Beta Distribution . . . . .	95
B.4	Weibull Distribution . . . . .	95
<b>C</b>	<b>K-means Clustering</b>	<b>97</b>

# List of Figures

Figure 2.1	Overall flowchart . . . . .	9
Figure 3.1	Calculation of optimal tilt angle for the PV panel . . . . .	11
Figure 3.2	Solar Irradiance Horizontal and Inclined . . . . .	12
Figure 3.3	Solar Irradiance Horizontal - Monthly Boxplot . . . . .	13
Figure 3.4	Solar Irradiance Horizontal - Hourly Boxplot . . . . .	13
Figure 3.5	Solar Irradiance Horizontal - Average Day . . . . .	14
Figure 3.6	Wind speed profile calculated with different values of power coefficient $\alpha_p$ . . . . .	17
Figure 3.7	Wind speed measured at 104 m - Monthly Boxplot . . . . .	18
Figure 3.8	Wind speed probability distribution at different heights of measurement . . . . .	18
Figure 3.9	Wind rose based on measurements at 104 m . . . . .	19
Figure 4.1	Sample of a power curve with cut-in and cut-out wind speed . . . . .	25
Figure 5.1	Annual load profile . . . . .	31
Figure 5.2	Daily average load profile . . . . .	32
Figure 5.3	Power curve of Enercon E-138 EP3 wind turbine . . . . .	37
Figure 6.1	Configuration of the units used for the planning phase . . . . .	40
Figure 6.2	Hierarchy structure of AHP . . . . .	43
Figure 6.3	Priorities calculated for each of the considered plans in the profit oriented approach . . . . .	46
Figure 6.4	Priorities calculated for each of the considered plans in the environmentally friendly approach . . . . .	47
Figure 7.1	Flowchart of operation optimization . . . . .	50
Figure 7.2	CDF comparison of empirical and selected distributions for hour 13:00 . . . . .	51
Figure 7.3	MC simulations convergence for hour 13:00 . . . . .	52
Figure 7.4	Solar cases . . . . .	53
Figure 7.5	Wind cases . . . . .	53

Figure 7.6	Load cases . . . . .	54
Figure 7.7	Elbow method for solar irradiance clusters . . . . .	54
Figure 7.8	Elbow method for wind speed clusters . . . . .	55
Figure 7.9	Elbow method for load clusters . . . . .	55
Figure 7.10	Diesel prices Western Australia 2001 - 2019 . . . . .	56
Figure 7.11	Monte Carlo simulations for future 300 months . . . . .	57
Figure 7.12	Diesel prediction for future 25 years . . . . .	58
Figure 8.1	Expected cost versus $\beta$ , Plan 2 . . . . .	68
Figure 8.2	CVaR versus $\beta$ , Plan 2 . . . . .	69
Figure 8.3	Expected cost versus CVaR for different values of $\beta$ , Plan 2 . . . . .	70
Figure 8.4	Hourly, power output of WTs, PVs and Diesel generator, for one of the generated MCS, with two values of $\beta$ , Plan 2 . . . . .	72
Figure 8.5	Hourly battery charging at discharging power, for one of the generated MCS, with two values of $\beta$ , Plan 2 . . . . .	72
Figure 8.6	Hourly state of charge of the battery, for one of the generated MCS, for optimized operation with three values of $\beta$ and base case (BC), Plan 2 . . . . .	73
Figure 8.7	Expected cost versus CVaR for different values of $\beta$ , Plan 7 . . . . .	75
Figure 8.8	Hourly power output of WTs, PVs and Diesel generator for one of the generated MCS, result of optimization with $\beta = 0.01$ and operation in the base case, Plan 7 . . . . .	76
Figure 8.9	Hourly state of charge of the battery for one of the generated MCS, result of optimization with $\beta = 0.01$ and operation in the base case, Plan 7 . . . . .	76
Figure 8.10	Expected cost versus $\beta$ plotted for different years of operation, Plan 7 . . . . .	77
Figure 8.11	CVaR versus $\beta$ plotted for different years of operation, Plan 7 . . . . .	78
Figure 8.12	Expected cost over the years of operation, plotted for two different values of $\beta$ , Plan 7 . . . . .	78
Figure 8.13	CVaR over the years of operation, plotted for two different values of $\beta$ , Plan 7 . . . . .	79

# List of Tables

Table 3.1	Monthly average solar global horizontal irradiance (GHI) . . . . .	14
Table 3.2	Average wind speed calculated from measurements at four different heights: 40, 60, 80 and 104 meters . . . . .	15
Table 3.3	Power law coefficient calculated between different measurement height . . . . .	16
Table 5.1	Assumed emissions from diesel generator . . . . .	34
Table 5.2	PV module costs and lifetime used for calculations . . . . .	34
Table 5.3	PV module costs and lifetime used for calculations . . . . .	35
Table 5.4	Battery storage costs and lifetime used for calculations . . . . .	36
Table 5.5	Wind turbine costs and lifetime used for calculations . . . . .	37
Table 6.1	Selected plans . . . . .	41
Table 6.2	Installed capacities of each of the considered technologies in the selected plans . . . . .	41
Table 6.3	Economical and technical details of the selected plans . . . . .	42
Table 6.4	The fundamental scale for deciding relative importance [34] . . . . .	43
Table 6.5	Selection Criteria . . . . .	44
Table 6.6	% change in NPC due to price increase of 30% . . . . .	45
Table 6.7	Profit oriented priorities . . . . .	45
Table 6.8	Environmentally Friendly Priorities . . . . .	46
Table 7.1	Variables used in the optimization . . . . .	60
Table 7.2	Constraints to define the operation of the plant . . . . .	62
Table 8.1	Cost of operation calculated for Plan 2 . . . . .	70
Table 8.2	Average state of charge of the battery for one of the generated MCS, with different values of $\beta$ , Plan 2 . . . . .	71
Table 8.3	Cost of operation in one of the scenarios for Plan 7 . . . . .	74
Table A.1	Economical Subattributes Priorities . . . . .	91
Table A.2	Robustness Subattributes Priorities . . . . .	91
Table A.3	Profit oriented cases . . . . .	92

Table A.4	Profit oriented cases . . . . .	92
Table A.5	Environmentally friendly case . . . . .	93
Table A.6	Environmentally friendly case . . . . .	93
Table A.7	Consistency Ratio . . . . .	94

# Nomenclature

## Abbreviations

AHP	Analytic Hierarchy Process
ANSI	American National Standards Institute
BC	Base Case
BESS	Battery Energy Storage System
CDF	Cumulative Distribution Function
CVaR	Conditional Value-at-Risk
DG	Distributed Generation
GDP	Gross Domestic Product
GHI	Global Horizontal Irradiance
IEC	International Electrotechnical Commission
LCOE	Levelized Cost of Electricity
MC	Monte-Carlo
MCDM	Multi-Criteria Decision-Making
MCS	Monte-Carlo Simulations
MILP	Mixed Integer Linear Programming
NPC	Net Present Cost [\$]
NREL	National Renewable Energy Laboratory
O&M	Operation and Maintenance
PV	Photovoltaic

RES	Renewable Energy Sources
RMSE	Root Mean Square Error
STC	Standard Test Conditions
VaR	Value-at-Risk
WCSS	Within-Cluster Sum-of-Squares
WS	Wind Speed
WT	Wind Turbine
WTG	Wind Turbine Generator

### Indices

$s$	Scenario
$t$	Timestep of the Optimization

### Parameters and Constants

$\alpha$	Confidence Level
$\alpha_P$	Power Law Coefficient
$\alpha_T$	Temperature Coefficient of Power [%/°C]
$\beta$	Risk Aversion Factor
$\dot{m}_{fuel}$	Mass Flow Rate of the Fuel [kg/h]
$\eta_{gen}$	Efficiency of the Generator [%]
$\eta_{mp,STC}$	Maximum Power Point Efficiency Under STC [%]
$\lambda$	Eigen Value
$\mu$	Mean
$\overline{G_T}$	Solar Radiation Incident on the PV Array in the Current Time Step [kW/m <sup>2</sup> ]
$\pi_s$	Probability of Scenario $s$
$\rho$	Actual Air Density [kg/m <sup>3</sup> ]
$\rho_{STP}$	Standard Air Density [kg/m <sup>3</sup> ]
$\sigma$	Standard Deviation

$C_i$	Consistency Index
$C_r$	Consistency Ratio
$CDF_{emp}^h$	Empirical CDF
$CDF_{sel}^h$	Selected CDF
$D_{t,s}$	Demand at time $t$ and scenario $s$ [kW]
$DT_d$	Minimum Down Time of the Diesel Generator [h]
$E_{nonren}$	Nonrenewable Electrical Production [kWh/yr]
$E_{served}$	Total Electrical Load Served [kWh/yr]
$eff$	Round Trip Efficiency of Charging and Discharging of the Battery [%]
$F_0$	Fuel Curve Intercept Coefficient of the Generator [l/h/kW]
$F_1$	Fuel Curve Slope of the Generator [l/h/kW]
$F_{min,d}$	Minimal Fuel Consumption of Diesel [l]
$f_{PV}$	PV Derating Factor
$f_{ren}$	Renewable Fraction [%]
$H_{nonren}$	Nonrenewable Thermal Production [kWh/yr]
$H_{served}$	Thermal Load Served
$i$	Real Discount Rate
$I_b$	Number of Installed Batteries [Number of Batteries]
$I_{pv}$	Installed Power of PVs [kW]
$I_{wt}$	Installed Power of Wind Turbines [kW]
$LHV_{fuel}$	Lower Heating Value [MJ/kg]
$n$	Lifetime of the Investment [yr]
$Nh$	Number of Hours Considered in RMSE Calculation
$OM_{b,e}$	Operation and Maintenance Cost of the Batteries, Dependent on the Throughput Energy [\$/kWh]
$OM_{b,y}$	Yearly Operation and Maintenance Cost of the Battery [\$/Number of Batteries]

$OM_d$	Operation and Maintenance Cost of the Diesel Generator [\$/h]
$OM_{pv,y}$	Yearly Operation and Maintenance Cost of the PVs, Dependent on the Amount of PVs [\$/kW]
$OM_{wt,e}$	Operation and Maintenance Cost of the Wind Turbines, Dependent on the Amount of Generated Energy [\$/kWh]
$OM_{wt,y}$	Yearly Operation and Maintenance Cost of the Wind Turbines, Dependent on the Amount of WTs [\$/kW]
$P_{gen}$	Electrical Output of the Generator [kW]
$P_{max,bc}$	Maximum Charging Power of the Battery [kW]
$P_{max,bd}$	Maximum Discharging Power of the Battery [kW]
$P_{max,d}$	Maximum Output Power of the Diesel Generator [kW]
$P_{min,d}$	Minimum Output Power of the Diesel Generator [kW]
$P_{pv,t,s}$	PV Power Output [kW]
$P_{WGT,STP}$	Wind Turbine Power Output at Standard Temperature and Pressure [kW]
$P_{WGT}$	Wind Turbine Power Output [kW]
$P_{wt,t,s}$	Power Output of All Installed WTs [kW]
$R_i$	Random Consistency Index
$R_y$	Net Cash Outflows-Inflows During Single Year [\$]
$S_{max}$	Maximum Possible Storage Content [%]
$SoC_{init}$	Initial SoC of the Battery [%]
$SoC_{max}$	Maximum SoC of the Battery [%]
$SoC_{min}$	Minimum SoC of the Battery [%]
$SU_d$	Start-up Cost of the Diesel Generator [\$/start]
$T$	Considered Optimization Period Expressed in Hours [h]
$T_a$	Ambient Temperature
$T_c$	PV Cell Temperature
$U_{hub}$	Wind Speed at the hub height [m/s]

$U_{meas}$	Wind Speed at the Measurement Height [m/s]
$UT_d$	Minimum up Time of the Diesel Generator [h]
$var$	Variance
$w$	Values in Eigenvector
$Y_{gen}$	Rated Capacity of the Generator [kW]
$Y_{PV}$	Rated Capacity of the PV Array [kW]
$Z$	Random Number for Each of the Predicted Steps in MC Simulation
$z_{hub}$	Height of the Hub of the Wind Turbine [m]
$z_{meas}$	Height of Measurement of the Wind Speed [m]
NOCT	Nominal Operating Cell Temperature [ $^{\circ}$ C]

### Variables

$\eta_{t,s}$	Auxiliary Non-Negative Variable
$\zeta_t$	Threshold to Recognize $(1-\alpha) \cdot 100$ Percent Worst Scenarios of Each Stochastic Environment at Hour $t$ .
$B_{c,t,s}$	Charging Power of the Battery [kW]
$b_{c,t,s}$	Charging Indicator of the Battery
$B_{d,t,s}$	Discharging Power of the Battery [kW]
$cost_{t,s}$	Operational Cost of Scenario $s$ in Hour $t$
$l_{pv,t,s}$	Loading of the PVs
$l_{wt,t,s}$	Loading of the WTs
$P_{d,t,s}$	Power Output of the Diesel Generator [kW]
$SoC_{t,s}$	State of Charge of the Battery [%]
$u_{d,t,s}$	Commitment Status of the Diesel Generator
$y_{d,t,s}$	Start-up Indicator of the Diesel Generator
$z_{d,t,s}$	Shutdown Indicator of Diesel Generator



# Chapter 1

## Introduction

Australia has a big mining potential, because of the amount of natural resources that it possesses. It has also been a country to invest over the years due to its stable economy, which guarantees a safe investment. However, there are some disadvantages. Such as, mines being in remote places and the Australian power grid having load and the sources separated from each other, generating a bottleneck in the transmission system.

Mining has been an activity performed by humans for 40,000 years [1], and is still performed today. It is one of the most lucrative sectors driving 45% of the global Gross Domestic Product (GDP). Several countries base their economy on their mining sector [2].

One of the difficulties of mining worldwide is that it must be carried out in remote places, therefore it is difficult to establish a mining site, since it requires having the basic needs covered before it can operate, such as water and electricity. In the case of electricity, there are several solutions to meet the necessities of the mine.

The most reliable but rather expensive solution is to build a line from the mine to a point of connection to the grid. However, it can be difficult, specially considering the logistic, and the need to achieve the required standards of the country where it is built e.g. IEC, ANSI, etc. In the case where a grid connection is not feasible, it is possible to connect a generator of the size required to energize the whole mine. This solution may satisfy the requirement of having a stable source of energy, but it is an expensive solution. Because the generator requires a lot of fuel and the cost of maintenance is significant. The above solution can be improved if renewable sources of energy, RES, are added to the mix of diesel generators. This translates into cheaper and greener energy, but due to meteorological dependence they can cause energy shortages or failures in satisfying the load. Therefore, to find the perfect solution for the combination of different energy sources, it is nec-

essary to analyze the different conditions that involve the load profile, location and weather conditions.

## 1.1 State of Art

### 1.1.1 Hybridization in Mines Energy Production

For the mines to operate properly and be able to maximize the profit, they are required to have a stable and reliable source of energy.

When a mine operates in islanded mode, the main issue is the energy supply. The most conventional approach is to use only a generator that satisfies the demand of the mine. Even though this way is reliable, it has space for improvement. The solution can be enhanced by adding a battery energy storage system (BESS) and renewable energy sources (RES), which improves the quality of the energy making it cheaper and more environmentally friendly.

In [3], a business study of renewable energy and storage was done for off-grid mining. It was mentioned in the brochure, that in this day and age hybrid solutions (part renewable part oil and gas) are the most common in mining sector. According to [3], the energy cost can be up to 15% of the revenue of the mine. This is why it is of high interest to decrease the cost of electricity. For the study, HOMER Pro microgrid modeling software was used. In [3], several cases were studied (Diesel + BESS, Diesel + Solar PV, Diesel + BESS + Solar PV), and compared to the base case of only diesel. In the study, levelized cost of electricity (LCOE) was used as a result. The solution of Diesel + BESS + Solar PV was the one with the lowest LCOE.

The Glencore Mine Raglan [4] is a metal-based mine located in Northern Quebec, Canada. The mine is not connected to hydroelectric or natural gas networks, and the use of diesel generators was required to operate it. The mine operation started in 1997, and in order to extend the lifetime the Sivumut Project was launched [5]. In this project, gradually the insertion of renewable energies started, specifically wind turbines. This was done in two steps. In August 2014 a wind turbine was erected on the mining site, and in 2015 an energy storage systems was installed to maximize the energy used from the wind turbine. In 2018, a second wind turbine was added to the site. According to one of their reports [6], these two wind turbines resulted in a yearly fuel savings of 4.4 million liters of diesel.

A relevant mining facility in the Western Australia region is the Agnew mine owned by Gold Fields [7]. Here, the Agnew Hybrid Renewable Project [8] by EDL is being delivered in the years 2019 to 2020. This project consists of a hybrid renewable microgrid for the Agnew mine, with a total installed capacity of 54[MW]. From the capacity, 18[MW] will be wind power and 4[MW] solar PV power, the re-

renewable sources are supported by a 13[MW] and 4[MWh] battery system. The rest of the capacity is performed by fossil fuels, 16[MW] of gas and 3[MW] of diesel generation. With this project, 46,300 tones of CO<sub>2</sub> are abated per year.

As mentioned in [3], today's trend in the mining sector energy production is a mix of fuel and renewable generation, and in the next few years, a full renewable generation for the mines is to be achieved.

### 1.1.2 HOMER Pro Used in Planning of Mines and Microgrid

The HOMER Pro microgrid software by HOMER energy is a powerful tool for optimizing microgrid systems. HOMER examines all possible combinations of systems and then sorts them according to a selected variable. This software is able to model the energy flow as well as make a business case of the results [9]

In the particular case shown in [3], it was used to calculate the effectiveness of adding a PV and/or adding a BESS. The mine had already a diesel engine working, adding the BESS would eliminate the operating reserve, and adding the PV would decrease the levelized cost of electricity (LCOE).

In [10], HOMER Pro was used to plan the strategy for islands in South Korea, for this three island scenarios were considered. The objective was to reduce the carbon emissions of microgrid islands. The lifetime of the project in [10] was of 20 years. The considered inflation rate was 1% and the discount rate was 1.23%. The data for each scenario was measured, then the technological data for each energy source was input in HOMER Pro and an optimization and economical analysis was made. In the results, the most used technologies were Solar PV, Wind, BESS and diesel, and a comparison of the LCOE was done. Only in one case the LCOE could be decreased compared to LCOE of a conventional system.

An autonomous hybrid power system was modelled in [11] using HOMER Pro for a town in Kenya. PV array and Wind turbine were considered as the main technology with a diesel genset as a backup and a battery bank as energy storage. In this paper, a load priority scheme was considered, where there were two types of loads, high-priority and low-priority. The load control model was done in Simulink MATLAB. In the initial sizing part, HOMER Pro was used, however for the operations of the microgrid, a more detailed model was necessary for the load priority control and BESS control.

HOMER Pro is a highly used software in the microgrid industry, it has a powerful optimization program for the planning phase of a system considering many technology combinations, also showing the economical assessment of the project. However, it has been seen that in some cases, a more detailed model on the operations of the mine may be required.

### 1.1.3 Decision Analysis

Sometimes in the industry, the criteria for making a decision can not be quantified, from choosing which employee to promote to choosing which of the selected power generating scenarios for a microgrid system. The planning stage of any project, including an energy supply system, has crucial importance. A popular tool for decision-making studies is analytic hierarchy process (AHP). could it be for

AHP is a structure for organizing different criteria that cannot be quantified and is necessary to make a decision. To generate a solution it is necessary to make a comparison between different alternatives, and then make relative scales. The comparisons are arranged in a hierarchical structure to organize judgments by breaking a problem down into different parts [12].

This tool can be used when different system configurations are being considered for an off-grid mine. Following certain criteria the most suitable scenario can be found.

In [13] a model for planning of energy sources for microgrid, using multi-criteria decision making based on AHP approach, was presented. The most critically influencing criteria considered in the study were: economic, structural, operational and maintenance, environmental and societal aspects. The total of nine combinations of generating units and grid were identified to choose from in the decision making process.

In [14], different scenarios for distributed generation (DG) in developing countries were compared. AHP was used in this study to obtain relative weights, between different attributes if the system, in an objective way.

### 1.1.4 Risk Analysis

In any power system, uncertainties can occur, whereas they are caused by unscheduled maintenance or meteorological variation. With the integration of renewable energy resources, these variations increase. That is why it is of high importance to account for them.

In [15], a risk-constrained optimization of the operation of an off-grid system was done. Here, the trade off between maximizing profits and the risk of getting low profits due to uncertainties is shown. The stochastic parameters in this paper were the PV power, wind power, load and electricity price. Several scenarios for each of the parameters were generated. A scenario-based stochastic optimization was done using the conditional value-at-risk (CVaR) as a representation. The CVaR for a given confidence level  $\alpha$  is defined as the expected value of the profit smaller than  $(1 - \alpha)$  quantile of the profit distribution [15]. The optimization was performed for several values of taken risk to show outcomes for different risk approaches.

A minimization of cost was done in [16], for a smart energy hub. A stochastic model was presented with real time electricity and natural gas prices as well as electricity demand. Here the objective function was a sum of prices and emission penalties. As well as in [15] several scenarios were generated using Monte Carlo simulations for the stochastic parameters, which in this case are electricity prices, natural gas prices and electricity demand. In [16], also CVaR was used to account for the risk, and several results were shown for different values of risk aversion factors.

In both [16] and [15], CPLEX solver from GAMS was used to find a solution of the mixed integer linear programming (MILP) model developed.

## 1.2 Problem Statement

The project aims at investigating a business case for an off-grid hybrid renewable solution to be able to meet a mine load demand, located in Western Australia. Several technologies will be considered, such as PV panels, wind turbines, BESS and diesel generators. An optimal energy solution is developed in such a way that it is competitive in the market and cost effective in the long term. The solution ensures to meet the demand of the mine as well as being market innovative.

## 1.3 Objectives

To solve the problems described in the previous section, the following project objectives have been set:

- Perform wind and solar resource assessment, based on measurements collected at the site.
- Indicate various possible energy solutions to satisfy the demand of the mine.
- Choose the best energy solution among the various indicated.
- Account for uncertainties in wind speed (WS), solar irradiance and load profile.
- Perform a risk oriented optimization of the best energy solution, obtaining an expected cost and conditional value at risk (CVaR).
- Analyze the impact of the increase of diesel prices throughout the mines lifetime

All of the objectives are leading to determine an economical, reliable and innovative energy solution for a mining site in Australia.

## 1.4 Assumptions

- There is no limit on the land available for the technologies installed to energize the mine.
- The cost of the inverter is incorporated to the cost of the battery and the PV, hence the cost of inverter in the system is not considered separately.
- The stability, losses and voltage drops are not considered in the simulations.
- The criteria for the hierarchy in the AHP weighting factors have been chosen arbitrarily and pair-wise comparison was made by the project team. No external opinion/expert judgment was included in such study.
- The equipment chosen for the simulations in HOMER Pro was not selected by the industrial partner.
- There is no limitation on the initial capital.
- The lifetime of the mine is considered as 25 years.
- Spacing of wind turbine generators in the area will not affect the wind profile, which will remain homogeneous for all generators.
- Every simulation was done with the time step of 1 hour.

## 1.5 Limitations

- HOMER Pro does not allow to optimize the size of two different generators for the same project, hence natural gas generator was not considered.
- The only types of electrical sources considered are: WTG, PV and diesel generator. The most commercially available and applicable technologies in mines were selected.
- The connection to the grid was not considered, because the mine is located in a remote place and no information about possible grid extensions was available.
- The data is just for 1 year, which is not optimal for a proper evaluation of renewable resources.
- A solution to be considered feasible, it has to meet the load at every hour during the year selected.

## Chapter 2

# Methodology

In this chapter the methodology used in this report will be explained. The software and tools used throughout the project will be described. In 2.1 the data used in the project will be briefly introduced. In 2.2, the potentials of energy resources will be introduced. In 2.3, the planning phase and operations of the mine will be described. The software that has been used and a flow chart will be shown.

### 2.1 Mine Data

The data measured on site in the year 2019 was provided by the industrial partner. This data consists of:

- Solar irradiance, hourly values for 365 days.
- Load profile of the mine, which is rather constant around  $0.9[P.U.]$ . It includes some maintenance time when it can decrease to  $0.1[P.U.]$ , also consists of hourly values for 365 days.
- Wind speed, for different heights, 40m, 60m, 80m and 104m. It is given every 10 minutes for 365 days.
- Prices of diesel have been obtained for the year 2019 in western Australia.
- The GPS coordinates of the mine were received from the industrial partner.

### 2.2 Resource Assessment

The first task to solve in this project is the study of the local energy resources potential. In Chapter 3, this study is explained, for solar irradiance and wind speed.

For solar irradiance, the available data set is analyzed and the seasonal and hourly profiles are extracted. Moreover, the best tilt angle for the given location is calculated. For the wind speed, the potential of the four hub heights received from the industrial partner are studied. Seasonal wind speed and direction of wind are studied accordingly.

## 2.3 Planning and Operation of the Mine

The flowchart of the proposed method for the study of the mine is presented in Figure 2.1. The flowchart comprises of preparation of the input data and two main phases namely Planning phase, and Scheduling and Risk Assessment phase.

For the planning of the mine, HOMER Pro software was used [9]. The software simulates the operation of a system by balancing the energy demand and generation for every time step. The way HOMER Pro calculates data for each of the technologies used, and the economical analysis is explained in Chapter 4. This approach is also used in the optimization of operation algorithm developed in coherence with HOMER Pro. In Chapter 5, the input data for HOMER Pro is described. This data was researched for this project and contains technological and economical parameters of each technology used throughout the project.

For the operations phase, an optimization algorithm was developed in python to study the selected case from the planning phase.

### 2.3.1 Planning

In HOMER Pro, the load profile of the mine and the measured solar and wind data from the location has been entered. Next, the decision about generation technologies to include in the planning phase has been made and the required data has been put in the software. The data consist of initial capital, operating and maintenance prices and lifetime, among other specific data for each technology.

The results from HOMER Pro consist of all the different combinations of the chosen technologies. It outputs data from each combination, such as different costs, emissions, etc. In addition to this, for each case, a time series of the generation of each technology is available.

Once the simulation in HOMER Pro was done, ten most relevant plans have been chosen from all the combinations. This is explained in 6. After that, a decision making algorithm has been used for selecting the best plan. The algorithm used is analytic hierarchy process (AHP). It consists of organizing different criteria for choosing a plan according to their relevance, and comparing all cases according to these criteria. Different selection criteria have been proposed, such as economical, environmental, technical and robustness, and the importance of each has been

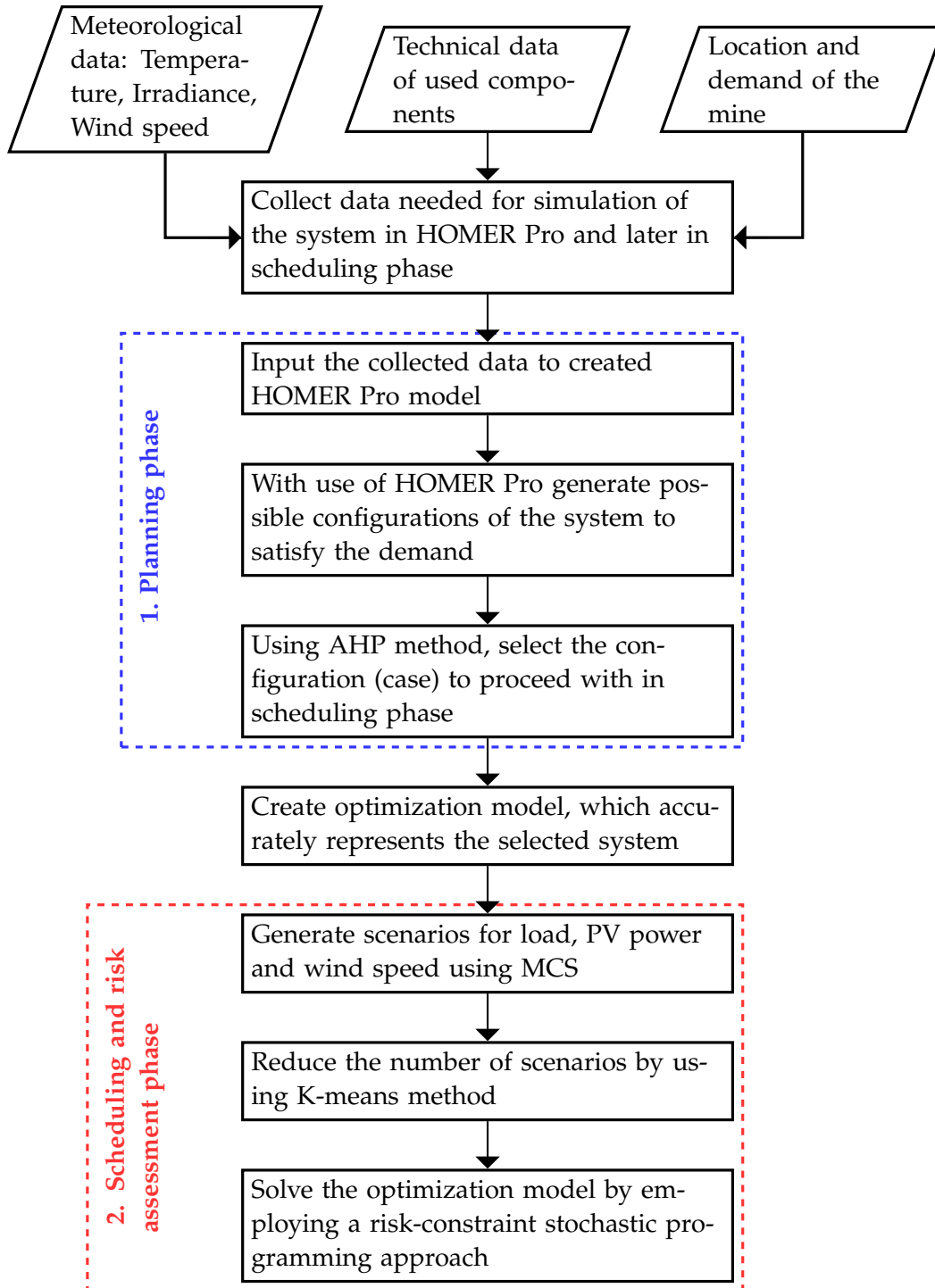


Figure 2.1: Overall flowchart

signifies through a weighting factor. With the importance of each criteria and the results from HOMER Pro, the algorithm has been used to compare all the ten cases and to choose the most suitable one.

### 2.3.2 Scheduling and Risk Assessment

The second phase of the project is Scheduling and Risk Assessment, here the operation part of the selected plan will be studied. The details of this can be found in Chapter 7.

Due to the high uncertainties on the renewable sources, and the daily load of the mine that is greatly effaced by different operating conditions, several cases have been generated and the risk of them have been studied in the next phase.

Firstly, several scenarios have been developed to assess the uncertainties using sequential Monte Carlo method. The stochastic variables in the study are, solar irradiance, load profile and wind speed. Available data has been fitted into three probability distribution functions, normal distribution, beta distribution and weibull distribution. The distribution with lowest error has been reverse sampled. For all the probabilistic study the library SciPy [17] for python has been used. Since the study of all the generated scenarios require high computational power, these have been clustered using K-means algorithm into a smaller set. For the clustering of the scenarios, the library scikit-learn [18] has been used.

Finally, the clusters have been used as an input for the optimization algorithm. A risk-constrained optimization algorithm has been developed, where the risk can be measured using conditional value at risk (CVaR) method.

In addition, a study of dieselprice and its effect on operating cost of the mine is done as a complement. to get more insight into that, diesel price data for the past years in the region of Western Australia has been gathered, and using Monte Carlo simulations, several predictions of the next 25 years (lifetime of the project) for diesel prices have been made. The mean value of all these future predictions has been calculated, and the risk-constrained optimization has been executed 25 times, one for each year, to study the change in expected cost and CVaR of the daily operations.

## Chapter 3

# Resource Assessment

In this chapter, the renewable generation resources availability and their potentials for the examined location will be studied. The resources mainly consist of solar irradiance and wind speed.

### 3.1 Solar Irradiance

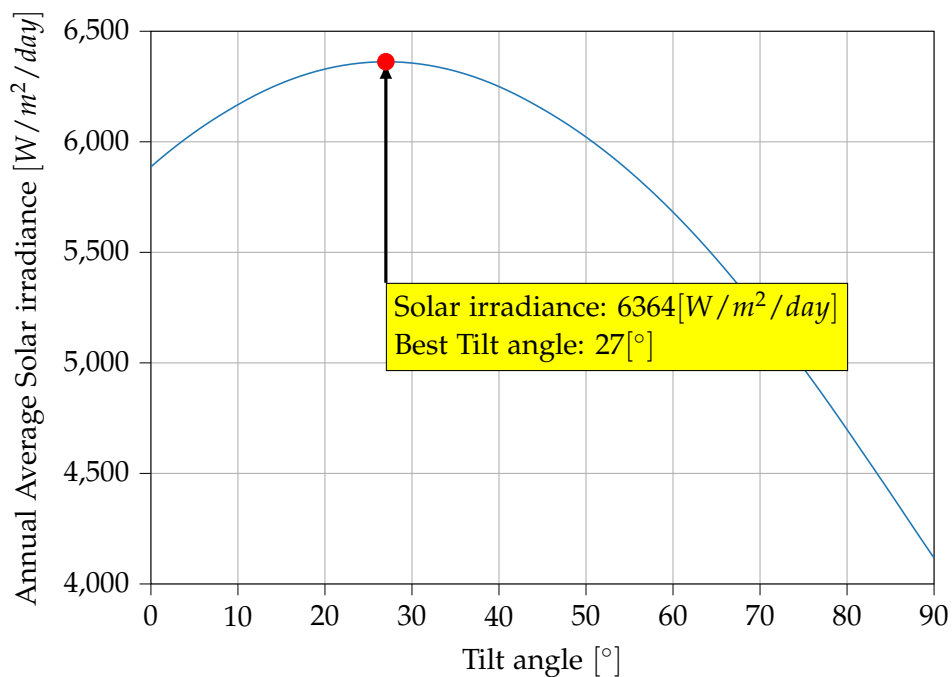
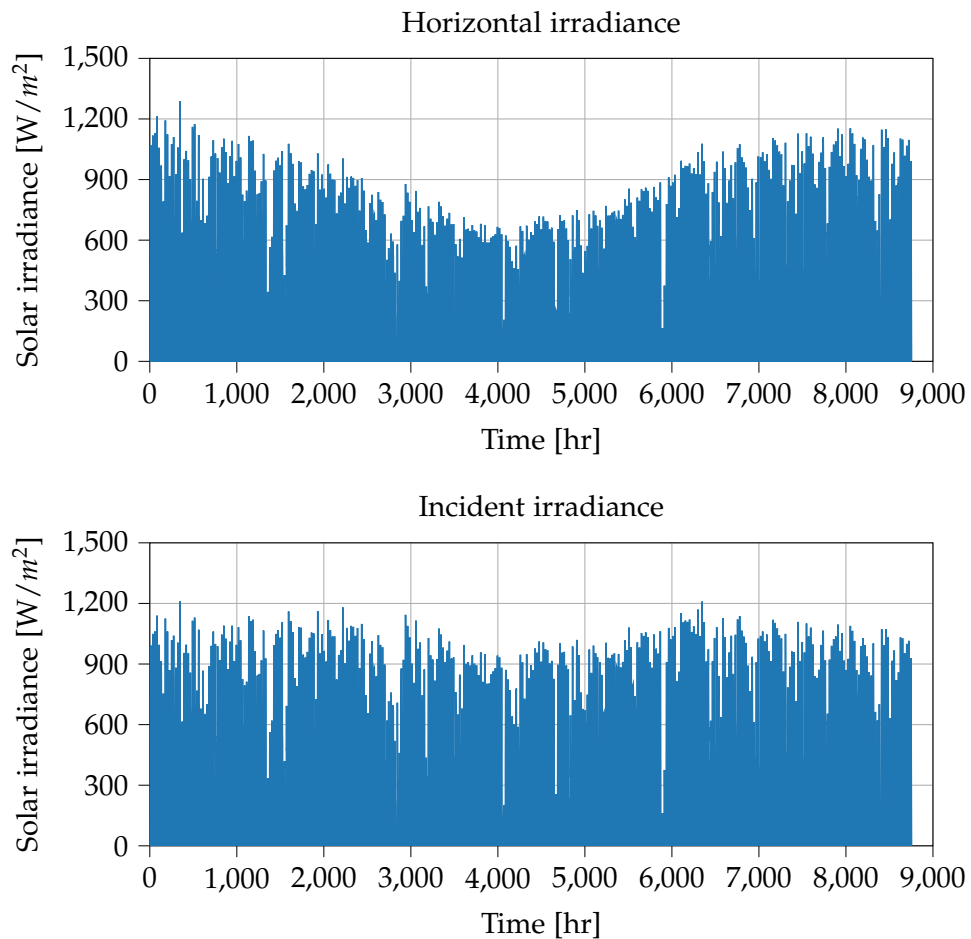


Figure 3.1: Calculation of optimal tilt angle for the PV panel

The measured solar irradiance for this project consists of average hourly values of Global Horizontal Irradiance (GHI) for 2019. For the location of the mining site in the southern hemisphere an azimuth angle of  $180^\circ$  is chosen. With the GHI the inclined solar irradiance for several angles has been calculated to obtain the best one. In Figure 3.1, the results are shown, the best tilt angle for the location can be observed. In this figure, from the (GHI) the daily average of inclined irradiance for 2019 has been calculated for angles between  $0^\circ$  and  $90^\circ$ . In the plot, the best tilt angle  $27^\circ$  and the daily average irradiance associated with it  $6364 [W/m^2/day]$  is shown.

In Figure 3.2, the horizontal and incident solar irradiance for the mine location for 2019 is shown. The global horizontal irradiance is obtained from the measurements made by the company. The incident irradiance is calculated based on the best tilt angle and the location.



**Figure 3.2:** Solar Irradiance Horizontal and Inclined

In Figures 3.3 and 3.4, boxplot of the inclined solar irradiance are shown monthly and hourly for the year 2019. In the hourly boxplot some night hours are not shown due to having a value of 0  $[W/m^2]$ . In this figures, the mean values and the first and third quartiles are shown. The seasonality of Western Australia (the south hemisphere) can be seen, where in the summer months, December and January the solar irradiance mean is higher. In the hourly boxplot, the peak hours are shown, from 10 to 12.

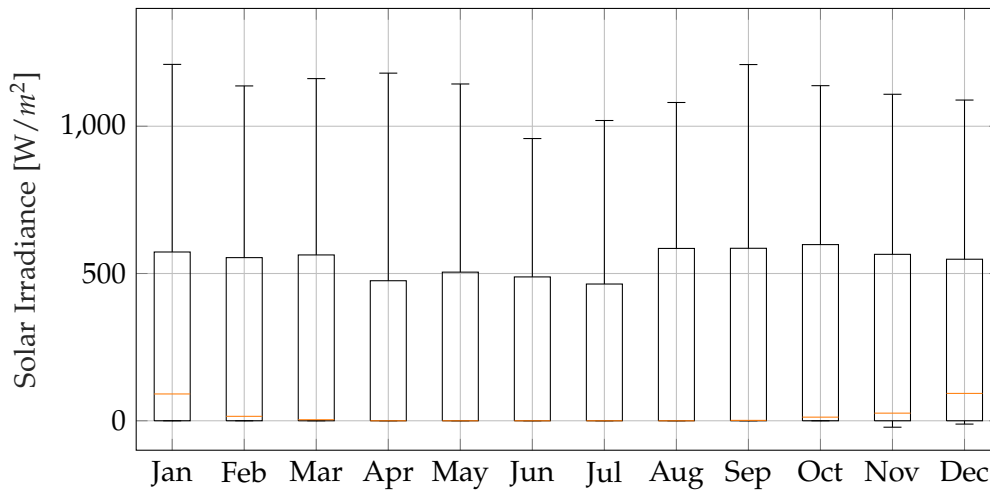


Figure 3.3: Solar Irradiance Horizontal - Monthly Boxplot

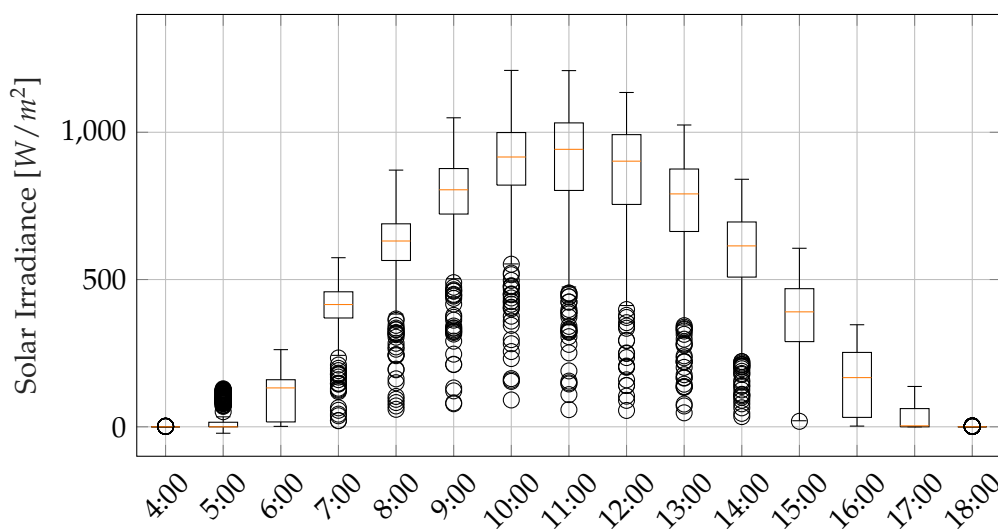


Figure 3.4: Solar Irradiance Horizontal - Hourly Boxplot

In Figure 3.5 the average day of GHI for the year 2019 is shown.

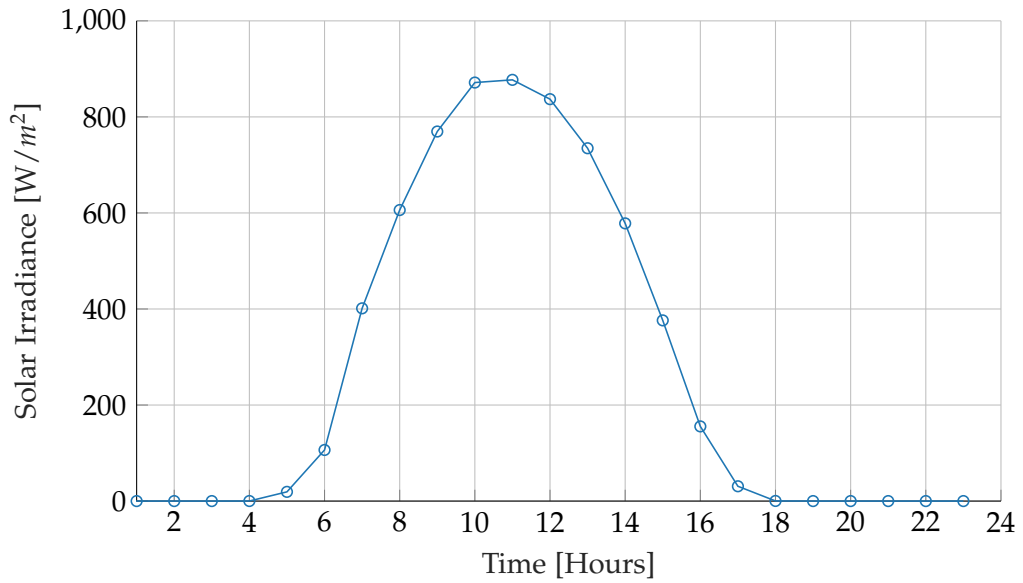


Figure 3.5: Solar Irradiance Horizontal - Average Day

In the table 3.1 the clearness index and the daily radiation average for each month can be observed for the GHI. The daily annual average of the GHI is  $5.89 [kWh/m^2/day]$ .

Table 3.1: Monthly average solar global horizontal irradiance (GHI)

Month	Clearness Index	Daily radiation [ $kWh/m^2/day$ ]
January	0.639	7.571
February	0.620	6.867
March	0.652	6.323
April	0.637	5.077
May	0.646	4.192
June	0.647	3.749
July	0.646	3.966
August	0.672	4.971
September	0.663	6.029
October	0.655	6.962
November	0.634	7.367
December	0.638	7.666

## 3.2 Wind Speed

The available wind speed and the wind direction measurements, which are going to be considered in this resource assessment, consist of 10 minutes average values. The wind speed measurements are performed on four different heights: 39.9, 60.1, 80 and 103.9 meters, which are going to be referred later too as 40, 60, 80 and 104 meters measurements. The wind direction measurements are performed at three different heights: 57.6, 77.1 and 97.9 meters.

The first overview of wind conditions at the site can be provided by the average wind speeds at the four measurement heights. The values are summarized in Table 3.2. Obviously, the highest average wind speed is measured at the highest hub height and is equal to 7.35 m/s. According to IEC 61400-1 standard [19] average wind speed of 7.5 m/s classifies the site to install wind turbines class III - suitable for low wind speeds. To obtain a higher average wind speed a higher hub height can be used.

**Table 3.2:** Average wind speed calculated from measurements at four different heights: 40, 60, 80 and 104 meters

Measurement height	Average Wind Speed
40 m	5.77 m/s
60 m	6.42 m/s
80 m	6.89 m/s
104 m	7.35 m/s

The calculation of wind speed at higher hub height can be done based on power law presented in Equation 3.1. Since, measurements from four different heights are available, the power law coefficients ( $\alpha_p$ ) between different heights can be calculated based on Equation 3.2. This way the calculations will be more accurate than when  $\alpha_p$  coefficient is assumed based on literature. The coefficients calculated between different hub heights are presented in Table 3.3. The comparison of how accurate the  $\alpha_p$  values represent the wind speed profile at the site, can be done by plotting the wind speed profile calculated with use of different  $\alpha_p$  values together with the average measured values at different heights. This was done on Figure 3.6. It can be seen that wind speed profile calculated with  $\alpha_{p,(40-60)}$  does not fit well the measurement at 104 meters. The remaining  $\alpha_{p,(60-80)}$  and  $\alpha_{p,(80-104)}$  give very similar result. The value of the former was calculated to be 0.245 and the latter to be 0.249. Therefore the  $\alpha_p$  chosen for calculations at this site is 0.25.

$$U_{hub} = U_{meas} \cdot \left( \frac{z_{hub}}{z_{meas}} \right)^{\alpha_p} \quad (3.1)$$

where:

$U_{hub}$  - the calculated wind speed at the hub height [m/s]

$U_{meas}$  - the wind speed at the measurement height [m/s]

$z_{hub}$  - the height of the hub [m]

$z_{meas}$  - the height of the measurement [m]

$\alpha_p$  - the power-law exponent

$$\alpha_{P,(1-2)} = \frac{\log \frac{U_1}{U_2}}{\log \frac{z_1}{z_2}} \quad (3.2)$$

where:

$U_1$  - the wind speed at height 1 [m/s]

$U_2$  - the wind speed at height 2 [m/s]

$z_1$  - the height 1 [m]

$z_2$  - the height 2 [m]

**Table 3.3:** Power law coefficient calculated between different measurement height

Calculated between	Symbol	Value
40 m and 60 m	$\alpha_{P,(40-60)}$	0.261
60 m and 80 m	$\alpha_{P,(60-80)}$	0.245
80 m and 100 m	$\alpha_{P,(80-104)}$	0.249

After calculation of power coefficient for the site considered in this project, the possibility to increase hub height was studied. It was done to see if a higher average wind speed can be obtained, for instance wind class II. This would enable to use WTs suitable for medium wind speed, and due to higher wind speed, the power production can be increased effectively. The requirement for wind class II is to have the average yearly wind speed equal to 8.5 m/s [19]. Using the previously calculated power law coefficient and power law presented in Equation 3.1, the calculation of the required hub height is done in Equation 3.3. Using measured average wind speed at 104 m. The result suggest a hub height of around 186 meters to reach the requirement of wind speed class II. WTs of this height are not being constructed. The highest existing WT has hub height of 178 m and is only considered as pilot project [20]. Therefore, there is no possibility to increase the

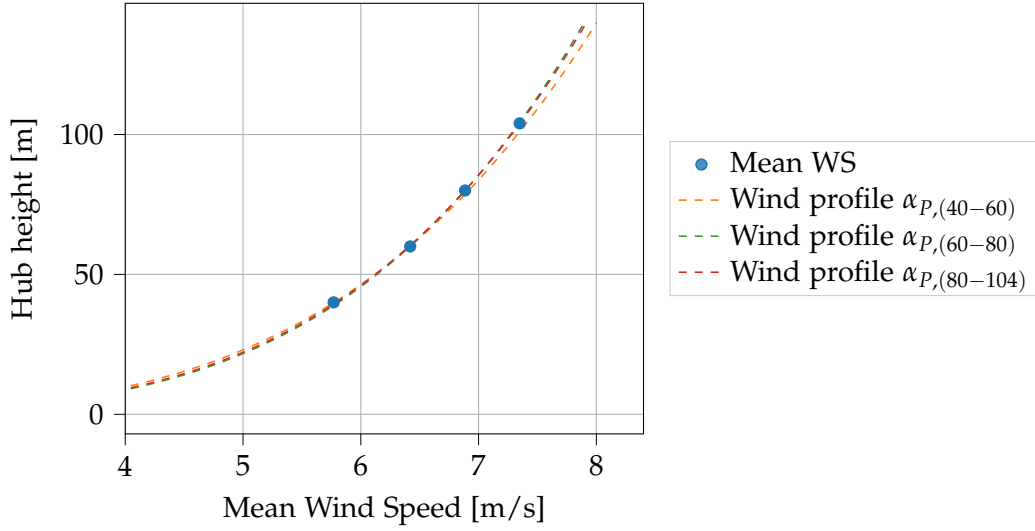


**Figure 3.6:** Wind speed profile calculated with different values of power coefficient  $\alpha_p$

average wind speed to 8.5 m/s. However, hub height can still be higher than 104 m to benefit from better wind conditions.

$$z_{hub} = \left( \frac{U_{hub}}{U_{meas}} \right)^{\frac{1}{\alpha_p}} \cdot z_{meas} = \left( \frac{8.5[m/s]}{7.35[m/s]} \right)^{\frac{1}{0.25}} \cdot 104[m] \approx 186[m] \quad (3.3)$$

Due to high variability of wind conditions and no visible daily pattern, unlike in solar radiation, there is no need to perform analysis of daily wind profile. More information can be retrieved based on monthly boxplot graph presented in Figure 3.7. It represents the monthly average values together with range of wind speeds recorded each month at 104 m height. The general conclusion can be that the wind speed is lower during the middle of the year and is highest in November and December. A similar conclusion was drawn from the measurements of solar irradiance. Therefore, based on this comparison, it cannot be said that wind and solar resources have complementary behaviour at this location. Another important observation, is that the wind speed variations are very high in each of the months, what proves that wind conditions are highly unpredictable.

A commonly used method to access the wind resources is to use the probability distribution. Figure 3.8 represents the wind speed probability distribution at the four measurement heights. The shape of the distribution is similar for all heights. The most probable wind speed to occur increases with the height of measurements. For 40, 60, 80 and 104 meters the most probable wind speeds are 6, 7, 8 and 9 respectively. This observation is in line with power law presented previously, where the wind speed increases with height.

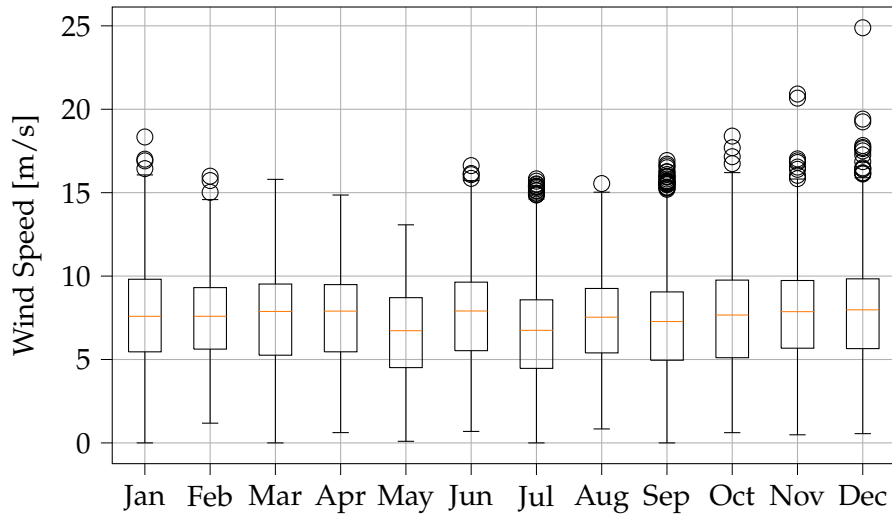


Figure 3.7: Wind speed measured at 104 m - Monthly Boxplot

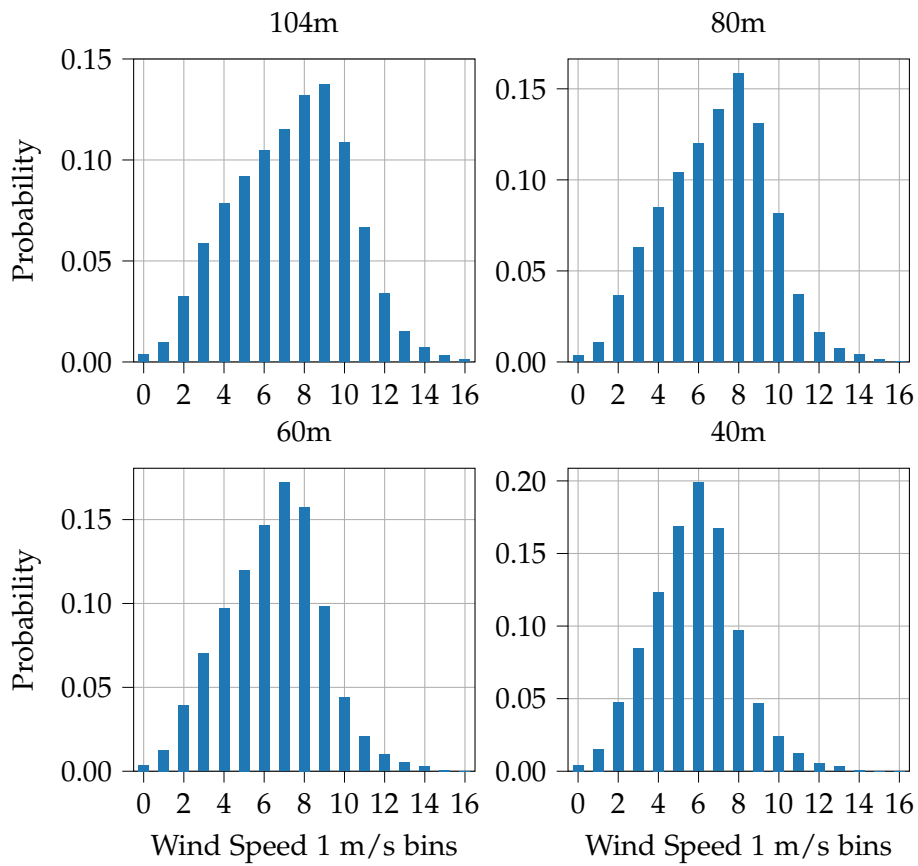


Figure 3.8: Wind speed probability distribution at different heights of measurement

Last analysis, was the distribution of wind resources across directions - wind rose. Wind roses are useful for siting wind turbines. When the wind turbines are placed in a landscape, it is important to have as few obstacles as possible, and smooth terrains in the direction from which a large share of wind comes [21]. The wind rose for the site was done based on the measurements of wind speed at 104 m and the measurements of wind directions at 97.9 m. By combining those two, it was possible to plot the probability of wind occurring in one of 16 selected directions (defined every 22.5°). The measurements were classified into four wind speed categories every 5 m/s, starting from 0. The ones above 20 m/s were not considered, since such high wind speed was rarely observed. Figure 3.9 represents the obtained wind rose. The dominant wind direction at the site is South-East, where the probability of wind from this direction is around 17.5%. Together with adjacent directions the probability is around 45%. Based on the results it would be advised to consider South-East direction as the dominant one during designing the layout of the plant.

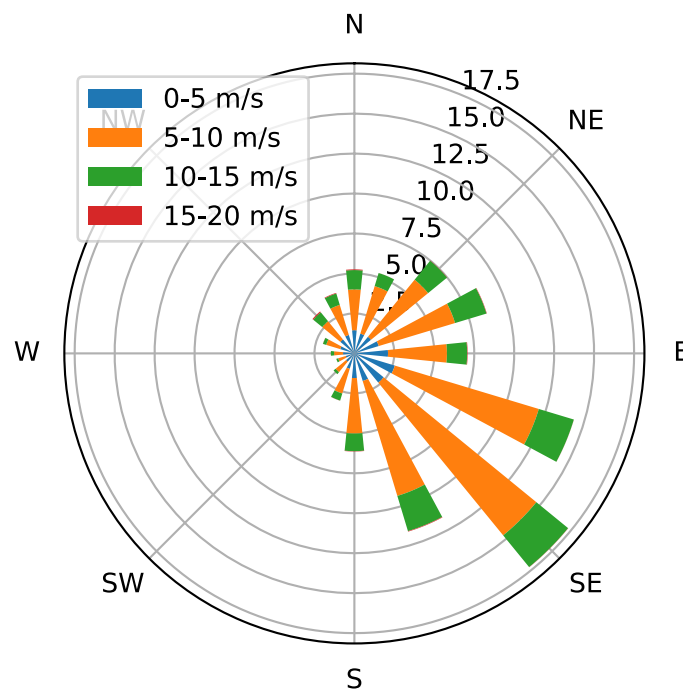


Figure 3.9: Wind rose based on measurements at 104 m



## Chapter 4

# HOMER Calculations

The presented below calculations methods are all retrieved from HOMER Pro on-line guide [22]. The knowledge of how the components are modelled in HOMER Pro is crucial both for good understanding of the analysis performed in HOMER Pro, as well as for the following calculation of operation of the selected systems. In this chapter, the components are divided in sections showing the technical equations. In addition to this, in the end the equations for the economical results are shown.

### 4.1 Generator

When modelling a conventional generator, the general variables for HOMER Pro are the lifetime, operating hours, minimum load ratio in percentage of capacity and minimum run time.

In addition to the general variables, HOMER Pro has fuel associated variables concerning the consumption, efficiency and emissions. First, the fuel type is to be selected. Diesel is the one chosen for this project. HOMER assumes that the fuel consumption is linear and it follows Equation 4.1:

$$F = F_0 \cdot Y_{gen} + F_1 \cdot P_{gen} \quad (4.1)$$

where:

$F_0$  - the fuel curve intercept coefficient [l/h/kW]

$F_1$  - the curve slope [l/h/kW]

$Y_{gen}$  - the rated capacity of the generator [kW]

$P_{gen}$  - the electrical output of the generator [kW]

If multiple points of measurements are used, HOMER will use an algorithm to approximate them to a line.

The efficiency of a generator in HOMER is defined as the electrical energy coming out divided by the chemical energy of the fuel and it follows Equation 4.2:

$$\eta_{gen} = \frac{3.6 \cdot P_{gen}}{\dot{m}_{fuel} \cdot LHV_{fuel}} \quad (4.2)$$

where:

$\dot{m}_{fuel}$  - the mass flow rate of the fuel [kg/hr]

$LHV_{fuel}$  - the lower heating value [MJ/kg]

The factor 3.6 comes from the conversion of  $1kWh = 3.6MJ$ . The mass flow rate of the fuel ( $\dot{m}_{fuel}$ ) is related to the fuel consumption ( $F$ ), depending on the units, if  $F$  is in kg they are the same, if not, a unit conversion must be done.

The last variables to enter in HOMER are the ones related to the emissions. Carbon monoxide, unburned hydrocarbons, particulate matter, nitrogen oxides and proportion of fuel sulfur converted to particulate matter, all of them in [g/units].

## 4.2 Idealized Battery

When modeling a lithium-ion battery some generic variables have to be entered for HOMER Pro. Firstly the nominal capacity in amp-hours and the nominal voltage or rated voltage, for lithium-ion battery is usually around 3.7 V. Next, the round trip efficiency, the ratio of energy put into the storage to the energy retrieved from it. HOMER Pro uses the same percentage of efficiency for input as for output of power. For load limits, two variables are considered. The minimum state of charge, establishes the minimum percentage of battery that can be, below this level, the battery would never run out. Maximum charge rate, measured in amp-hour. Finally the maximum charge and discharge current need to be entered in amps.

For the lifetime of the battery, there are two options. Time lifetime, where after a fixed length of time the battery will be replaced. Throughput lifetime, after a fixed amount of energy in kWh the battery is replaced. A third option is available where it combines the last two, lifetime and throughput, the battery will be replaced when one of them reaches the limit first.

### 4.3 Photovoltaic Panel

The variables used in HOMER Pro to simulate a photovoltaic panel, PV, are the rated capacity of the PV, the derating factor, the temperature coefficient of power and the PV cell temperature under standard test conditions.

The inputs that the PV requires to run a simulation in HOMER Pro are the temperature and the irradiance of the place where the PV is located. HOMER Pro offers a tool to obtain this data from the internet based on the location, but for this project the data obtained by the industrial partners and presented in 3 is used.

The way HOMER Pro calculates the power output is shown in the equation 4.3. This equation is a simplified way to calculate the power output based on the irradiance and temperature input, and it does not depend on the components inside of the PV.

$$P_{PV} = Y_{PV} f_{PV} \frac{\overline{G_T}}{\overline{G_{T,STC}}} [1 + \alpha_T (T_c - T_{c,STC})] \quad (4.3)$$

where:

$Y_{PV}$  - the rated capacity of the PV array, meaning its power output under standard test conditions [kW]

$f_{PV}$  - the PV derating factor

$\overline{G_T}$  - the solar radiation incident on the PV array in the current time step [ $kW/m^2$ ].

$\overline{G_{T,STC}}$  - the incident radiation at standard test conditions [ $1kW/m^2$ ]

$\alpha_T$  - the temperature coefficient of power [%/°C].

$T_c$  - the PV cell temperature in the current time step [°C], which is calculated according to Equation 4.4

$T_{c,STC}$  - the PV cell temperature under standard test conditions [25°C].

$$T_c = \frac{T_a + (T_{c,NOCT} - T_{a,NOCT}) \left( \frac{G_T}{G_{T,NOCT}} \right) \left[ 1 - \frac{\eta_{mp,STC}(1 - \alpha_P T_{c,STC})}{0.9} \right]}{1 + (T_{c,NOCT} - T_{a,NOCT}) \left( \frac{G_T}{G_{T,NOCT}} \right) \left( \frac{\alpha_P \eta_{mp,STC}}{0.9} \right)} \quad (4.4)$$

Where:

$T_a$  - the ambient temperature [°C]

$T_{a,NOCT}$  - the NOCT [°C], module specific

$T_{a,NOCT}$  - the ambient temperature at which NOCT is defined [20°C]

$\eta_{mp,STC}$  - the maximum power point efficiency under standard test conditions [%]

HOMER Pro allows to calculate the power output without considering the temperature factor, thus simplifying the equation 4.3, the power is modelled using the equation 4.5.

$$P_{PV} = Y_{PV} f_{PV} \frac{\overline{G_T}}{\overline{G_{T,STC}}} \quad (4.5)$$

## 4.4 Wind Turbine

The calculation of power output from the wind turbine is done in three steps. Firstly, the wind speed at the hub height of the wind turbine is calculated. Based on the calculated speed the power output of the wind turbine is determined. Lastly, the power output can be adjusted based on the actual air density value.

### 4.4.1 Calculation of Wind Speed at the Hub Height

For each time step of the simulation, the measured wind speed at the measurement height is used to calculate the wind speed at the hub height. The calculations can be done using either logarithmic law or power law. The former is presented in Equation 4.6 and the latter in Equation 4.7.

$$U_{hub} = U_{meas} \cdot \frac{\ln\left(\frac{z_{hub}}{z_0}\right)}{\ln\left(\frac{z_{meas}}{z_0}\right)} \quad (4.6)$$

$$U_{hub} = U_{meas} \cdot \left(\frac{z_{hub}}{z_{meas}}\right)^{\alpha_P} \quad (4.7)$$

where:

$U_{hub}$  - the calculated wind speed at the hub height [m/s]

$U_{meas}$  - the wind speed at the measurement height [m/s]

$z_{hub}$  - the height of the hub [m]

$z_{meas}$  - the height of the measurement [m]

$\alpha_P$  - the power-law exponent

#### 4.4.2 Calculation of Wind Turbine Power Output at the Standard Air Density

For this calculation, the necessary input is the power curve of the selected wind turbine. The power curve contains information about the power output of the wind turbine at different wind speeds. An example is presented on Figure 4.1. The power generation starts after the cut-in wind speed is exceeded and stops when the wind speed is higher than cut out speed. The power curve in HOMER is defined based on discrete power curve points. The power output for wind speed between the defined points is calculated based on linear approximation.

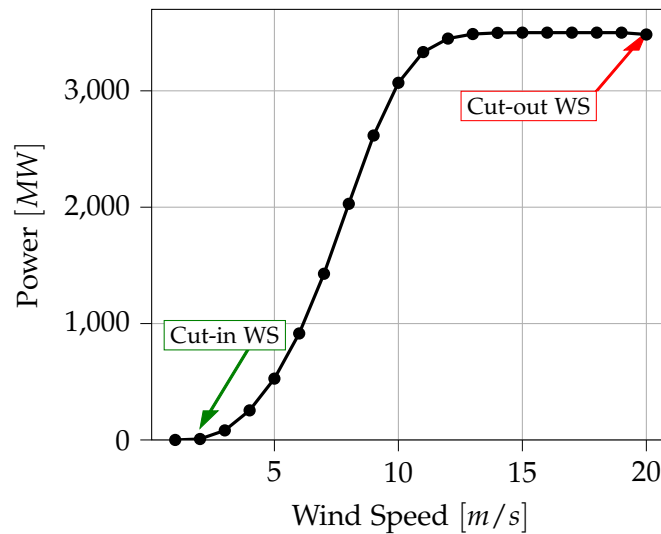


Figure 4.1: Sample of a power curve with cut-in and cut-out wind speed

When the wind speed at the hub height is determined, it is used to calculate the power output based on the power curve of the selected wind turbine. For the wind speed in each hour of operation, the corresponding power output is found. If the wind speed is lower than the cut-in speed or it exceeds the cut-out speed the power output is equal to 0.

#### 4.4.3 Applying Density Correction

The power curve typically specifies the turbine performance under conditions of standard air density ( $[\rho_0 = 1.225 \text{ kg/m}^3]$ ). To adjust to the actual conditions, the power output, determined based on the power curve, is multiplied by the air density ratio, according to Equation 4.8.

$$P_{WGT} = \frac{\rho}{\rho_0} \cdot P_{WGT,STP} \quad (4.8)$$

where:

$P_{WGT}$  - the wind turbine power output

$\rho$  - the actual air density  $kg/m^3$

$\rho_0$  - the standard air density –  $1,225kg/m^3$

$P_{WGT,STP}$  - the power output at standard temperature and pressure

## 4.5 Emissions

The emissions can be estimated for six pollutants: Carbon Dioxide ( $CO_2$ ), Carbon Monoxide ( $CO$ ), Unburned Hydrocarbons ( $UHC$ ), Particulate Matter ( $PM$ ), Sulfur Dioxide ( $SO_2$ ) and Nitrogen Oxides ( $NO_x$ ).

The emitted pollutants depend on the fuel used and the properties of the generator. The important properties of fuel to calculate the emission are:

- Carbon Content [%]
- Sulfur Content [%]

The remaining emissions are specified in the properties of the generator as emission factors (kg of pollutant emitted per unit of fuel consumed). Factors for four pollutants should be specified directly:  $CO$ ,  $UHC$ ,  $PM$  and  $NO_x$ . The remaining two ( $CO_2$  and  $SO_2$ ) are calculated based on carbon and sulfur content of the fuel, taking into account the other emitted pollutants and with the following assumptions:

1. Any carbon in the fuel that is not emitted as carbon monoxide or unburned hydrocarbons is emitted as carbon dioxide.
2. The carbon fraction of the unburned hydrocarbon emissions is the same as that of the fuel.
3. Any sulfur in the burned fuel that is not emitted as particulate matter is emitted as sulfur dioxide.

## 4.6 Techno-Economic Indicators

### 4.6.1 Renewable Fraction

The renewable fraction is calculated by HOMER Pro following Equation 4.9:

$$f_{ren} = 1 - \frac{E_{nonren} + H_{nonren}}{E_{served} + H_{served}} \quad (4.9)$$

where:

$E_{nonren}$  - nonrenewable electrical production [kWh/yr]

$E_{served}$  - total electrical load served [kWh/yr]

$H_{nonren}$  - nonrenewable thermal production [kWh/yr]

$H_{served}$  - total thermal load served [kWh/yr]

### 4.6.2 Net Present Cost

The net present cost (NPC) of a system is the difference between the present value of all the costs and the present value of all the revenues of system. HOMER Pro calculates the NPC as a sum of the total discounted cash flow in each year of the project lifetime. The calculation can be presented with Equation 4.10.

$$NPC = \sum_{t=1}^n \frac{R_y}{(1+i)^y} \quad (4.10)$$

where:

$R_y$  - the net cash outflows-inflows during single year  $y$  [\$]

$n$  - the lifetime of the investment [yr]

$i$  - the real discount rate

### 4.6.3 Levelized Cost of Electricity

Levelized Cost of Electricity [LCOE] is the average cost per kWh of useful electrical energy produced by the system. It is commonly used to compare profitability of energy sector investments and can be calculated according to Equation 4.11.

$$LCOE = \frac{C_{ann}}{E_{served}} \quad (4.11)$$

where:

$C_{ann}$  - the total annualized cost [\$/year]

The total annualized cost is the annualized value of the total net present cost. HOMER calculates the total annualized cost using Equation 4.12.

$$C_{ann} = CRF(i, t) \cdot NPC \quad (4.12)$$

where:

$CRF$  - a function returning the capital recovery factor, which is a ratio used to calculate the present value of an annuity (a series of equal annual cash flows). The  $CRF$  can be calculated with Equation 4.13

$$CRF(i, t) = \frac{i(1+i)^t}{(1+i)^t - 1} \quad (4.13)$$

#### 4.6.4 Initial Capital Cost

The initial capital cost is the sum of total installed costs of all components at the beginning of the project.

#### 4.6.5 Operating Cost

The operating cost is the annualized value of all costs and revenues other than initial capital cost and can be expressed by Equation 4.14

$$C_{operating} = C_{ann} - C_{ann,cap} \quad (4.14)$$

where:

$C_{ann,cap}$  - the total annualized capital cost [\$/yr]

### 4.7 Dispatch Algorithm

HOMER Pro has three available controller set ups for the dispatch algorithm, which are: HOMER Predictive Selection, HOMER Cycle Charging and HOMER Load Following. The principle of the first is that it has a 24 hour insight into the loads and renewable resources. However, it cannot be used when sizes of the components are to be optimized. HOMER Cycle Charging assumes that whenever a generator is turned on it operated at full load. This behaviour is not desirable in a hybrid power generation and is not used in the calculations in the project. For this

project, the dispatch strategy used in optimizing the hourly operation of the power plant is HOMER Load Following. In this dispatch strategy the generator produces only enough power to meet the load in each time step. Charging of the battery is left to renewable energy sources. If it is economically advantageous, the generator may still ramp up and produce power to sell it to the grid. The power sources are dispatched to serve the load at the least total cost in each time step. The total cost includes cost of fuel, *O&M* and replacement costs.



# Chapter 5

## Input Data

In this chapter the data needed for performing the analysis will be presented. To perform a correct simulation reliable input is required. Some of the data has been obtained from the industrial partner and the rest has been gathered through review of related literature and available open access resources.

### 5.1 Load

In Figure 5.1 the load profile of the mine in P.U. is shown for 2019, the mean value is  $0.8975[P.U.]$ . As it can be seen, the load profile is very constant through the whole year, despite some occasional dropdowns due to maintenance.

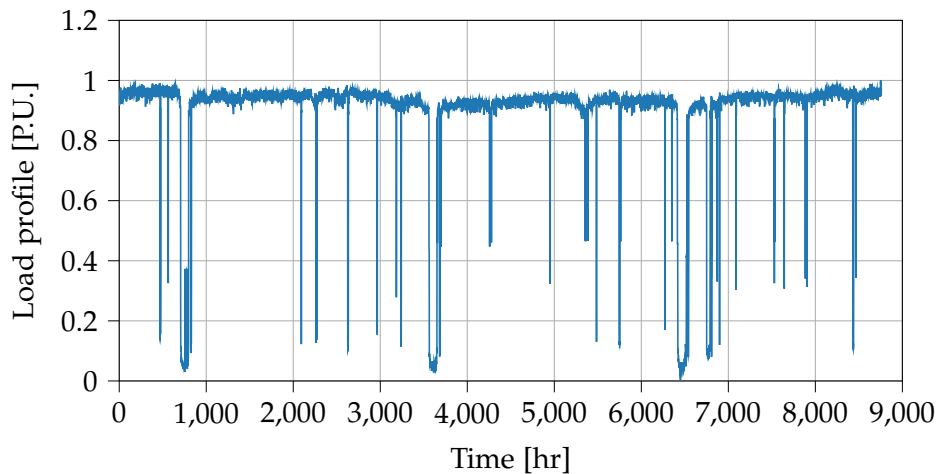


**Figure 5.1:** Annual load profile

In Figure 5.2, the average daily demand in P.U. is shown, it can be observed

that the demand is steady. The uncertainties in the load profile studied later on are due to the maintenance of the equipment shown in Figure 5.1.

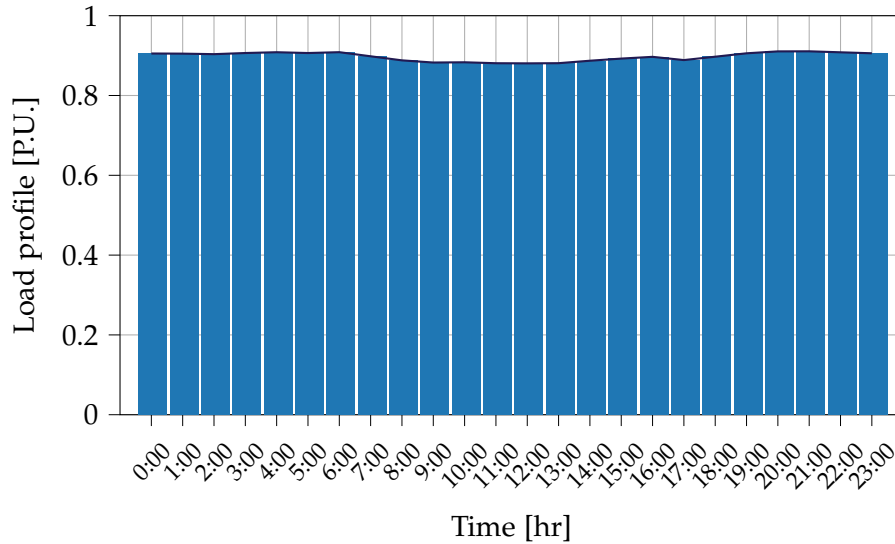


Figure 5.2: Daily average load profile

## 5.2 Economics

### 5.2.1 Inflation

The inflation in Australia has varied between a 1.3% and a 2.1% since 2016 to 2020. In the last quarter of 2019 the variation was of a 1.9 %. Because of this the inflation rate was selected to be of 1.8% [23].

### 5.2.2 Discount Rate

According to [24] the discount rates for renewable energy project in Australia have average value of 6.75% and 7.5% for solar and onshore wind respectively. Therefore, the assumed discount rate in this project is chosen to be 7%.

### 5.2.3 Project Lifetime

The project lifetime is expected to be around 25 years.

## 5.3 Wind Speed Data

The wind speed data used in the project are 10 minutes average values measured at four heights: 40, 60, 80 and 104 meters. Since the calculations are done hourly the wind speed data for one hour is calculated as mean value for the six 10 minutes intervals in one hour. The measurements from 80 meters are chosen for the calculations since the measurements for 104 meters contain measurement errors - random extremely high measurements during a day with average wind.

The calculation of wind speed at the hub height is done with the power law presented in Chapter 4.4.1. The power law exponent is 0.25 and is calculated based on the measurements from different heights. The calculations are presented in Chapter 3.2.

## 5.4 Diesel Generator

According to [25] the prices for diesel generators in 2020 are expected to be approximately 405\$/kW and the variable Operation and Maintenance (O&M) costs should be assumed to be 7\$/MWh. The lifetime of diesel generator is expressed in hours of operation and is assumed to be 22500 hours, which is an average value according to [26]. Another important input for the calculation of diesel generator is the price of diesel. The price is assumed to be 1.019\$/l according to the mean prices of diesel in Australia in 2019 [27].

In order to be able to optimize the size of the diesel generator needed in the system the diesel generator is defined as Autoset Generator.

Apart from the prices of the technology and fuel, the needed inputs are: minimum load ratio, minimum runtime, fuel curve and emissions.

The minimum load ratio specifies what is the minimum load the diesel generator can operate on. According to [28] operating diesel generator under 30% of rated power for a long time has negative impact for the unit, therefore the minimum load ratio is set to 30%.

For practical reasons the minimum runtime is set to 15 min.

This way the fuel curve has default values and cannot be modified as the Autosize generator was selected. It is defined as described in 4.1, the intercept coefficient is 0.0147 and the slope is 0.236.

Finally, the emissions are assumed to be the default values proposed by HOMER and are summarized in Table 5.1.

**Table 5.1:** Assumed emissions from diesel generator

Emission [g/L of fuel]	Value
CO	16.5
UHC	0.72
PM	0.1
NO <sub>x</sub>	15.5
Sulfur Converted to PM [%]	2.2

The data used for defining the diesel generator in HOMER is summarized in Table 5.2

**Table 5.2:** PV module costs and lifetime used for calculations

Installation cost [ $M\$/MWh_p$ ]	0.405
O&M [ $\$/MWh_{output}$ ]	7
Lifetime [hours]	22500
Diesel Price [ $\$/l$ ]	1.019
Minimum Load Ratio [%]	30
Emissions	Table 5.1

## 5.5 PV

There is a sustained decline in the prices of utility-scale solar PV [29]. According to [25] the prices dropped by around 60% from 2015 to 2020. The price for utility scale PV is estimated to be  $0.495M\$/MWh_p$ . Another important cost, which must be considered are the O&M costs. These were also decreasing over the past years but not as rapidly as the installation costs. The O&M costs for PV are estimated to be  $7.32\$/kW/year$ .

The life time of the PV modules exceeds 30 years but the power output is degrading with time. The efficiency loss in modern PV modules is approximately 13% after 25 years of operation. This means that the power output of the PV system after 25 years will be approximately 87% of the initial power output. The PV price includes the cost of inverter, however the lifetime of inverter is shorter (approx. 15 years) and it must be replaced before the PV modules. This is accounted for by decreasing the replacement price of PV modules and setting replacement price for the inverter.

For the calculations, the technical data and orientation of the PV modules details are also necessary. These are: efficiency, NOCT, power temperature coefficient, panel slope and panel azimuth. The panel slope calculation was presented in Chapter 3.1 and the optimal slope chosen to be  $27^\circ$ . The other parameters are

listed in Table 5.3, where all the values used as inputs to simulating the model are summarized.

**Table 5.3:** PV module costs and lifetime used for calculations

Installation cost [ $M\$/MWh_p$ ]	0.495
Yearly O&M [ $\$/kW/year$ ]	7.32
Lifetime [ $years$ ]	30
Power output after 25 years [%]	87
Efficiency [%]	13
NOCT [ $^{\circ}C$ ]	47
Power Temperature Coefficient [ $\%/^{\circ}C$ ]	-0.5
Panel Slope [ $^{\circ}$ ]	27
Panel Azimuth [ $^{\circ}$ ]	180

## 5.6 Battery Storage

### 5.6.1 Economics

According to [30] the total cost for a 2-hour battery in 2018 is  $454[\$/kWh]$ , this is taken as the capital price. A 2-hour battery is defined as a battery capable of delivering the rated power during 2 hours. The capital cost is calculated including several components such as inverters, structures, etc. However the individual Li-ion battery cost is  $209[\$/kWh]$ , this last cost is taken as replacement cost, since the equipment related to the battery does not need such a frequent replacement.

According to [31] the battery operating and maintenance cost in this case is estimated as  $11.35[\$/kWh-yr]$ , assuming that in 2018 the OPEX was  $2.5[\%]$  of the CAPEX per year.

### 5.6.2 Lifetime

According to the National Renewable Energy Laboratory (NREL) studies mentioned in the previous paragraph, the lifetime of the battery is 15 years, assuming 1 cycle per day. Since in this project a higher use of the battery is predicted, the lifetime of the battery can be adjusted according to the investigations made in [32], which ends into a 10-year life span.. In the same paper, a test of energy throughput lifetime is done for a specific Li-ion battery. This test is extrapolated to the battery considered in HOMER Pro.

In the test a  $75[Ah]$  and  $4.2[V]$  battery and a daily Amp-hour throughput of  $69[Ah]$  (discharge direction, with positive current) is considered. Assuming repeated cycling in this mode for 365 days/year, the battery lasts 7.3 years to 70% of

75[Ah].

The energy throughput of the NREL Battery test in percentage of the nominal capacity is calculated in Equations 5.1 and 5.2:

$$EnergyThroughput[Ah] = 69 \cdot 365 \cdot 7.3 = 183,850.5[Ah] \quad (5.1)$$

$$EnergyThroughput[\%] = \frac{EnergyThroughput[Ah]}{75[Ah]} \cdot 100 = 245,134[\%] \quad (5.2)$$

The battery considered in HOMER Pro is a 167[Ah] capacity and 600[V]. The energy throughput of this battery is calculated in 5.3 and 5.4:

$$EnergyThroughput[Ah] = \frac{167 \cdot 245,134}{100} = 424,403.78[Ah] \quad (5.3)$$

$$\begin{aligned} EnergyThroughput[Kwh] &= \frac{EnergyThroughput[Ah] \cdot V}{1000} \\ &= \frac{424,403.78 \cdot 600}{1,000} = 254,642.27 \quad (5.4) \end{aligned}$$

For this project a minimum state of charge of the battery of 30[%] is considered. The summary of the data input in HOMER is showed in table 5.4.

**Table 5.4:** Battery storage costs and lifetime used for calculations

Capital investment [\$/kWh]	454
Replacement cost [\$/kWh]	209
Yearly O&M [\$/kWh – yr]	11.35
Hourly O&M [\$/kWh <sub>output</sub> ]	0.00236
Lifetime [years]	10
Lifetime [kWh]	254,642
Minimum SOC [%]	30

## 5.7 Wind Turbine

The investment cost of onshore wind turbines (WTs) is decreasing over the years. However, the decrease rate is significantly lower than for PV modules [29]. According to [25] the price decreased by around 16% from 2015 to 2020. The price for large scale WTs (assumed capacity of 3.5 MW) is approximately 1.32 M\$/MW.

The O&M cost reach around 16.5  $\$/kW/year$ . The lifetime of the WT is estimated to be 27 years.

For calculating the power output of the WT it is necessary to know the power curve. Based on the analysis performed in Chapter 3.2 the chosen WT is Enercon E-138 EP3. First reason is that it is suitable for wind class III [33], which is the class at the site. Secondly, the power curve of the wind turbine is available in HOMER. It's rated power output is 3.5 MW which is the power for which the prices per MW where estimated. The power curve used for calculations is presented on Figure 5.3. Another parameter which must be chosen is the hub height of the wind turbine. The default value suggested by HOMER is 135 m. The average yearly wind speed at this height can be calculated using Equation 3.1 and is around 7.84 m/s. This value is suitable for using this wind turbine and therefore hub height of 135 m was chosen.

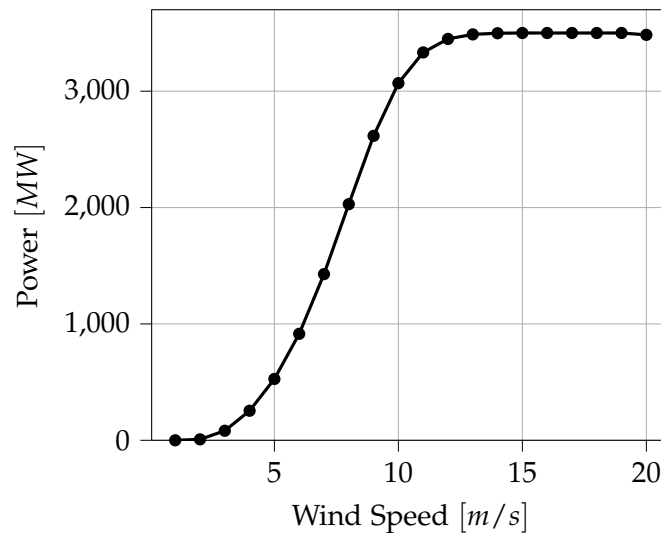


**Figure 5.3:** Power curve of Enercon E-138 EP3 wind turbine

The summary of the input to the model is presented in Table 5.5.

**Table 5.5:** Wind turbine costs and lifetime used for calculations

Installation cost [ $M\$/MWh_p$ ]	1.32
Yearly O&M [ $\$/kW/year$ ]	16.5
Hourly O&M [ $\$/kWh_{output}$ ]	0.00177
Lifetime [ $years$ ]	27



## Chapter 6

# HOMER Pro Results and Plan Selection

First part of the chapter presents the possible configurations of the energy system for the mining site, which were obtained with use of HOMER Pro. The aim is to indicate the best configuration. This objective is achieved using Multi-Criteria Decision-Making (MCDM), based on Analytic Hierarchy Process (AHP).

### 6.1 Results from HOMER Pro

The first step of decision making process is to indicate the possible configurations of the power plant. Based on all the data presented in Chapter 5 the HOMER Pro model was created. The units considered in the model are:

- Photovoltaic modules
- Wind turbines
- Batteries
- Diesel generator
- Converter

The configuration of the system is presented in Figure 6.1. The models behind all of the units are presented in Chapter 4. The size of all of them is optimized in HOMER Pro in order to satisfy the demand at every instance and minimize NPC. HOMER Pro optimizes all possible configurations of the system and displays the results in order of increasing NPC. Since the number of generated configurations would not enable to consider them all in the decision making step, 10 of them are

chosen. The selection of the plans was done to represent various types of possible energy solution for the mine. Plans with low NPC, low initial investment and with different mix of technologies were chosen.

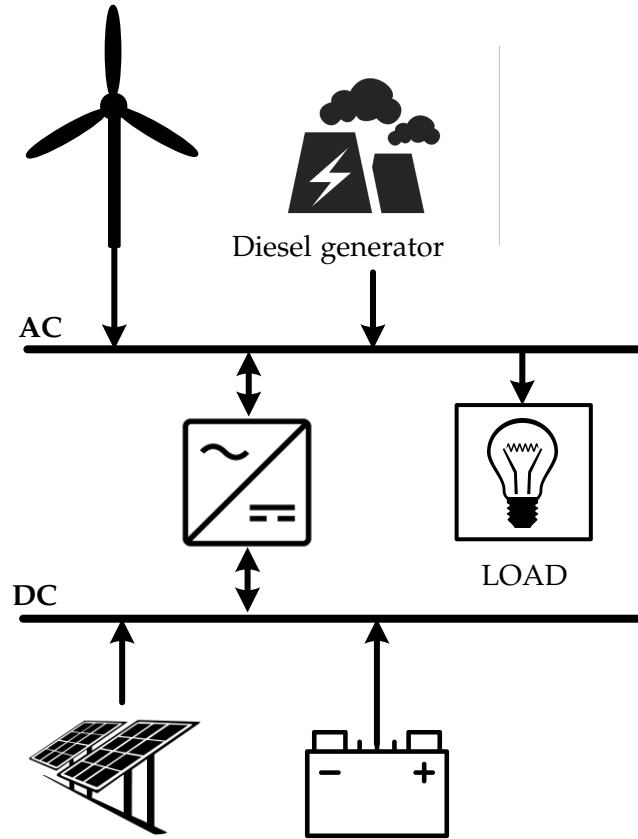


**Figure 6.1:** Configuration of the units used for the planning phase

In Table 6.1 the different plans selected from the HOMER Pro calculations are shown along with a short description of the reason for choosing them to be considered in the decision making process. The capacities of technologies installed in each of the selected plans are presented in Table 6.2. The economical and technical details are presented in Table 6.3. These values are used in the decision making process. It is worth mentioning that, the operating cost calculated with use of HOMER Pro does not take into account the variable costs of operation of WTs and BESS, which are associated with the output power of the generating unit. This is due to limitations of HOMER Pro. These costs are accounted for in the later stage when the optimization of operation is performed.

**Table 6.1:** Selected plans

<b>Plan no.</b>	<b>Configuration plans</b>	<b>Description</b>
1	Diesel	Base Case, Lowest Initial Investment
2	PV + Wind turbines + Diesel + Battery	Lowest NPC
3	PV + Wind turbines + Diesel + Battery	Low NPC, high renewable fraction
4	PV + Wind turbines + Diesel	Low NPC, high renewable fraction
5	Wind turbine + Diesel + Battery	High renewable fraction without PV
6	PV + Diesel + Battery	Low excess electricity with renewables, without WT
7	PV + Wind turbine + Diesel + Battery	Lower installed power of renewables
8	PV + Wind turbine + Diesel	Lower installed power of renewables without battery
9	PV + Wind turbines + Diesel + Battery	Solution with renewables with low excess electricity
10	Wind turbines + Diesel + Battery	Solution without PV

**Table 6.2:** Installed capacities of each of the considered technologies in the selected plans

<b>Plan nr</b>	<b>PV [MW]</b>	<b>WT [MW]</b>	<b>Diesel Generator [MW]</b>	<b>Battery [MWh]</b>
1	0.0	0.0	60.0	0.0
2	97.0	101.5	55.0	64.4
3	90.0	94.5	55.0	67.8
4	106.0	122.5	55.0	0.0
5	0	122.5	55.0	100.8
6	120.0	0	55.0	40.5
7	60.0	63.0	50.0	38.6
8	60.0	63.0	55.0	0.0
9	30.0	31.5	50.0	11.9
10	0.0	94.5	55.0	90

**Table 6.3:** Economical and technical details of the selected plans

Plan nr	NPC [M\$]	COE [\$/kWh]	Operating cost [M\$/yr]	Initial capital [M\$]	Ren Frac [%]	Excess Elec [%]
1	1881.8	0.315	131.86	24.30	0.00	0.00
2	444.0	0.074	14.93	233.66	91.95	38.72
3	447.3	0.075	15.96	222.55	91.25	34.67
4	468.6	0.078	16.44	236.94	90.51	48.21
5	605.4	0.101	26.65	229.93	83.83	35.27
6	1273.2	0.213	83.28	100.13	37.08	11.28
7	572.3	0.096	29.92	150.77	79.55	14.21
8	643.4	0.108	36.07	135.27	78.78	15.13
9	1157.3	0.194	76.32	82.15	46.49	1.77
10	647.8	0.108	32.64	188.03	79.1	21.62

## 6.2 Description of AHP

To compare the different cases obtained by HOMER Pro and to make a decision regarding the best cases, a multi-criteria decision-making algorithm (MCDM) has been used. The tool used for MCDM is analytic hierarchy process (AHP). This process consist of subjective comparison of all the plans of the system by arranging them in a matrix to determine relative priorities [12].

AHP compares two at a time elements of a system arranged in a matrix to determine relative priorities among all elements of that system. The priorities of the elements are the values of the eigen vector of the largest real positive Eigen value [12]. An algorithm approach to AHP is as follows:

1. It is necessary to make a hierarchy as shown in the figure 6.2. The first level is the main objective of the whole problem. The second level shows the different criteria that are related to the main objective. And the lowest level are the different solution to solve the problem.
2. Then it is necessary to obtain pairwise comparison of the different elements by introducing expert judgements and scale them from 1 to 9 based on the scale presented in Table 6.4. This comparisons are used to make a reciprocal matrix of  $n \times n$ , where  $n$  is the number of elements to be compared.
3. The eigen values of said matrix are calculated by solving the equation 6.1.
4. The eigen values are ranked according to their values, from the highest value as the most important value. The eigenvector of the largerst real positive

eigenvalue is the priority vector of the matrix.

- In order to corroborate the results it is necessary to value the consistency and sensitivity of the result. The formula shown in the equation 6.2 is the consistency index which is the average magnitude of the smaller eigen values, which shows the deviation of consistency in the AHP method. Now the consistency index is divided by the random consistency index shown in the equation 6.3, this results in the consistency ratio of the comparison matrix. The random consistency index depends on the matrix size, so it has to be calculate beforehand, to verify the results, and is given by the equation 6.4. For good consistency the consistency ratio should not exceed 0.1.

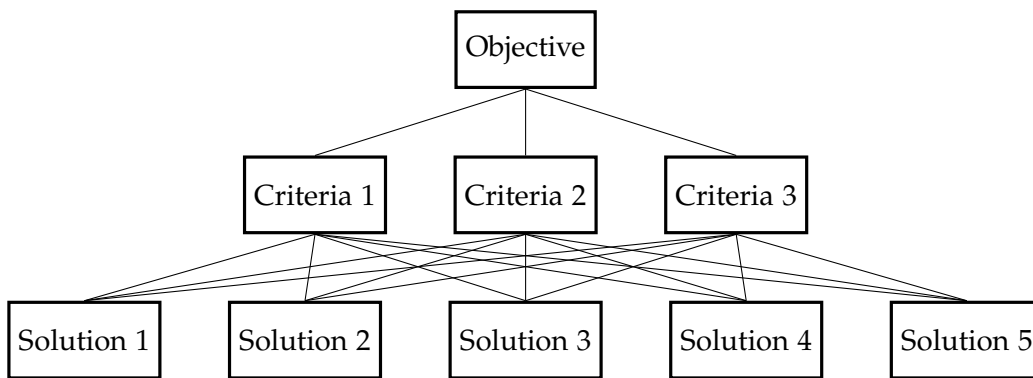


Figure 6.2: Hierarchy structure of AHP

Table 6.4: The fundamental scale for deciding relative importance [34]

Intensity of importance	Description
1	Equal importance
3	Moderate importance
5	Strong importance
7	Very strong importance
9	Extremely strong importance
2,4,6,8	Intermediate values

$$\begin{bmatrix} 1 & a_{12} & a_{13} & \dots & a_{1n} \\ 1/a_{12} & 1 & a_{23} & \dots & a_{2n} \\ 1/a_{13} & 1/a_{23} & 1 & \dots & a_{3n} \\ \vdots & \vdots & \vdots & \ddots & \vdots \\ 1/a_{1n} & 1/a_{2n} & 1/a_{3n} & \dots & 1 \end{bmatrix} \begin{bmatrix} w_1 \\ w_2 \\ w_3 \\ \vdots \\ w_n \end{bmatrix} = \lambda \begin{bmatrix} w_1 \\ w_2 \\ w_3 \\ \vdots \\ w_n \end{bmatrix} \quad (6.1)$$

$$C_i = (\lambda_{max} - n)/(n - 1) \quad (6.2)$$

$$C_r = (\lambda_{max} - n)/(n - 1)/R_i \quad (6.3)$$

$$R_i = 1.98(n - 2)/n \quad (6.4)$$

### 6.3 Criteria

In Table 6.5, the criteria followed in this project for the decision making are shown. The most relevant attributes for this project have been chosen. Four main attributes are selected, Economical, Robustness, Environmental and Technical. Under each of the main attributes, different subattributes are selected.

**Table 6.5:** Selection Criteria

Attribute	Subattribute
Economical	NPC [\$] Initial Capital [\$] Operating cost [\$ / yr] System/Excess Electricity [%]
Robustness	Diesel PV Wind Turbine Battery
Environmental	CO2 Emissions SO2 Emissions NOx PM
Technical	Ren Frac [%]

These criteria are later used for the comparison of each plan and finally to choose the most relevant one. Since the relevancy of each subattribute is subjective, two different cases have been chosen, a profit oriented one and an environmentally friendly. Regardless of each case, the sub-attributes priorities are the same for the whole study. The economical and robustness priorities can be observed in Appendix A, for the environmental priorities all of them are equally relevant and a priority coefficient of 0.25 is used.

### 6.3.1 Robustness Assessment

Whereas all the attributes presented in 6.5 are self explanatory, the robustness requires a brief description of how it is calculated. In the project, the robustness is defined as the influence of change in price on the final result (NPC). The less influence the higher the robustness. Hence, the influence of price increase of diesel fuel, PV modules, wind turbine and battery was analyzed. The calculations considered 30% increase in all of the factors and the corresponding increase in NPC was analyzed. The results are presented in Table 6.6. The obtained values were later used to decide on the robustness priorities presented in Appendix A.

**Table 6.6:** % change in NPC due to price increase of 30%

Plan nr	Diesel	PV	Wind Turbine	Battery
1	24.92%	0.00%	0.00%	0.00%
2	8.92%	3.24%	9.06%	2.53%
3	9.65%	2.99%	8.38%	2.64%
4	10.14%	3.38%	10.37%	0.00%
5	12.90%	0.00%	8.02%	2.90%
6	23.04%	1.40%	0.00%	0.55%
7	16.91%	1.56%	4.36%	1.46%
8	17.14%	1.39%	3.88%	0.00%
9	22.32%	0.39%	1.08%	0.18%
10	15.58%	0.00%	5.78%	2.42%

## 6.4 Profit Oriented

This is a profit oriented case, where the most relevant attribute is the economical and the robustness respectively, followed by the technical and environmental. The comparison of each attribute for this case, later used in the decision making, can be seen in Table 6.7. In the last column the coefficients for each criteria are shown.

**Table 6.7:** Profit oriented priorities

Criteria	Economical	Robustness	Environmental	Technical	Priority
Economical	1	2	6	5	0.5219
Robustness	1/2	1	4	3	0.2928
Environmental	1/6	1/4	1	1/2	0.0715
Technical	1/5	1/3	2	1	0.1137
				Cr	0,0114

The AHP results for the profit oriented case can be observed in Appendix A. A

summary of the results is presented in Figure 6.3, where the calculated priorities are plotted for all 10 plans. It can be seen that the plan with highest priority and therefore the most suitable for profit oriented approach is plan number 2 (PV + Wind turbine + Diesel + Battery). This plan has the lowest NPC of 444M\$, an initial investment of 233.66M\$, and an operating cost of 14.9M\$/yr. It has a renewable fraction of 91.95% and an excess electricity of 38.72%. The two other plans with high priority are plan number 3 and plan number 4. Both of them have similar characteristic to the selected plan number 2. This is: low NPC and high renewable fraction.

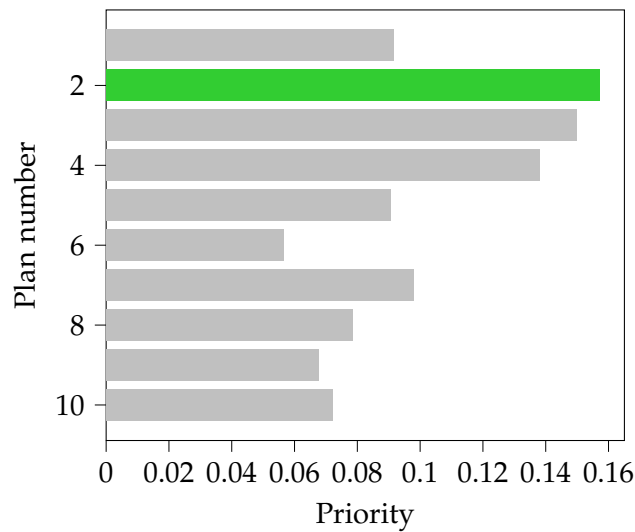


Figure 6.3: Priorities calculated for each of the considered plans in the profit oriented approach

## 6.5 Environmentally Friendly

In the environmentally friendly case, the most relevant attributes are the environmental and the technical respectively, followed by the economical and robustness. In Table 6.8 the pairwise comparison of each attribute and the final priority coefficient are shown.

Table 6.8: Environmentally Friendly Priorities

Criteria	Economical	Robustness	Environmental	Technical	Priority
Economical	1	2	1/4	1/3	0.1319
Robustness	1/2	1	1/5	1/2	0.0971
Environmental	4	5	1	2	0.5005
Technical	3	2	1/2	1	0.2706
				Cr	0,0352

The AHP results for the environmentally friendly case can be observed in Appendix A. A summary is presented on Figure 6.4. It can be seen that the plan with highest priority and therefore the most suitable plan for this case is plan number 2 (PV + Wind turbine + Diesel + Battery). This is the same as the best plan selected by the profit oriented approach. In this approach the second and third best plan are also chosen to be plan number 3 and plan number 4. The difference can be seen in the priorities of the remaining plans.

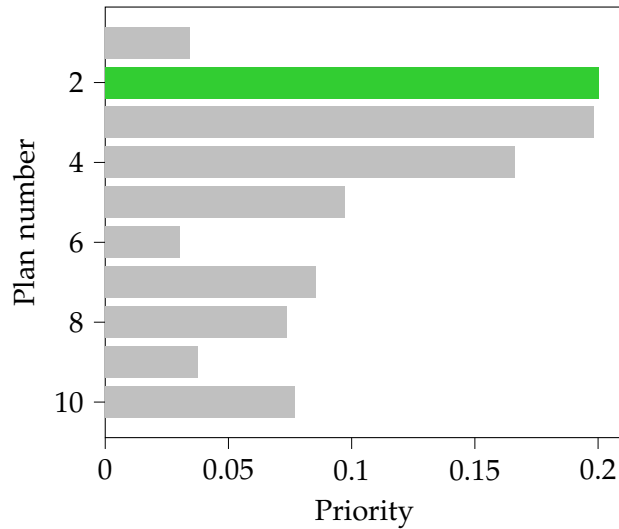


**Figure 6.4:** Priorities calculated for each of the considered plans in the environmentally friendly approach

## 6.6 Verification of AHP

Verification of AHP is one of the steps of the algorithmic approach, as mentioned in Chapter 6.2. The consistency of the result can be verified by calculating the consistency ratio as presented in Equation 6.3. It is calculated for the matrix of pairwise comparisons for each of the criteria and the categories. Its value is recommended to not exceed 10% [35] for the result to be trustworthy. The performed calculations proved that all the values satisfy the condition to be below 10% and therefore the calculations are considered to be reliable. The specific values are presented in Appendix A.4.



## Chapter 7

# Optimization of Operation

Having selected the plan to proceed with in the previous chapter, its hourly operation optimization can be performed. In order to do so, it is necessary to describe the system as a set of constraints and construct the objective function to be minimized. The focus of this project is to operate the system in a way to minimize the operation and maintenance cost over a 24 hour period. A risk-constraint optimization is used to minimize the cost under uncertainties in renewable resources and load profile of the mine. These will be accounted for using conditional value-at-risk (CVaR) method.

The flowchart of operation optimization is presented in Figure 7.1. The first step is to collect the necessary input data, which was described in Chapter 5. The next step is to incorporate the calculation methods of the components used in the system to the optimization problem. These were presented in Chapter 4. To perform the optimization the input of wind speed, PV power and load are needed. These are generated based on the measurements delivered by the industrial partner and with use of steps shown in Figure 7.1. Finally, the risk is incorporated into the optimization and the optimization model is solved.

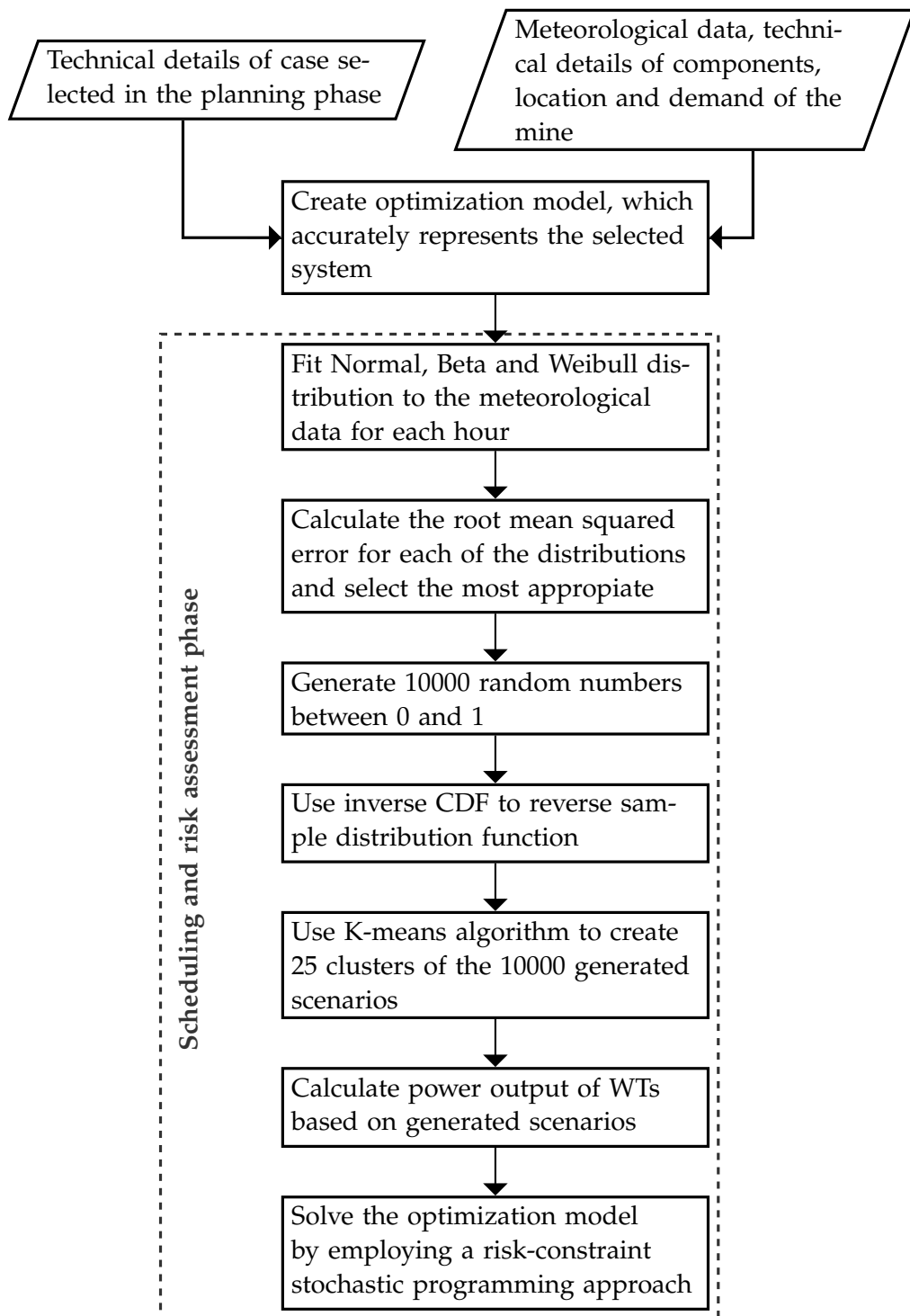


Figure 7.1: Flowchart of operation optimization

## 7.1 Evaluation of Uncertainties

For this project, data measured in 2019 is used for the planning and operating phase, since the renewable energy resources are volatile, uncertainty scenarios have been added to the optimization formulation to account for these. In this section, this study will be explained.

Three variables have been used for the evaluation of uncertainties, PV power, wind speed and load profile of the mine, since these are most likely to vary due to uncertainties. 10000 different cases for each stochastic variables have been generated, and then for computational reasons, this cases have been clustered to 25 that will be used in the optimization algorithm.

The method for generating all the cases from the measured data is the one described in [36]. The data obtained from the industrial partner for year 2019 is divided into 24 hours. For each hour, the empirical cumulative distribution function (CDF) is calculated. Then the CDF of three most used distributions, Normal, Beta and Weibull are obtained. The SciPy [17] library for python has been used for this process and the distribution functions are described in Appendix B. In Figure 7.2 the CDFs can be observed for a randomly selected hour.

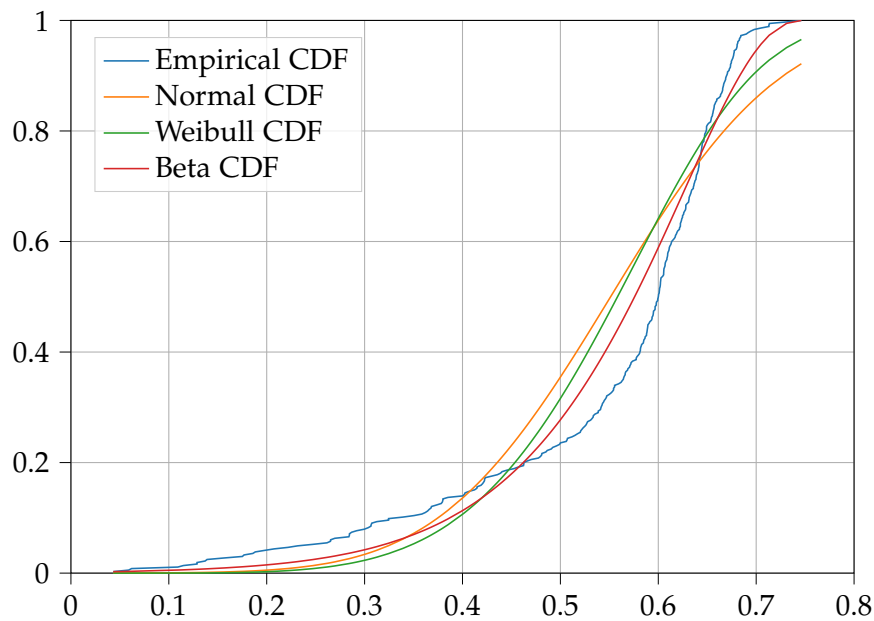


Figure 7.2: CDF comparison of empirical and selected distributions for hour 13:00

After obtaining the CDFs the root mean square error (RMSE) is calculated for each of them and the lowest error distribution is chosen as the best fit. The RMSE equation is shown in Equation 7.1.

$$RMSE = \sqrt{\frac{1}{Nh} \sum_{h=1}^{Nh} \cdot (CDF_{emp}^h - CDF_{sel}^h)^2} \quad (7.1)$$

where:

$Nh$  - number of hours

$CDF_{emp}^h$  - empirical CDF

$CDF_{sel}^h$  - selected CDF

Then 10000 random values between 0 and 1 are generated and the inverse CDF is used to find the values of those random numbers. This is done for every hour of the day for PV Power and for load, whereas for wind speed, since the data is every 10 minutes, 144 intervals are used for 1 day.

In Figure 7.3, the result of PV power for hour 13:00 can be observed for several MC simulations. It can be seen that for higher simulations the average of the generated cases are closer to the measured average of that hour for year 2019, 0.551 [kW]. 10000 MC simulations were done, because the computational time was acceptable and the results were accurate enough.

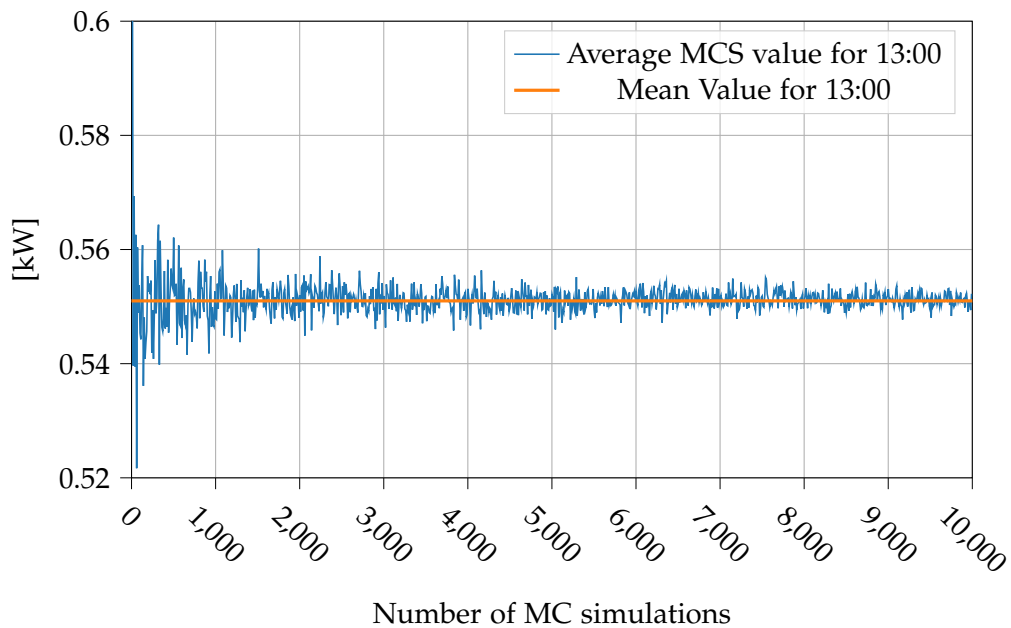


**Figure 7.3:** MC simulations convergence for hour 13:00

After generating all 10000 day cases for the stochastic variables, the cases are reduced to 25 using a case reduction algorithm. In this project K-means clustering

is used for the reduction, based on [15]. For K-means algorithm the library scikit-learn [18] for python has been used, this is described in Appendix C.

In Figures 7.4, 7.5 and 7.6 the 25 cases and the mean of the three stochastic variables are displayed.

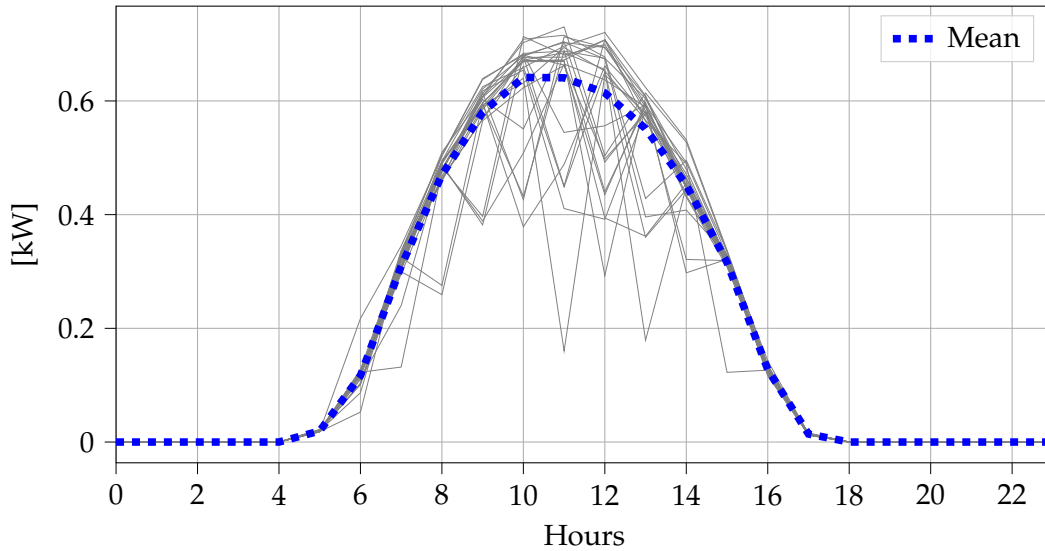


Figure 7.4: Solar cases

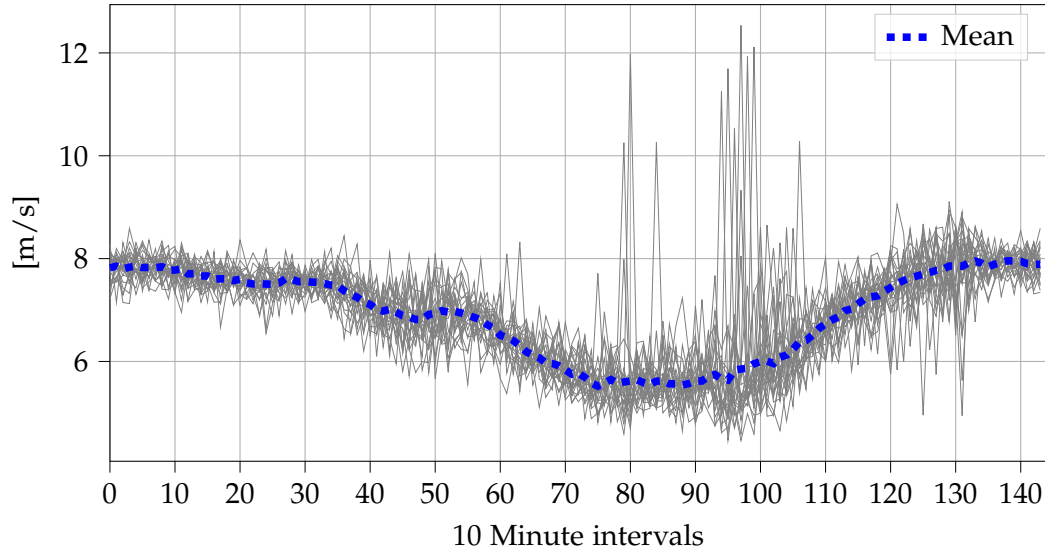


Figure 7.5: Wind cases

As mentioned before, the wind data obtained by the industrial partner is not measured hourly but every ten minutes, that is why the Figure 7.5 has 144 timesteps.

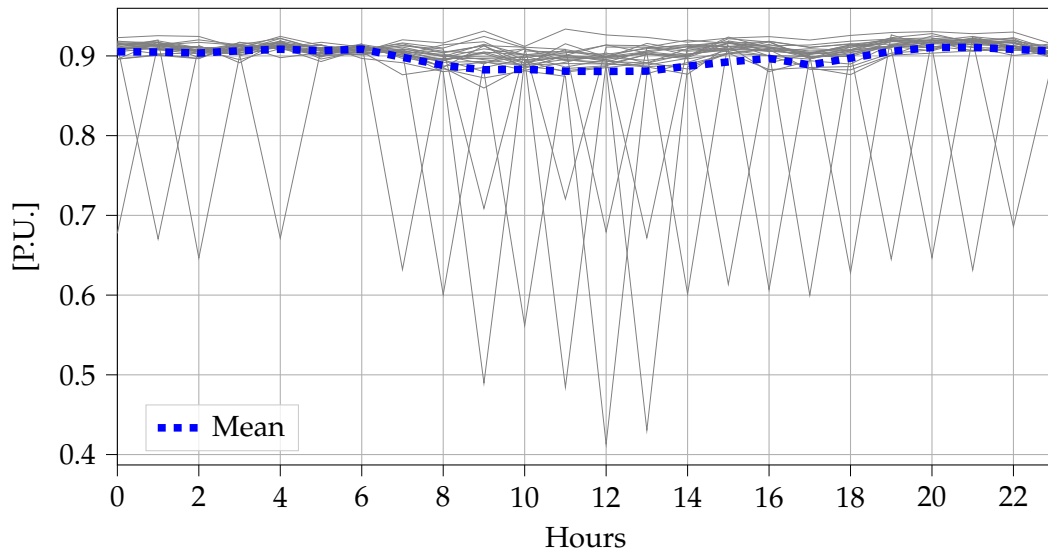


Figure 7.6: Load cases

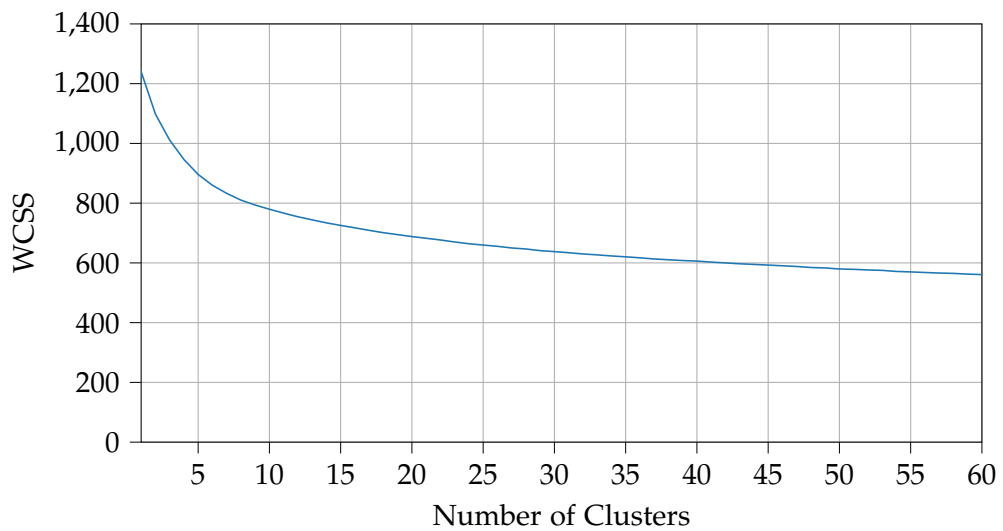


Figure 7.7: Elbow method for solar irradiance clusters

In Figure 7.6, it can be observed that in some of the generated cases the load spikes downwards. This is because in the data provided by the industrial partner, several days in the year the load is reduced to very low numbers, because of drill maintenance period where it is required to inch the drill at low speed. The load profile of the mine can be seen in Figure 5.1, where the maintenance of the drill was also mentioned.

For selecting the number of clusters in the K-means algorithm, a simple elbow

method was done. In Appendix C the within-cluster sum-of-squares (WCSS) is explained. For the elbow method the WCSS was calculated for clusters between 1 and 60. In Figures 7.7, 7.8 and 7.9, the results of the elbow method are shown, based on these results, the number of clusters (25) is chosen. This number is chosen because a larger amount of clusters will not have a considerable difference of WCSS, and will require larger computational power.

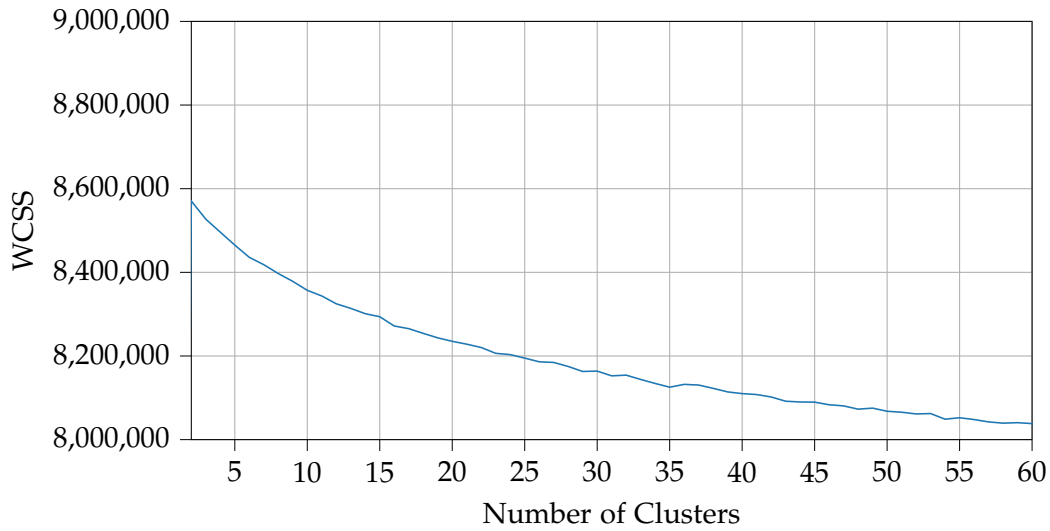


Figure 7.8: Elbow method for wind speed clusters

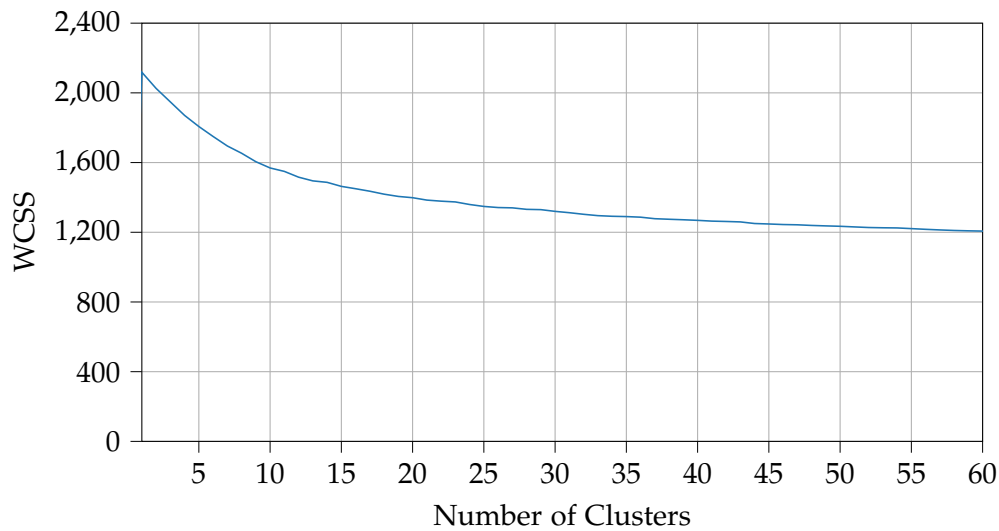


Figure 7.9: Elbow method for load clusters

## 7.2 Diesel Prediction

The lifetime of this mine is 25 years. Since in some cases the main cost of the daily operation of the mine is the fuel price, a study of the future of diesel prices needs to be done. For this study, past years data of diesel prices have been collected from The Department of Mines, Industry Regulation and Safety of Western Australia [27]. From this site, the monthly prices from January 2001 to December 2019 have been obtained, this data can be observed in Figure 7.10.



Figure 7.10: Diesel prices Western Australia 2001 - 2019

In Figure 7.10, an average increase of the prices for the past 19 years can be observed. With this data, a forecasting model has been developed using a simple Monte Carlo simulation based on [37]. First the logarithmic returns of the data have been calculated. Then, the mean, variance and standard deviation of the logarithmic returns are obtained. With these values the Monthly returns are calculated in Equation 7.2:

$$\text{MonthlyReturns} = \exp(\text{drift} + \sigma \cdot Z) \quad (7.2)$$

where:

$$\text{drift} = \mu - 0.5 \cdot \text{var}$$

*var* - variance

$\mu$  - mean

$\sigma$  - standard deviation

$Z$  - random number for each of the predicted steps

Since the historical data used is monthly, and the project lifetime is 25 years, 300 steps (months) have been predicted. Finally the last historical point is taken as the start point for the simulation, and the future price list is calculated in Equation 7.3:

$$\sum_{t=1}^{300} FuturePrices[t] = FuturePrices[t - 1] \cdot MonthlyReturns[t] \quad (7.3)$$

where:

*FuturePrices* - list of the forecasted prices

This has been executed 10000 times, the results can be observed in Figure 7.11, although only the first 25 out of 10000 simulations are shown due to plotting memory limits.

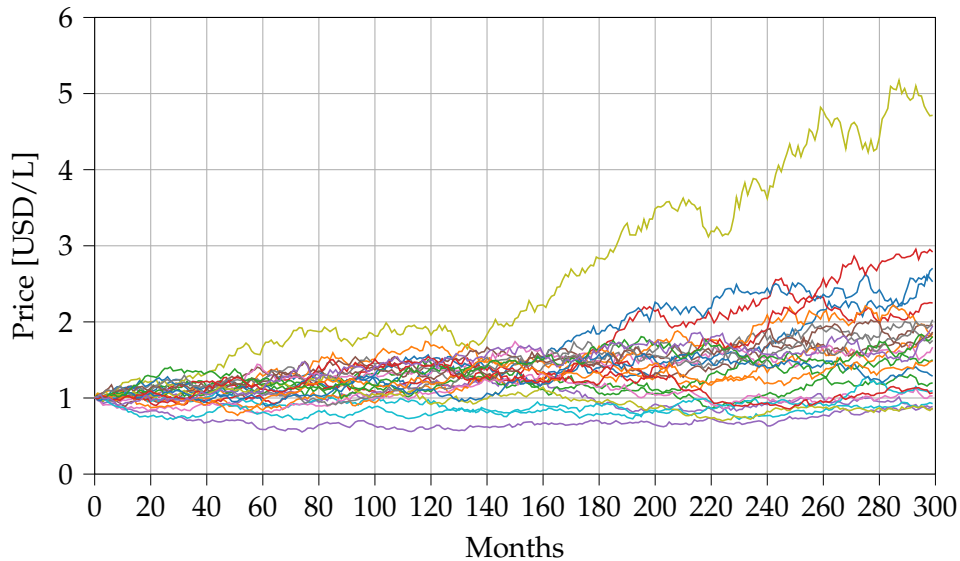


Figure 7.11: Monte Carlo simulations for future 300 months

Finally the average of all the Monte Carlo simulations have been obtained, and the yearly average has been calculated to obtain the predicted yearly diesel price values for the next 25 years. This values can be observed in Figure 7.12.

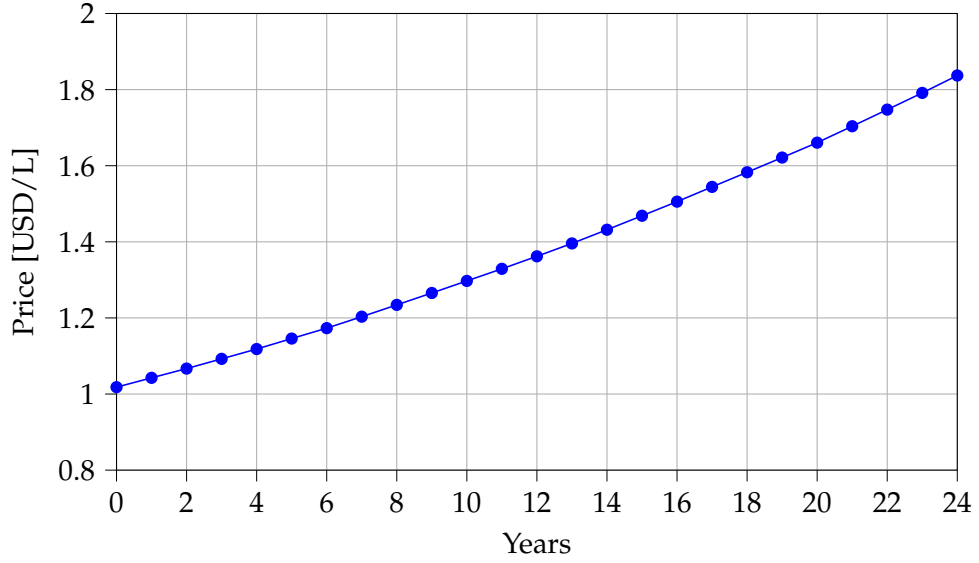


Figure 7.12: Diesel prediction for future 25 years

### 7.3 Incorporating Risk Management

Popular risk managing functions are value-at-risk (VaR) and conditional value-at-risk (CVaR). VaR is a measure which is widely used in industry regulations. It is, however, not well suited to work with cases where the losses are not normally distributed [38]. Moreover, it does not provide information on the extent of losses in the tail of the loss distribution. Therefore, it is incapable of distinguishing between situations where losses that are worse are only a little bit worse, and those where they are overwhelming. CVaR, on the other hand, accounts for the losses exceeding VaR. Hence, it provides adequate picture of risk reflected in extreme tails. A great advantage is that CVaR can be optimized and constrained with linear programming methods, whereas VaR is relatively difficult to optimize [39].

Having said that, CVaR measure was chosen for this study. For a discrete distribution and at given confidence level  $\alpha$  the equation for minimizing CVaR is formulated as follows [15] [16] [40]:

$$CVaR = \min(\zeta_t + \frac{1}{1-\alpha} \sum_{s=1}^{N_s} \pi_s \eta_{t,s}) \quad (7.4)$$

Subjected to:

$$\eta_{t,s} - cost_{t,s} + \zeta_t \geq 0 \quad (7.5)$$

$$\eta_{s,t} \geq 0 \quad (7.6)$$

Where:

$\alpha$  - confidence level

$\zeta_t$  - threshold to recognize  $(1-\alpha)\cdot 100$  percent worst scenarios of each stochastic environment at hour  $t$ . It equals to VaR, which means that  $(1-\alpha)\cdot 100$  costs in hour  $t$  are higher or equal to  $\zeta_t$

$cost_{t,s}$  - operational cost of scenario  $s$  in hour  $t$

$\eta_{t,s}$  - auxiliary non-negative variable, equal to the difference between  $cost_{t,s}$  and  $\zeta_t$  when the  $cost_{t,s}$  is higher than  $\zeta_t$ .

$\pi_s$  - probability of scenario  $s$

## 7.4 Formulation of Optimization

### 7.4.1 Variables

The first step of building a problem is to define the variables, which are going to be optimized. These are later used in the constraints and the objective function. Since the selected plan comprises of PV, WT, Diesel generator and Battery, the variables must be selected to accurately describe operation of each of these elements. They are defined for every hour of the optimization period ( $t$ ), as well as for each of the considered scenarios ( $s$ ) generated according to the algorithm described in Chapter 7.1. The variables are summarized and described in Table 7.1. The ones introduced in the previous section, used for calculation of CVaR, are not going to be presented again in this section.

The constants used for the limits are:

- $P_{max,d}$  - maximum output power of the diesel generator
- $P_{min,d}$  - minimum output power of the diesel generator
- $P_{max,bc}$  - maximum charging power of the battery
- $P_{max,bd}$  - maximum discharging power of the battery
- $SoC_{min}$  - minimum SoC of the battery
- $SoC_{max}$  - maximum SoC of the battery

**Table 7.1:** Variables used in the optimization

<b>Name</b>	<b>Type</b>	<b>Lower limit</b>	<b>Upper limit</b>	<b>Description</b>
$u_{d,t,s}$	Binary	-	-	Commitment status of the diesel generator
$P_{d,t,s}$	Continuous	$P_{min,d}$	$P_{max,d}$	Power output of the diesel generator
$y_{d,t,s}$	Binary	-	-	Start-up indicator of the diesel generator
$z_{d,t,s}$	Binary	-	-	Shutdown indicator of diesel generator
$l_{wt,t,s}$	Continuous	0	1	Enables part loading of the WTs
$l_{pv,t,s}$	Continuous	0	1	Enables part loading of the PVs
$B_{c,t,s}$	Continuous	0	$P_{max,bc}$	Charging power of the battery
$B_{d,t,s}$	Continuous	0	$P_{max,bd}$	Discharging power of the battery
$b_{c,t,s}$	Binary	-	-	Charging indicator of the battery
$b_{d,t,s}$	Binary	-	-	Discharging indicator of the battery
$SoC_{t,s}$	Continuous	$SoC_{min}$	$SoC_{max}$	State of charge of the battery

The variables  $l_{wt,t,s}$  and  $l_{pv,t,s}$  are introduced to the system in order to enable part loading of the WTs and PV. Considering the units to be able to reduce the output power is advantageous when building the equality constraint for satisfying the demand. In island operation of the system the renewable energy sources should be able to part load in order to not exceed the demand. The part loading of WTs can be achieved by introducing active power control. Examples of two possible approaches were presented in [41] and these are: pitch control and torque control. The active power output of PV can be reduced by modifying the maximum power point tracking algorithm, as presented in [42]. If these variables are not introduced the constraint can only be defined as inequality constraint where the power output of the mine must be greater or equal to the demand. This approach can be valuable when the advantages of grid connection are considered and the surplus electricity production can be fed into the grid.

An additional clarification may be needed to explain the used binary variables:

$u_{d,t,s}$ ,  $y_{d,t,s}$ ,  $z_{d,t,s}$ ,  $b_{c,t,s}$  and  $b_{d,t,s}$ . The first three are used to define the state of operation of the diesel generator.  $u_{d,t,s}$  specifies if the unit is in operation, this information is valuable to calculate costs of operation associated with the number of hours of in operation.  $y_{d,t,s}$  and  $z_{d,t,s}$  specify if the unit started or stopped the production in this hour. Having these enables to define the minimum on and off time of the unit, as well as specifying starting costs. The last binary variables are associated with the operation of the battery.  $b_{c,t,s}$  specifies if the battery is charging in this hour and  $b_{d,t,s}$  whether it is discharging. These variables are introduced to prohibit simultaneous charging and discharging of the battery.

### 7.4.2 Constraints

The constraints can be divided into two main categories: the bounds of variables and the additional ones, which describe the operation of the system. The bounds are defined in Table 7.1 and are the upper and lower limit that the variable can reach. The binary variables do not have any bounds specified, as they can only take two values: 0 or 1. Once the variables are defined, it is possible to describe the selected system with a set of constraints. This must be done accurately in order to represent the real operation of the system. The two main constraints are: the equality of supply and demand in the mine and stored energy balance. All the constraints, describing the operation of the system, are summarized in Table 7.2. The formulation is done for every hour of the optimization period  $t$  in each of the considered scenarios  $s$ , as presented in the first column of the table. The terms other than variables used in the formulation are:

- $P_{pv,t,s}$  - calculated PV power in hour  $t$  and scenario  $s$
- $P_{wt,t,s}$  - calculated power output of all installed WTs in hour  $t$  and scenario  $s$
- $D_{t,s}$  - demand to satisfy in hour  $t$  and scenario  $s$
- $eff$  - round trip efficiency of charging and discharging of the battery
- $S_{max}$  - maximum possible storage content
- $SoC_{init}$  - initial SoC of the battery
- $UT_d$  - minimum up time of the diesel generator
- $DT_d$  - minimum down time of the diesel generator

**Table 7.2:** Constraints to define the operation of the plant

Constraint	Description
$D_{t,s} = l_{wt,t,s} \cdot P_{wt,t,s} + l_{pv,t,s} \cdot P_{pv,t,s} + P_{d,t,s} + B_{d,t,s} - B_{c,t,s} \quad (7.7)$	Equality of supply and demand
$SoC_{t,s} + B_{c,t,s} \cdot \frac{\sqrt{eff}}{S_{max}} - \frac{B_{d,t,s}}{\sqrt{eff} \cdot S_{max}} = SoC_{t+1,s} \quad (7.8)$	Stored energy balance
$u_{d,t,s} \geq \frac{P_{d,t,s}}{P_{max,d}} \quad (7.9)$	Defining the state of operation of the diesel
$u_{d,t+1,s} - u_{d,t,s} = y_{d,t+1,s} - z_{d,t+1,s} \quad (7.10)$	Defining the start and stop of the diesel
$y_{d,t+1,s} + z_{d,t+1,s} \leq 1 \quad (7.11)$	No simultaneous start and stop of diesel generator
$b_{c,t,s} \geq \frac{B_{c,t,s}}{P_{max,bc}} \quad (7.12)$	Defining the charging indicator
$b_{d,t,s} \geq \frac{B_{d,t,s}}{P_{max,bd}} \quad (7.13)$	Defining the discharging indicator
$b_{d,t,s} + b_{c,t,s} \leq 1 \quad (7.14)$	No simultaneous charging and discharging
$UT_d \cdot y_{d,t,s} \leq \sum_{h=t}^{t+UT_d-1} u_{d,h,s} \quad (7.15)$	Defining minimum up time of diesel
$\sum_{h=t}^{t+DT_d-2,s} z_{d,h,s} \leq 1 - u_{d,t+DT_d-1,s} \quad (7.16)$	Defining minimum down time
$SoC_{0,s} = SoC_{init,s} \quad (7.17)$	Initial storage constraint

The listed constraints can be altered to represent a different configuration of the system. The minimum up and down time of the diesel generator was introduced in order to avoid frequent switching on and off of the unit. These can be set to any desired value or removed if it is not considered an issue.

According to [43] the ramping rate of internal combustion engines is equal to around 25% of full load per minute. Since the time step considered in the optimization is 1 hour, the ramping effect does not need to be considered. However, if the lower ramping rate is advised, in order of hours, this can be taken into account by introducing an additional constraint:

$$(P_{d,t} - P_{d,t+1})^2 \leq RampingRate^2$$

In the constraint the absolute value of the difference between the previous and current load cannot be higher than the selected ramping rate.

### 7.4.3 Objective Function

The final step of defining the optimization problem is the formulation of the objective function to minimize. As mentioned previously, this is the cost of operation and maintenance of the plant in an uncertain environment. It comprises of cost of fuel and operation and maintenance of all of the components. To account for the uncertainties weighted CVaR value of cost is added to the optimization problem through risk aversion factor  $\beta$ .

The fuel cost is defined with Equation 7.18, where it depends linearly on the diesel generator load but an offset is introduced. The linear coefficient, which defines the relationship between the used fuel in  $l/h$  and the output power in  $MW$  is equal to 0.244 and is retrieved from generator data in HOMER Pro. The operation and maintenance cost of the diesel generator depends on the number of hours in operation and is expressed with Equation 7.20. If additional cost associated with the start of diesel generator should be considered it can be done by adding Equation 7.19 to the objective function. The O&M cost of PV, and part of O&M costs of WTs and battery, are fixed yearly values, which only depend on the installed power of technologies, and are defined with Equation 7.21. The remaining O&M costs of WTs and battery are associated with the amount of generated energy and energy throughput respectively and are expressed with Equation 7.22. Having all of the cost components defined, the operation cost of a scenario  $cost_s$  can be defined as a sum of all above as in Equation 7.24. The parameters used in the objective function are:

- $F_{min,d}$  - minimal fuel consumption of diesel [l]
- $SU_d$  - start-up cost of the diesel generator [\$/start]

- $OM_d$  - operation and maintenance cost of the diesel generator [\$/h]
- $OM_{wt,y}$  - yearly operation and maintenance cost of the wind turbines [\$/kW]
- $OM_{pv,y}$  - yearly operation and maintenance cost of the PVs [\$/kW]
- $OM_{b,y}$  - yearly operation and maintenance cost of the battery [\$/nr of batteries]
- $OM_{wt,e}$  - operation and maintenance cost of the wind turbines, dependent on the amount of generated energy [\$/kWh]
- $OM_{b,e}$  - operation and maintenance cost of the wind turbines, dependent on the throughput energy [\$/kWh]
- $I_{wt}$  - installed power of wind turbines [kW]
- $I_{pv}$  - installed power of PVs
- $I_b$  - number of installed batteries
- $T$  - considered optimization period expressed in hours, in this project selected to be 24 hours

$$\sum_t^T (u_{d,t,s} \cdot F_{min,d} + P_{d,t,s} \cdot 0.244) \cdot DP \quad (7.18)$$

$$\sum_t^T (y_{d,t,s} \cdot SU_d) \quad (7.19)$$

$$\sum_t^T (u_{d,t,s} \cdot OM_d \cdot P_{max,d}) \quad (7.20)$$

$$(OM_{wt,y} \cdot I_{wt} + OM_{pv,y} \cdot I_{pv} + OM_{b,y} \cdot I_b) \cdot \frac{T}{8760} \quad (7.21)$$

$$\sum_t^T (I_{wt,t} \cdot P_{wt,t,s} \cdot OM_{wt,e} + \frac{B_{c,t,s} + B_{d,t,s}}{2} \cdot OM_{b,e}) \quad (7.22)$$

$$cost_s = Equation7.18 + Equation7.20 + Equation7.19 + Equation7.21 \quad (7.23)$$

Finally, after defining the cost per scenario the objective function to minimize can be expressed with Equation 7.24. The second part of the equation incorporates the risk measurement CVaR to the objective function through the risk aversion factor  $\beta$ .

$$\text{Min} \sum_{s=1}^{N_s} \pi_s \cdot \text{cost}_s + \beta \cdot \text{CVaR} \quad (7.24)$$



# Chapter 8

## Results

This chapter represents the results of optimization described in the previous chapter. The optimization problem is a linear problem with binary decision variables. Therefore a Mixed Integer Linear Programming (MILP) solver was used. The chosen solver is Gurobi [44] and the problem is defined using PuLP open-source package in Python programming language [45].

The operation was optimized for Plan 2 and Plan 7 described in Chapter 6. The former was selected in the decision making process based on AHP and is considered to be the best Plan for the mining site. Plan 7 is added to the analysis to represent the influence of diesel prices on the expected cost of operation. Due to lower power installed in renewable energy sources, the diesel engine is used more frequently. Hence, the impact of diesel prices prediction over the 25 years of mine lifetime can be analyzed. Moreover, Plan 7 has a significantly lower initial investment compared to Plan 2, what may be an important factor for the mining operator. Finally, it was ranked as the 5<sup>th</sup> best plan in both Environmentally friendly and Profit oriented approach for AHP. The better plans were similar to the analyzed Plan 2 in terms of initial investment and renewable fraction. One exception is Plan 1, which came before Plan 7 in the case of Profit oriented approach. However, since it considers only diesel generator, it does not comply with the aim of the project to establish an off-grid hybrid renewable solution.

### 8.1 Results of Optimization - Plan 2

Plan 2 was selected in the decision making stage, in Chapter 6, to be the one that suits all the decision criteria best. The configuration of the used technologies in Plan 2 is:

- 97 MW of installed PVs

- 101.5 MW of installed WTs
- 55 MW of installed diesel generators
- 64.4 MWh of installed battery

The optimization problem, formulated in the previous chapter, was adjusted to accurately represent the selected plan. The optimization was done for 25 different cases of PV power, wind speed and load, generated with use of MCS and with confidence level ( $\alpha$ ) of 95%. Moreover, 10 different levels of risk aversion factor ( $\beta$ ) were considered to observe how the level of risk, incorporated in the optimization, affects the expected profit and CVaR.

### 8.1.1 Risk Assessment in Plan 2

The operator of the mine is interested to get a deep insight into the expected cost of operation as well as the one in the worst possible scenario. The latter, considering the possibilities of uncertainties, may have a great influence on the final result. The risk is incorporated to the optimization by the risk aversion factor  $\beta$ . The value of  $\beta$  varies from 0.1 to 10. The former represents near-zero risk aversion and with increase of beta the risk aversion increases.

The expected cost of operation of the mine for 24 hours period and different levels of risk aversion factor ( $\beta$ ) is shown in Figure 8.1. With the increase of  $\beta$  the operating cost of the mine increases. The difference between the lowest cost (for  $\beta = 0.1$ ) and the highest cost (for  $\beta = 10$ ) is around 0.26%.

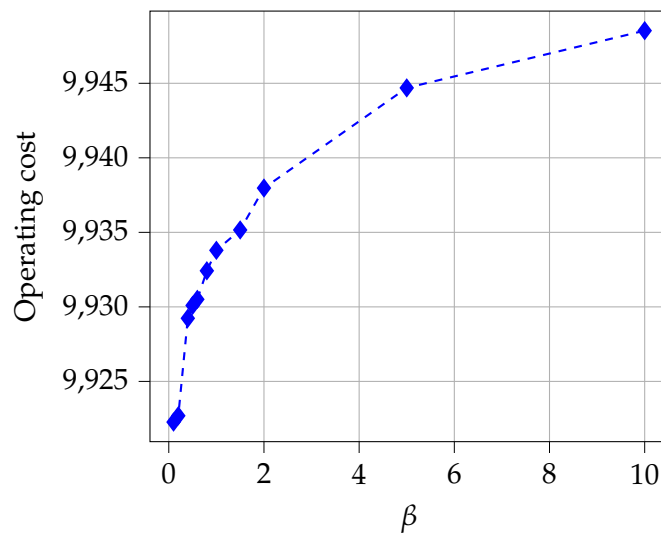


Figure 8.1: Expected cost versus  $\beta$ , Plan 2

Figure 8.2 represents the effect of increasing  $\beta$  on the conditional value at risk. The tendency is opposite to the one observed for the cost of operation. With the increase of  $\beta$  the CVaR value decreases and the difference between the extreme values is around 0.40%.

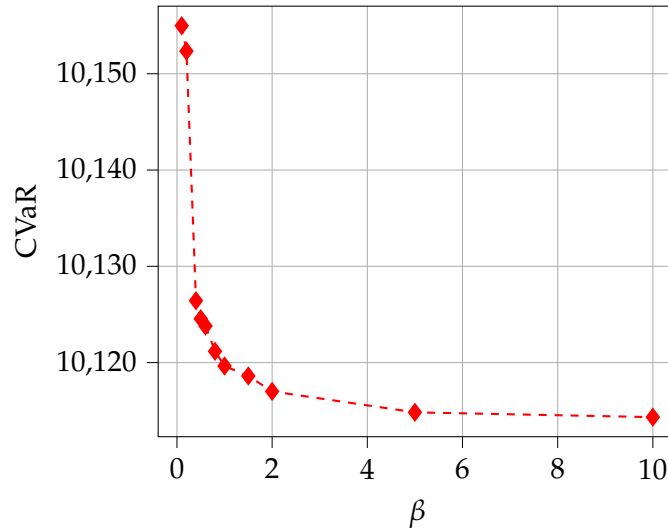
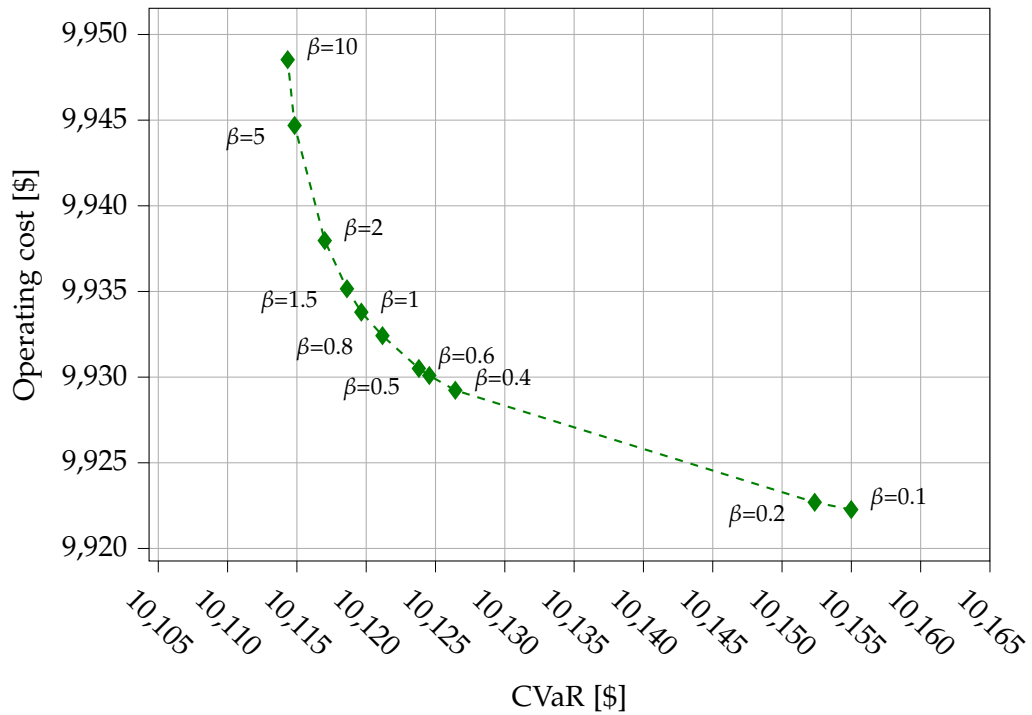


Figure 8.2: CVaR versus  $\beta$ , Plan 2

The final comparison shows the dependency between the expected cost of operation and the CVaR for different levels of risk aversion factor. This is presented in Figure 8.3. As stated previously, with the increase of  $\beta$  CVaR is reduced and the cost increases. Change of  $\beta$  from 0.1 to 0.4 has significant influence on both variables. However, the change of  $\beta$  from 2 to 10 increases the expected cost without decreasing the CVaR value significantly. The CVaR for  $\beta=0.1$  is 102.3% of the expected operating cost. When  $\beta=10$  is considered, CVaR is 101.7% of the expected cost.

All things considered, the variation of operation cost and CVaR are not of high magnitude due to rather low variable operation costs of renewable energy sources.

The expected cost was calculated based on the optimization problem presented in Chapter 7. The arising question is if the optimization reduces the cost when compared to a simple algorithm for operation of the battery and diesel generator. The simple operation assumed for this project is that the battery is always charged by RES if the production from RES is higher than the demand and the SoC of the battery is lower than 100%. If the production from RES is lower than the demand the battery is discharged to supply the needed power. In case it is not possible to cover the demand by discharging the battery, the diesel generator is used. This simple algorithm is referred to as base case, and is close to the optimized operation, however, it does not take into account the level of O&M cost of the components.



**Figure 8.3:** Expected cost versus CVaR for different values of  $\beta$ , Plan 2

**Table 8.1:** Cost of operation calculated for Plan 2

Approach	Cost of operation
Optimization with $\beta = 0.1$	9922 \$
Optimization with $\beta = 10$	9949 \$
Base case	10076 \$
Diesel generator only	325464 \$

The costs calculated for one of the scenarios, in optimal cases and base case, are represented in Table 8.1. The optimized cost, calculated for  $\beta = 0.1$ , is 1.5% lower than the cost in the base case. Even when the high level of risk is considered in the optimization, the cost is still 1.3% lower than the base case.

Finally, the cost of operation of Plan 2 can be compared to the O&M cost if only diesel generator is used to satisfy the demand of the mine. This cost is listed in Table 8.1 and is around 33 times higher, for this typical day, than the cost in Plan 2. That proves that the selected plan could not only provide a reliable power generation, but also very low daily operating cost.

### 8.1.2 Hourly Operation of Plan 2

This section represents the hourly dispatch of the units to satisfy the demand of the mine. The simulations were performed jointly for all 25 scenarios to account for CVaR in the optimization. An example of hourly dispatch for one of the scenarios is presented in this chapter. The aim is to show the optimal dispatch of the units during the day and compare the optimized operation with low level and high levels of risk aversion factor. The hourly dispatch for the day is plotted for  $\beta$  equal to 0.1 and 10.

Figure 8.4 represents the optimized hourly operation of the power generating units - PVs, WTs and diesel generator. The difference between  $\beta = 0.1$  and  $\beta = 10$  is mainly in the operation of PV modules, which are allowed to generate more power in the peak during the middle of the day. For the low risk level the PV output power is lower. The additional power, generated in high risk level, is used to charge the battery. This behaviour is presented in Figure 8.5 where it can be seen that the battery is charged and discharged more frequently and with higher power for  $\beta = 10$ . For the representation of SoC hourly optimized values, additional  $\beta$  value of 1 was introduced. It was done to show the dependency of SoC on the level of risk incorporated to the optimization. Moreover, the SoC calculated in the base case was included. Looking at the Figure 8.6, the battery is reaching higher SoC when the risk aversion factor increases. The same observation can be made for the average SoC, presented in Table 8.2. With the increase of  $\beta$  value the average SoC of the battery increases. This is because of the uncertainties, which are incorporated to higher extend into the optimization. Keeping the battery charged throughout the operation assures a better resilience to unexpected changes. The behaviour proves that the CVaR method, presented in this project, works correctly. The SoC calculated in the base case differs significantly from the one obtained in the optimal case. The battery is kept fully charged throughout the day, even though it is not needed for operation of the mine. Operating the battery with this naive approach increases the O&M cost of the mine.

**Table 8.2:** Average state of charge of the battery for one of the generated MCS, with different values of  $\beta$ , Plan 2

$\beta$	Average SoC
0.1	32.4%
1	37.5%
10	40.2%

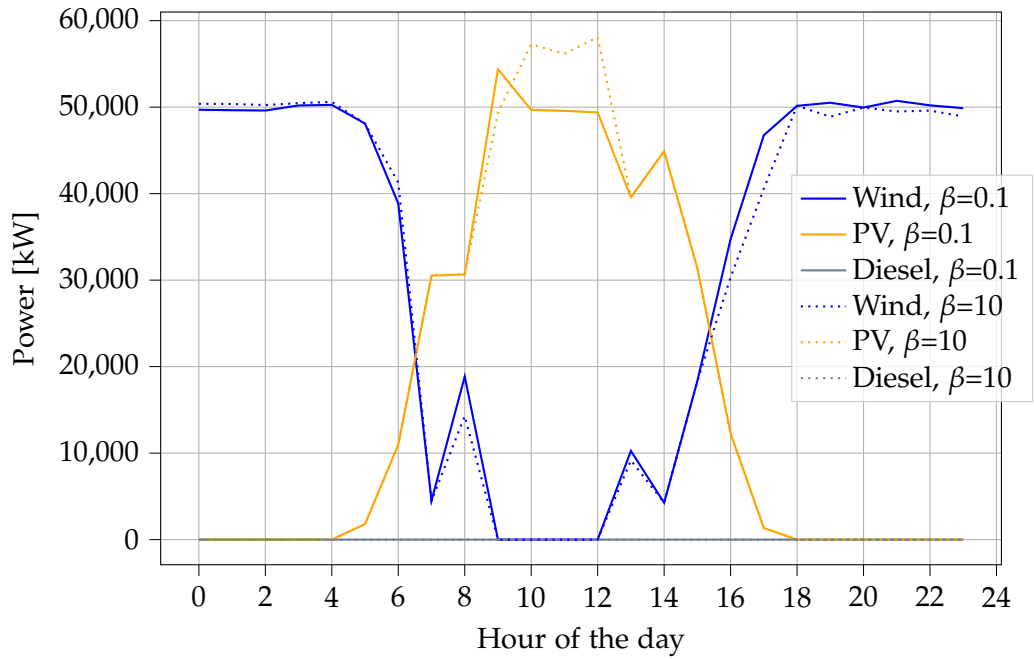


**Figure 8.4:** Hourly, power output of WTs, PVs and Diesel generator, for one of the generated MCS, with two values of  $\beta$ , Plan 2

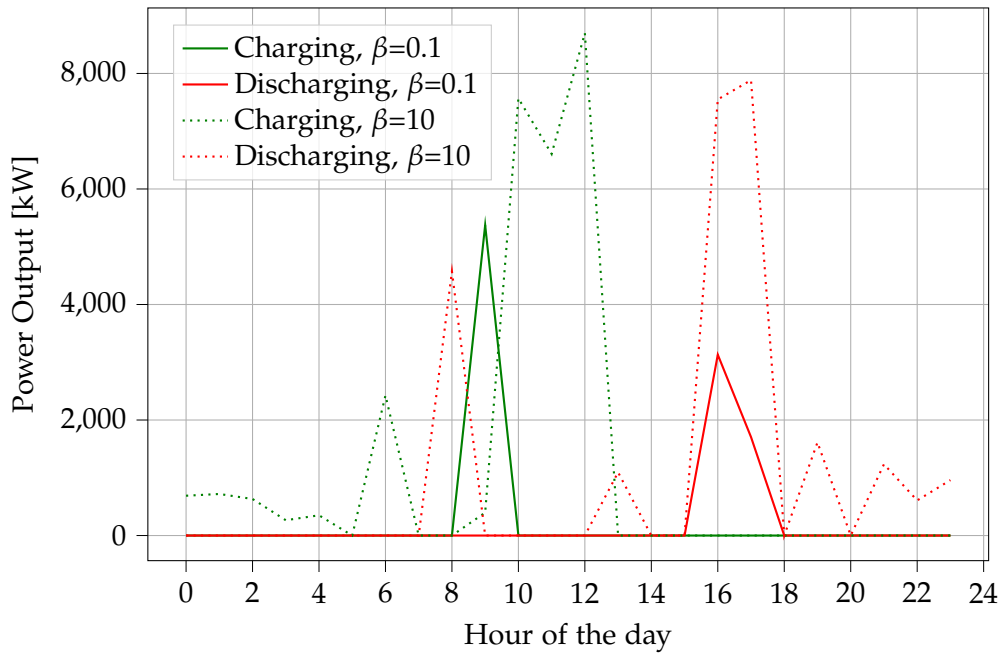


**Figure 8.5:** Hourly battery charging at discharging power, for one of the generated MCS, with two values of  $\beta$ , Plan 2

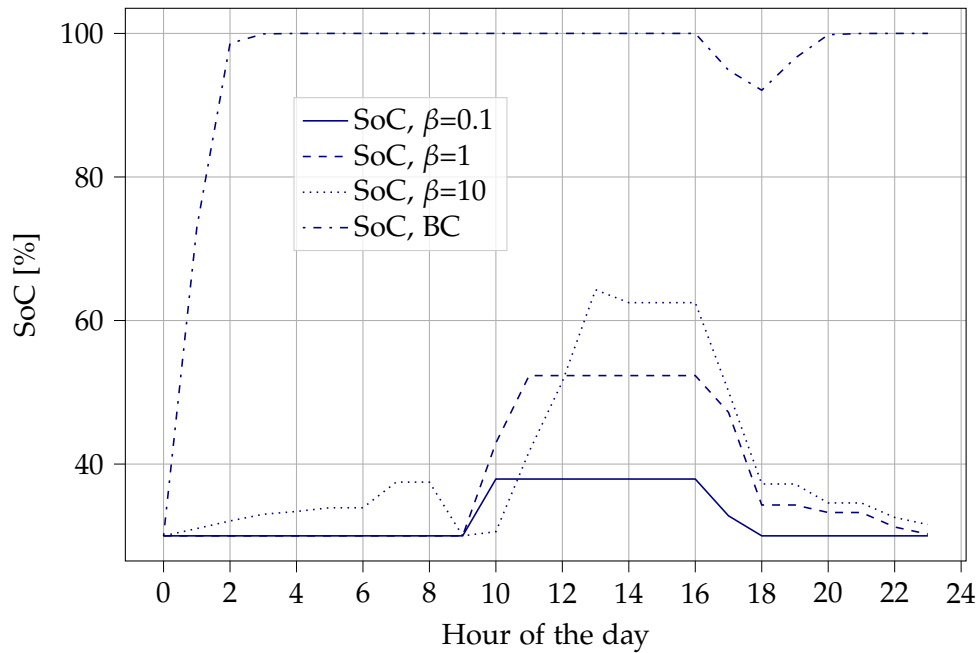


**Figure 8.6:** Hourly state of charge of the battery, for one of the generated MCS, for optimized operation with three values of  $\beta$  and base case (BC), Plan 2

## 8.2 Results of Optimization - Plan 7

Plan 7 was selected as an alternative to Plan 2 with lower initial investment. It is also used to show the influence of diesel prices changes over the 25 years of mine lifetime. The configuration of the used technologies in Plan 7 is:

- 60 MW of installed PVs
- 63 MW of installed WTs
- 55 MW of installed diesel generators
- 38.6 MWh of installed battery

The optimization problem, formulated in Chapter 7 was adjusted to accurately represent the selected plan. The optimization was performed similarly to the optimization of Plan 2. It was done for 25 different cases of PV power, wind speed and load, generated with use of MCS and with confidence level ( $\alpha$ ) of 95%. Moreover, 11 different levels of risk aversion factor ( $\beta$ ) were considered to observe how the level of risk, incorporated in the optimization, affects the expected profit and CVaR.

### 8.2.1 Risk Assessment in Plan 7

The risk is incorporated into optimization by the risk aversion factor  $\beta$ . For Plan 7, the value of  $\beta$  varies from 0.01 to 300. The range is bigger than in the case of Plan 2 because significant changes in expected operating cost were still observed for higher  $\beta$  values.

The dependency between expected cost of operation and the CVaR for different levels of risk aversion factor is represented on Figure 8.7. With the increase of  $\beta$  CVaR is reduced and the expected cost increases. A significant decrease in CVaR value is already observed when the value of risk aversion factor is changed from 0.01 to 0.1 and to 0.5. At the same time the expected operating cost does not increase significantly. When the  $\beta$  value is further increased up to 300, the CVaR does not decrease, whereas the expected cost raises at high rate. The difference between minimal cost (for  $\beta = 0.01$ ) and maximal cost (for  $\beta = 300$ ) is around 5.47%. The difference in maximal and minimal CVaR for the same range of beta is around 7.23%.

The operating cost calculated in the optimization is significantly lower than in the previously described base case. With the naive operation of the units the cost is around 22% higher than in the optimal case with lowest risk aversion factor.

One more important remark is that the expected operation cost of Plan 7, over one day of operation, is significantly higher than the one calculated for Plan 2. The expected cost for the same risk aversion factor  $\beta = 0.1$  is 43042\$ for Plan 7 and only 9922\$ for Plan 2, meaning that it increases about 4 times. This is caused by high cost of operation of diesel generator.

**Table 8.3:** Cost of operation in one of the scenarios for Plan 7

Approach	Cost of operation
Optimization with $\beta = 0.01$	43042 \$
Optimization with $\beta = 300$	45396 \$
Base case	52575 \$
Diesel generator only	325464 \$

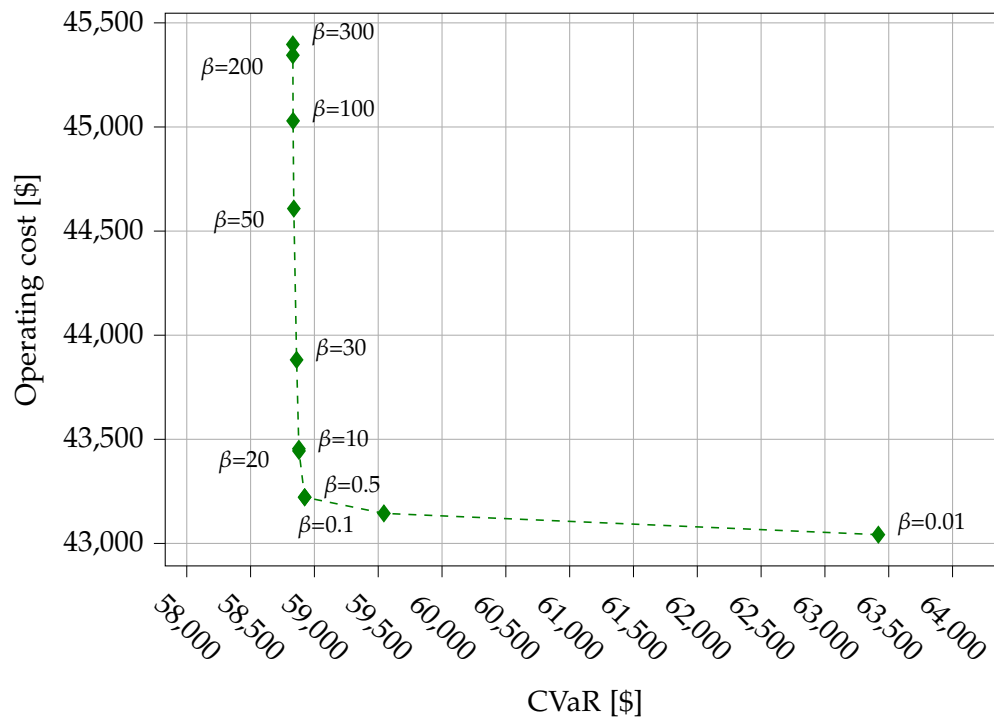
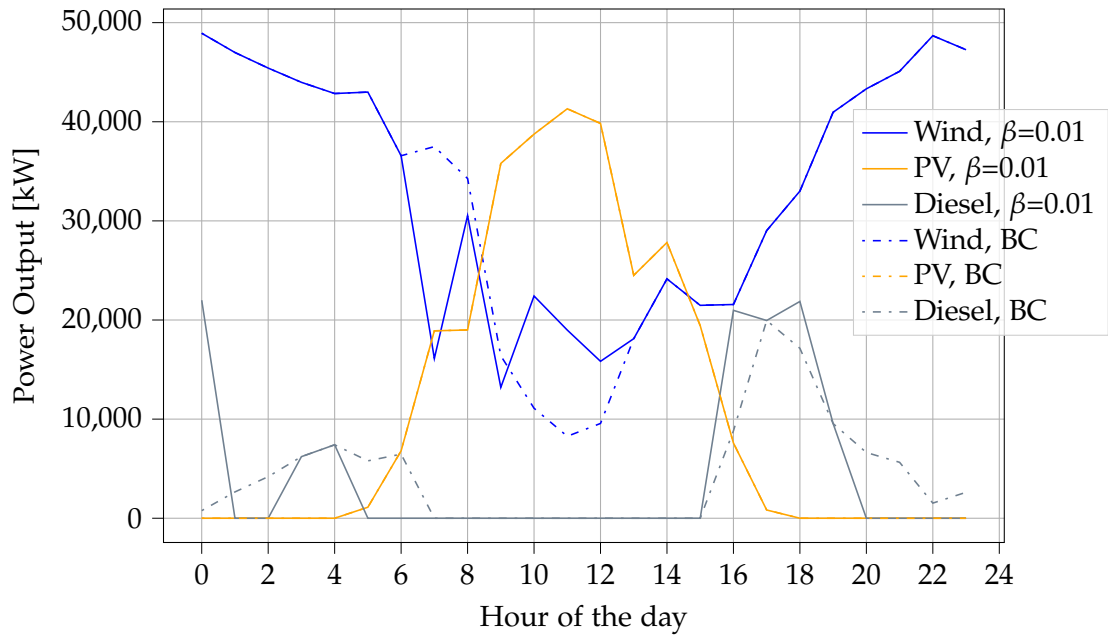


Figure 8.7: Expected cost versus CVaR for different values of  $\beta$ , Plan 7

### 8.2.2 Hourly Operation in Plan 7

This section represents the hourly dispatch of the units to satisfy the demand of the mine. The simulations were performed jointly for all 25 scenarios generated with MC simulation to account for CVaR in the optimization. In this section, an example of hourly dispatch of the units for one of the scenarios is presented. The optimized operation is plotted for the lowest ( $\beta = 0.01$ ) and is compared with operation calculated in the base case. When Plan 7 is considered, the difference between the optimized operation and the base case is more visible than for plan 2.

The hourly dispatch of the units, for optimized operation and the base case, is presented in Figure 8.8. The main difference is that the diesel generator is kept turned on during more hours throughout the day in the naive dispatch. Moreover, in the hours when the diesel generator is turned on in both optimized and simple operation, the output power of the diesel is lower or equal in the base case. However, the optimized operation uses the battery more, as can be seen in 8.9. This behaviour enables to turn on the generator less frequently but with higher output power. The advantage of this behaviour is that the diesel generator is operated with higher efficiencies. This results in lower operation cost for the optimized operation, as mentioned in previous section.



**Figure 8.8:** Hourly power output of WTs, PVs and Diesel generator for one of the generated MCS, result of optimization with  $\beta = 0.01$  and operation in the base case, Plan 7

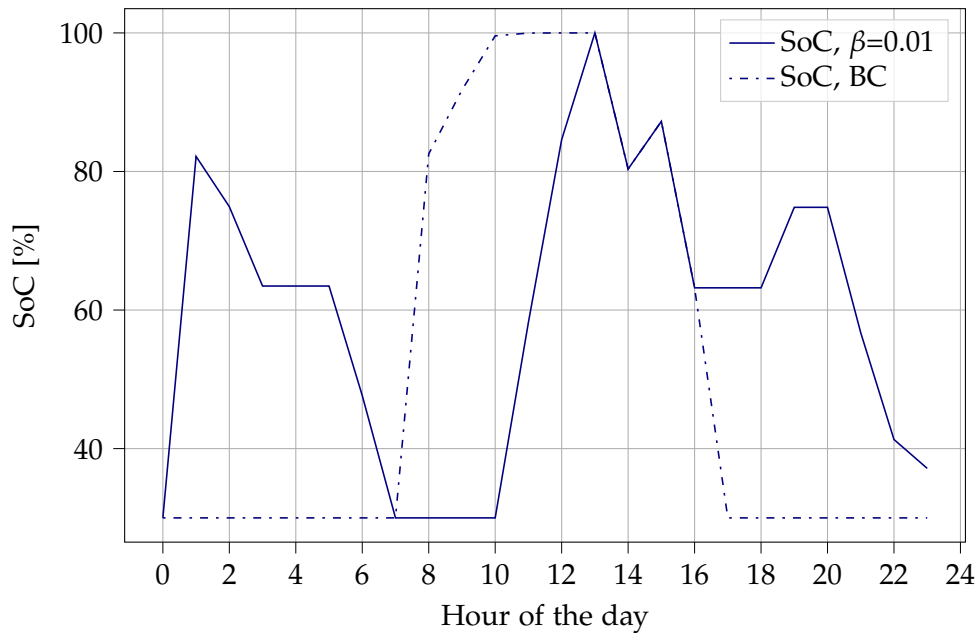


**Figure 8.9:** Hourly state of charge of the battery for one of the generated MCS, result of optimization with  $\beta = 0.01$  and operation in the base case, Plan 7

### 8.2.3 Influence of Changing Diesel Prices in Plan 7

The main reason for introducing Plan 7 in the analysis is to observe the influence of diesel prices expected in the planning period on the cost of operation. This cannot be done in Plan 2, which mostly operates only on renewable energy sources.

The optimization of Plan 7, described previously, was performed 25 times to reflect the change in diesel price over the 25 years of mine operation. The predicted values of diesel price are represented in Figure 7.12.

The influence of diesel prices on the expected operating cost for different  $\beta$  values can be seen on Figure 8.10. With the increase of diesel prices over the years the expected operating cost increases. However, the shape of the dependency between the expected operating cost and  $\beta$  remains the same. This is caused by the fact that the uncertainties in PV power, wind speed and load are considered the same for each of the 25 years of operation.

CVaR is also expected to increase with the increase of diesel prices over the years. This can be seen on Figure 8.10, which represent the relationship between CVaR and  $\beta$  for six years of operation. The graph only takes into account three lowest values of  $\beta$  because no significant variations in CVaR are observed for higher risk aversion factors.

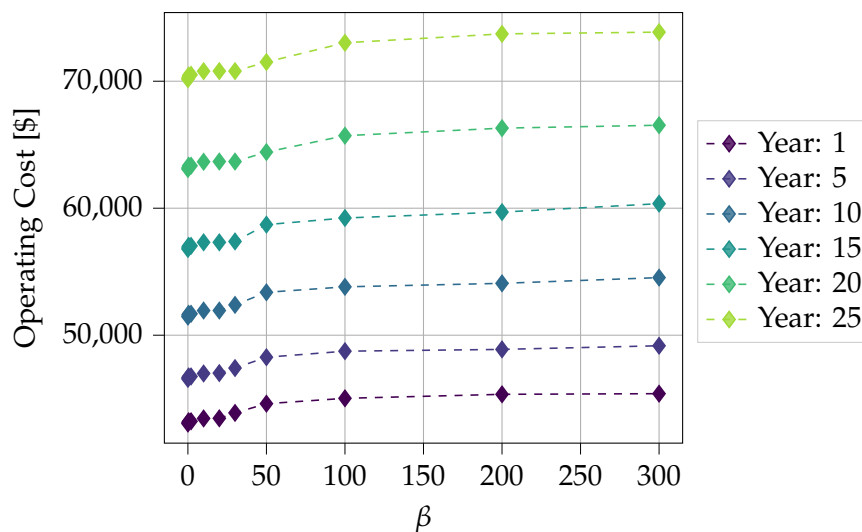


Figure 8.10: Expected cost versus  $\beta$  plotted for different years of operation, Plan 7

The influence of diesel prices expected over the years of operation can be seen on Figures 8.12 and 8.13. These represent the expected operation cost and CVaR respectively. The values are plotted for two values of risk aversion factor:  $\beta = 0.01$  and  $\beta = 300$ . Again, the increasing trend of operating cost and CVaR over the years can be seen. This is expected, since the predicted diesel prices are also increasing.

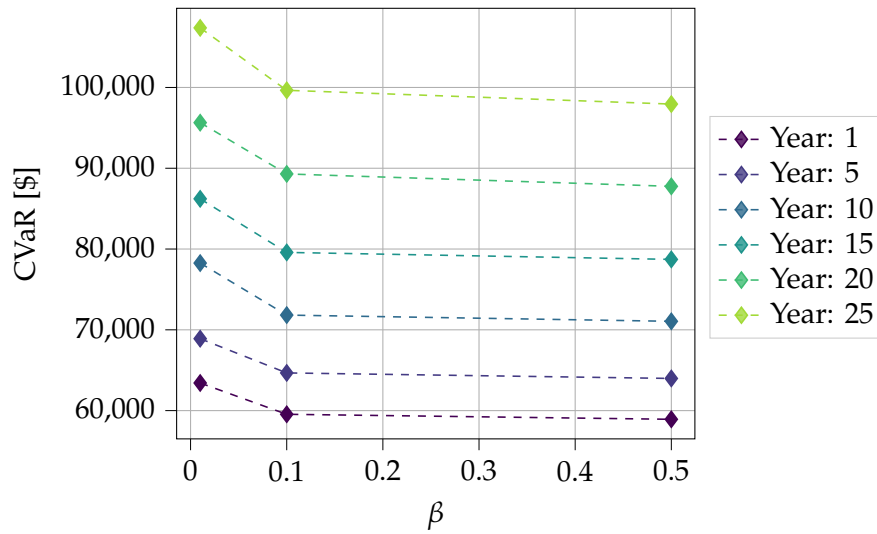


Figure 8.11: CVaR versus  $\beta$  plotted for different years of operation, Plan 7

The increase in operating cost from the first to the last year of operation for  $\beta = 0.01$  is around 63.0% whereas for  $\beta = 300$  is around 62.7%. The increase of CVaR for  $\beta = 0.01$  is around 69.3% and for  $\beta = 300$  around 66.3%. Meanwhile the increase in the expected diesel price over the 25 years is around 80.2%.

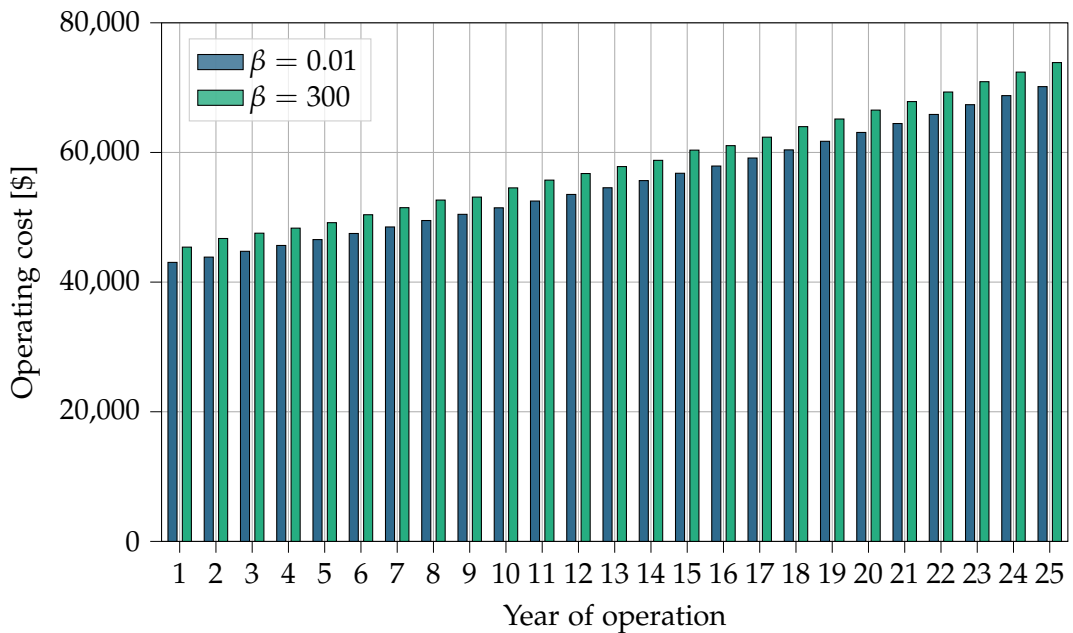


Figure 8.12: Expected cost over the years of operation, plotted for two different values of  $\beta$ , Plan 7

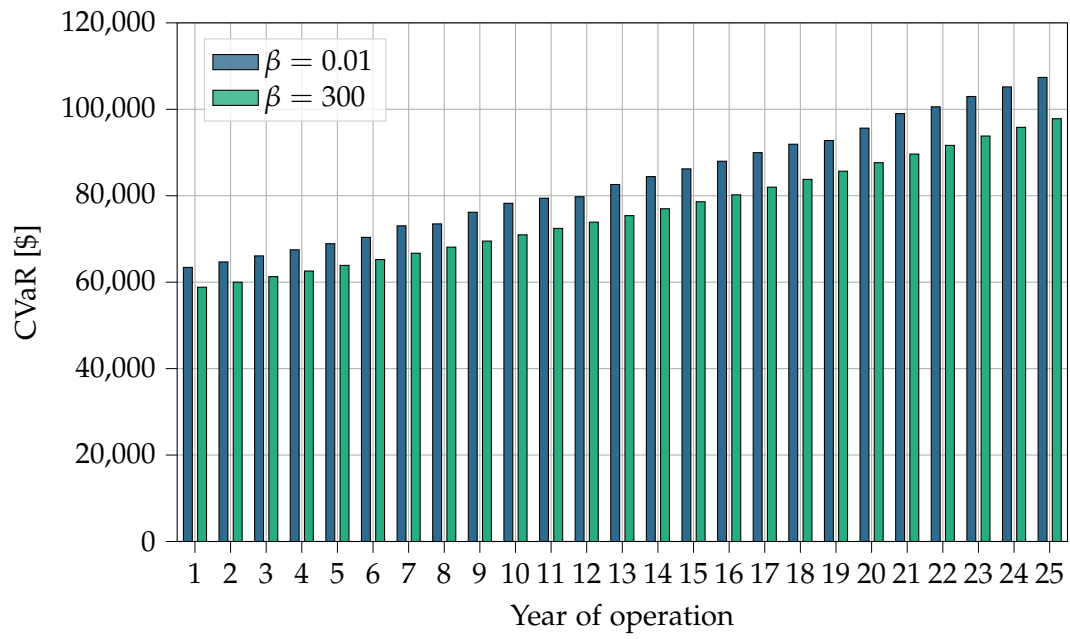


Figure 8.13: CVaR over the years of operation, plotted for two different values of  $\beta$ , Plan 7



## Chapter 9

# Conclusions and Future Work

### 9.1 Conclusions

The focus of the project was to determine an economical, reliable and innovative energy solution for a mining site in Australia. In order to do it several objectives were established and all of them are addressed in the report.

The first step was to perform solar and wind resource assessment, based on the measurements collected at the site. The analysis of solar resources proved that there was a visible seasonality. However, the most important part of the assessment was to indicate the optimal tilt for PV panels installed on a fixed axis. It was done by calculating the annual average solar irradiance for angles in range of  $0 - 90^\circ$ . The best tilt angle was found to be  $27^\circ$  and was later used for the calculation of PV power output at the site. The wind resources analysis considered measurements of wind speed at four different heights. This enabled the calculation of the power law coefficient, which was later used in calculations of wind speed at the hub height of the wind turbine. The power law coefficient ( $\alpha_p$ ) was calculated to be 0.25. Moreover, it was found that the average wind speed measured at the site classifies it to install wind turbines class III - suitable for low wind speed. Finally, based on wind rose, South-East direction was found to be the dominant one. This information can be taken into account by the designers of the wind power plant, because it is important to have as few obstacles as possible in the direction from which a large share of wind comes.

HOMER Pro was used to indicate the various possible energy solutions to satisfy the demand of the mine. The technical details of the used technologies and measurements of solar irradiance, temperature and wind speed were used as input to HOMER Pro. Based on this information and the load time series, the possible configurations of technologies, which satisfy the load at all instances, were found. It was found that configurations with high power of renewable energy sources had

lower NPC after 25 years of operation of the mine. At the same time the initial investment was higher for these configurations. From all the possibilities, ten plans were selected to be taken into account in the decision making process. The choice was made in a way to represent various possibilities of technology mix and taking into account the most important criteria of low NPC.

Having selected the ten plans, the next aim was to indicate the best one based on the selected multi-criteria decision-making algorithm - AHP. Four main criteria were considered: Economical, Robustness, Environmental and Technical. The AHP was performed for two approaches: Profit Oriented and Environmentally Friendly. The Plan selected in both approaches was the same - Plan 2. It had the lowest NPC and high renewable fraction. It is a reasonable conclusion taking into account the fact that NPC is the most important economical measure, and the percent of electricity produced from renewable sources assures low emissions.

The final step was to perform optimization of operation of the selected Plan 2. The aim of the optimization was to minimize the expected cost of operation of the hybrid power plant under the uncertainties in PV Power, wind speed and load profile. The CVaR approach was used to model the trade-off between minimizing the cost of operation and the risk of getting high costs of operation in undesired scenarios. The level of risk incorporated to the optimization problem was controlled by risk aversion factor  $\beta$ . It could be seen that with increase of  $\beta$  the expected cost of operation increased, while the CVaR decreased. The change in the two measures was 0.26% and -0.4% respectively. Generally, the variation of operation cost and CVaR were not of high magnitude due to rather low variable operation costs of renewable energy sources, from which most of energy was produced in Plan 2. The CVaR for  $\beta = 0.1$  was 102.3% of the expected operating cost. When  $\beta = 10$  was considered, CVaR was 101.7% of the expected cost. This proves that the operating cost will not be increased significantly even considering the worst scenario. Comparison of the optimized operation with a simple algorithm for charging and discharging proved that the first approach results in lower cost of operation. The difference, when the risk aversion factor was considered to be 0.1, was calculated to be 1.5%. The daily expected cost of operation of Plan 2 compared to cost of operation if the mine would only be energized by diesel generator, was around 33 times lower. This proves the advantage of a system with high power of RES. Based on the optimized, hourly dispatch of the units in Plan 2 it could be seen that increasing the level of risk incorporated had impact on the optimal dispatch of the units. An important observation was that the average SoC of the battery increases with the increase of  $\beta$ . This was a desired behaviour because it assures better resilience of the system to unexpected changes.

An additional analysis was performed to see the influence of changes in diesel prices expected in the 25 years of operation on the cost of operation of the plant. Since the electricity in Plan 2 was mostly produced from renewable energy sources

it was not suitable for this analysis. Therefore, Plan 7 was selected. The expected diesel prices in the next 25 years were obtained based on historical data for western Australia with use of Monte Carlo Simulation. The average of the simulations was used as prediction and it could be seen that the diesel prices are expected to rise in the coming years. This information was incorporated to the optimization of Plan 7. The conclusion is that for this plan, with renewable fraction of around 80%, the impact of diesel prices on the cost of operation is significant. Compared to Plan 2 the daily cost increased 4 times, what was caused by high cost of operation of diesel generator. The analysis of the influence of the increase of diesel prices showed that with the expected increase of diesel prices of 80.2% the increase in operating cost from the first to the last year of operation for  $\beta=0.01$  was around 63.0% whereas for  $\beta=300$  was around 62.7%. This shows the advantage of a system with higher power installed in renewable technologies (Plan 2) over the one, which uses diesel generator more extensively (Plan 7).

All things considered, the selected Plan 2 fulfilled the aim of the project being an innovative, economical and reliable solution. The influence of uncertainties in the PV power, wind speed and load was not of high magnitude. The system was also resilient to changes in diesel prices, because of high fraction of electricity produced from renewable energy source.

## 9.2 Future Work

In this section, some suggestions for further improving the results of this report are explained.

One of the main parts of the project was the selection of energy resources for the mine and HOMER Pro was used for it. In the beginning of the project, concentrated solar power (CSP) was also considered for this project, since the solar irradiance in Western Australia was high. However since HOMER Pro does not have a model for this it was discarded. For a future study, an accurate model of CSP could be implemented in MATLAB and included in HOMER Pro. The CSP could also be added with thermal energy storage such as molten salts.

This project was for an offgrid mine and at all times island mode has been considered. Since the site coordinates have been provided by the industrial partner, a possible grid connection could be analyzed. The distance to the nearest grid point could be calculated and the cost per km of line plus the cost of connection could be researched. With this approach the cases could be studied for both offgrid and ongrid and the most cost effective could be chosen.

Finally, the planning phase of the project could also be developed in python and be ran with the operations in a loop. This way more detailed and customized results will be obtained. Also more control over the different technologies will

be available, and more details could be implemented, such as battery degradation curves.

# Bibliography

- [1] *malarch @ web.archive.org*.  
[Online]. Available: <https://web.archive.org/web/20160303221001/http://www.sntc.org.sz/cultural/malarch.asp>.
- [2] *rep\_id:3650 @ www.miningweekly.com*.  
[Online]. Available: <http://www.miningweekly.com/article/global-mining-drives-45-plus-of-world-gdp-cutifani-2012-07-04>.
- [3] ABB, “ABB Microgrid Business Case Brochure”, ABB, Tech. Rep., 2017, p. 7.  
[Online]. Available: <https://software.response.e.abb.com/microgrid-business-case-mining>.
- [4] Glencore, *GLENCORE - Mine Raglan*.  
[Online]. Available: <https://www.mineraglan.ca/en/Pages/home.aspx>.
- [5] GLENCORE, “GLENCORE - Mine Raglan (Sivumut project)”, Tech. Rep.  
[Online]. Available: [https://www.mineraglan.ca/en/what-we-do/Documents/Sivumut\\_EN\\_FINAL\\_2017\\_\(court\).pdf](https://www.mineraglan.ca/en/what-we-do/Documents/Sivumut_EN_FINAL_2017_(court).pdf).
- [6] “RAGLAN MINE - Our engagement”, GLENCORE, Tech. Rep., 2018, p. 8.  
[Online]. Available: [https://www.mineraglan.ca/en/media/publications/EngagementBooklets/notre%20engagement2018\\_EN.pdf#search=wind](https://www.mineraglan.ca/en/media/publications/EngagementBooklets/notre%20engagement2018_EN.pdf#search=wind).
- [7] *Gold Fields*. [Online]. Available: <https://www.goldfields.com/index.php>.
- [8] EDL, “Agnew Hybrid Renewable Project”, EDL, Tech. Rep., 2019, p. 2.  
[Online]. Available: <https://edlenergy.com/wp-content/uploads/2019/07/EDL-Fact-Sheet-Agnew.pdf>.
- [9] *HOMER Pro - Microgrid Software for Designing Optimized Hybrid Microgrids*.  
[Online]. Available:  
<https://www.homerenergy.com/products/pro/index.html>.
- [10] S. Jin, H. Kim, T. H. Kim, H. Shin, K. Kwag, and W. Kim, “A Study on Designing Off-grid System Using HOMER Pro - A Case Study”, in *2018 IEEE International Conference on Industrial Engineering and Engineering Management (IEEM)*, Dec. 2018, pp. 1851–1855.  
DOI: 10.1109/IEEM.2018.8607423.

- [11] S. G. Fikari, S. G. Sigarchian, and H. R. Chamorro, "Modeling and simulation of an autonomous hybrid power system", in *2017 52nd International Universities Power Engineering Conference (UPEC)*, Aug. 2017, pp. 1–6. DOI: 10.1109/UPEC.2017.8231915.
- [12] R. K. Rietz and S. Suryanarayanan, "A review of the application of analytic hierarchy process to the planning and operation of electric power microgrids", *40th North American Power Symposium, NAPS2008*, vol. 80401, pp. 1–6, 2008. DOI: 10.1109/NAPS.2008.5307403.
- [13] S. S. Bohra, A. Anvari-Moghaddam, and B. Mohammadi-Ivatloo, "AHP-Assisted Multi-Criteria Decision-Making Model for Planning of Microgrids", pp. 4557–4562, 2019. DOI: 10.1109/iecon.2019.8926887.
- [14] A. P. Agalgaonkar, S. V. Kulkarni, and S. A. Khaparde, "Evaluation of configuration plans for DGs in developing countries using tradeoff analysis and MADM", *Proceedings of the IEEE Power Engineering Society Transmission and Distribution Conference*, vol. 21, no. 2, pp. 278–285, 2006. DOI: 10.1109/TDC.2006.1668504.
- [15] M. Vahedipour-Dahraie, A. Anvari-Moghaddam, and J. M. Guerrero, "Evaluation of reliability in risk-constrained scheduling of autonomous microgrids with demand response and renewable resources", *IET Renewable Power Generation*, vol. 12, no. 6, pp. 657–667, 2018, ISSN: 17521424. DOI: 10.1049/iet-rpg.2017.0720.
- [16] M. Roustai, M. Rayati, A. Sheikhi, and A. M. Ranjbar, "A scenario-based optimization of Smart Energy Hub operation in a stochastic environment using conditional-value-at-risk", *Sustainable Cities and Society*, vol. 39, no. January, pp. 309–316, 2018, ISSN: 22106707. DOI: 10.1016/j.scs.2018.01.045. [Online]. Available: <https://doi.org/10.1016/j.scs.2018.01.045>.
- [17] The SciPy community, *SciPy.org*. [Online]. Available: <https://docs.scipy.org/doc/scipy/reference/index.html#>.
- [18] F. Pedregosa, G. Varoquaux, A. Gramfort, V. Michel, B. Thirion, O. Grisel, M. Blondel, P. Prettenhofer, R. Weiss, V. Dubourg, J. Vanderplas, A. Passos, D. Cournapeau, M. Brucher, M. Perrot, and E. Duchesnay, "Scikit-learn Machine Learning in {P}ython", *Journal of Machine Learning Research*, vol. 12, pp. 2825–2830, 2011.
- [19] S. Ali, S. M. Lee, and C. M. Jang, "Techno-economic assessment of wind energy potential at three locations in South Korea using long-Term measured wind data", *Energies*, vol. 10, no. 9, pp. 1–23, 2017, ISSN: 19961073. DOI: 10.3390/en10091442.

- [20] *World's tallest wind turbine built in Germany - Electrek*. [Online]. Available: <https://electrek.co/2017/11/02/worlds-tallest-wind-turbine-built-in-germany/>.
- [21] *The Wind Rose*. [Online]. Available: <http://xn--drmstrre-64ad.dk/wp-content/wind/miller/windpower%20web/en/tour/wres/rose.htm>.
- [22] *HOMER Pro Online Guide*. [Online]. Available: <https://www.homerenergy.com/products/pro/docs/3.13/index.html>.
- [23] *measures-cpi @ www.rba.gov.au*. [Online]. Available: <https://www.rba.gov.au/inflation/measures-cpi.html>.
- [24] *How do you value a renewable energy project?* [Online]. Available: <https://www.ivsc.org/news/article/how-do-you-value-a-renewable-energy-project>.
- [25] Energinet and D. E. Agency, "Technology Data - Generation of Electricity and District heating", Tech. Rep., 2019.
- [26] T. Adefarati and R. Bansal, "Energizing Renewable Energy Systems and Distribution Generation", *Pathways to a Smarter Power System*, pp. 29–65, Jan. 2019. doi: 10.1016/B978-0-08-102592-5.00002-8. [Online]. Available: <https://www.sciencedirect.com/science/article/pii/B9780081025925000028>.
- [27] *FuelWatch Historical Price Search*. [Online]. Available: [https://www.fuelwatch.wa.gov.au/fuelwatch/pages/public/historicalPriceSearch.aspx?fbclid=IwAR1f1FCv5J2Ec229b7kkFd83uoFuTVYJgyQY1kYX60o\\_6hN0tyvma9fDyvs](https://www.fuelwatch.wa.gov.au/fuelwatch/pages/public/historicalPriceSearch.aspx?fbclid=IwAR1f1FCv5J2Ec229b7kkFd83uoFuTVYJgyQY1kYX60o_6hN0tyvma9fDyvs).
- [28] B. Jabeck, "The impact of generator set underloading", *Caterpillar, Inc*, pp. 1–4, 2015.
- [29] *Renewable power generation costs in 2018*. [Online]. Available: [https://www.irena.org/-/media/Files/IRENA/Agency/Publication/2018/Jan/IRENA\\_2017\\_Power\\_Costs\\_2018.pdf](https://www.irena.org/-/media/Files/IRENA/Agency/Publication/2018/Jan/IRENA_2017_Power_Costs_2018.pdf).
- [30] R. Fu, T. Remo, and R. Margolis, "2018 U.S. Utility-Scale Photovoltaics-Plus-Energy Storage System Costs Benchmark", National Renewable Energy Laboratory, Tech. Rep., 2018. [Online]. Available: <https://www.nrel.gov/docs/fy19osti/71714.pdf>.
- [31] W. Cole and A. W. Frazier, "Cost Projections for Utility-Scale Battery Storage", National Renewable Energy Laboratory, Tech. Rep., 2019, p. 23. [Online]. Available: <https://www.nrel.gov/docs/fy19osti/73222.pdf>.

- [32] P. K. Smith, A. Saxon, M. Keyser, B. Lundstrom, Z. Cao, A. Roc, and S. Corp, "Life Prediction Model for Grid-Connected Li-ion Battery Energy Storage System: Preprint", National Renewable Energy Laboratory, Washington, Tech. Rep., 2017, p. 9.  
[Online]. Available: <https://www.nrel.gov/docs/fy17osti/67102.pdf>.
- [33] *E-138 EP3*. [Online]. Available: <https://www.enercon.de/en/products/ep-3/e-138-ep3/>.
- [34] T. L. Saaty, "A scaling method for priorities in hierarchical structures", *Journal of Mathematical Psychology*, vol. 15, no. 3, pp. 234–281, 1977, ISSN: 0022-2496. DOI: [https://doi.org/10.1016/0022-2496\(77\)90033-5](https://doi.org/10.1016/0022-2496(77)90033-5).  
[Online]. Available: <http://www.sciencedirect.com/science/article/pii/0022249677900335>.
- [35] T. L. Saaty, *Fundamentals of Decision Making and Priority Theory With the Analytic Hierarchy Process*, ser. AHP series. RWS Publications, 2000, ISBN: 9781888603156.  
[Online]. Available: <https://books.google.dk/books?id=wct10T1bbIUC>.
- [36] E. A. Mohamed and Y. G. Hegazy, "A Novel Probablistic Strategy for Modeling Photovoltaic Based Distributed Generators", *International Journal of Energy and Power Engineering*, vol. 9, pp. 904–907, 2015.
- [37] L. Lester, *Python Risk Management: Monte Carlo Simulations - Towards Data Science*, 2020.  
[Online]. Available: <https://towardsdatascience.com/python-risk-management-monte-carlo-simulations-7d41c891cb5>.
- [38] R. T. Rockafellar and S. Uryasev, "Conditional value-at-risk for general loss distributions", *Journal of Banking and Finance*, vol. 26, no. 7, pp. 1443–1471, 2002, ISSN: 03784266. DOI: 10.1016/S0378-4266(02)00271-6.
- [39] S. Sarykalin, G. Serraino, and S. Uryasev, "Value-at-Risk vs. Conditional Value-at-Risk in Risk Management and Optimization", *State-of-the-Art Decision-Making Tools in the Information-Intensive Age*, no. September 2008, pp. 270–294, 2008. DOI: 10.1287/educ.1080.0052.
- [40] M. Tavakoli, F. Shokridehaki, M. Funsho Akorede, M. Marzband, I. Vechiu, and E. Poursmaeil, "CVaR-based energy management scheme for optimal resilience and operational cost in commercial building microgrids", *International Journal of Electrical Power and Energy Systems*, vol. 100, no. January, pp. 1–9, 2018, ISSN: 01420615. DOI: 10.1016/j.ijepes.2018.02.022. [Online]. Available: <https://doi.org/10.1016/j.ijepes.2018.02.022>.

- [41] J. Aho, P. Fleming, and L. Y. Pao, "Active power control of wind turbines for ancillary services: A comparison of pitch and torque control methodologies", *Proceedings of the American Control Conference*, vol. 2016-July, pp. 1407–1412, 2016, issn: 07431619.  
doi: 10.1109/ACC.2016.7525114.
- [42] A. Sangwongwanich, Y. Yang, and F. Blaabjerg, "Development of flexible active power control strategies for grid-connected photovoltaic inverters by modifying MPPT algorithms", *2017 IEEE 3rd International Future Energy Electronics Conference and ECCE Asia, IFEEC - ECCE Asia 2017*, no. June, pp. 87–92, 2017.  
doi: 10.1109/IFEEC.2017.7992423.
- [43] European Engine Power Plants Association, "Engine Power Plants Technology & Applications", 2015.
- [44] L. L. C. Gurobi Optimization, *Gurobi Optimizer Reference Manual*, 2020.  
[Online]. Available: <http://www.gurobi.com>.
- [45] S. Mitchell, S. M. Consulting, and I. Dunning, *PuLP: A Linear Programming Toolkit for Python*, 2011.



# Appendix A

## Decision Making (AHP) - Results

### A.1 Subattributes Priority

Economical					
Criteria	NPC	Initial Capital	Operating cost	Excess Electricity	Priority
NPC	1	3	5	7	0.5817
Initial Capital	1/3	1	2	4	0.2314
Operating cost	1/5	1/2	1	2	0.1205
Excess Electricity	1/7	1/4	1/2	1	0.0664
				Cr	0.0095

**Table A.1:** Economical Subattributes Priorities

Robustness					
Criteria	Diesel	PV	WT	Battery	Priority
Diesel	1	5	7	3	0.5872
PV	1/5	1	2	1/2	0.1228
WT	1/7	1/2	1	1/3	0.0722
Battery	1/3	2	3	1	0.2179
				Cr	0.0065

**Table A.2:** Robustness Subattributes Priorities

## A.2 Profit Oriented Results

**Table A.3:** Profit oriented cases

Plan no.	Economic					Robustness			
	NPC	Initial Capital	Operating Cost	Excess Elec.	Diesel	PV	WT	Battery	
1	0.0139	0.3934	0.0136	0.2889	0.0397	0.1525	0.2250	0.1497	
2	0.2210	0.0292	0.1780	0.0210	0.1869	0.0467	0.0308	0.0487	
3	0.1951	0.0297	0.1780	0.0271	0.1869	0.0467	0.0366	0.0487	
4	0.1522	0.0292	0.1780	0.0142	0.1869	0.0467	0.0272	0.1497	
5	0.0927	0.0297	0.1179	0.0258	0.1154	0.1525	0.0353	0.0932	
6	0.0277	0.1290	0.0239	0.1123	0.0397	0.0833	0.2283	0.1316	
7	0.1342	0.0757	0.1179	0.0765	0.0683	0.0833	0.0984	0.0726	
8	0.0680	0.0787	0.0823	0.0765	0.0683	0.0833	0.0984	0.1316	
9	0.0273	0.1597	0.0280	0.2854	0.0397	0.1525	0.1257	0.1316	
10	0.0680	0.0459	0.0823	0.0725	0.0683	0.1525	0.0941	0.0427	
Cr	0.0292	0.0200	0.0498	0.0693	0.0052	0.0021	0.0489	0.0198	

**Table A.4:** Profit oriented cases

Plan no.	Environmental				Technical		Priority
	CO2	SO2	NOx	PM	Ren. Frac.		
1	0.0120	0.0120	0.0120	0.0120	0.0131	0.0916	
2	0.2382	0.2382	0.2382	0.2382	0.1766	0.1572	
3	0.2382	0.2382	0.2382	0.2382	0.1766	0.1498	
4	0.1761	0.1761	0.1761	0.1761	0.1766	0.1380	
5	0.0972	0.0972	0.0972	0.0972	0.1026	0.0907	
6	0.0175	0.0175	0.0175	0.0175	0.0242	0.0564	
7	0.0725	0.0725	0.0725	0.0725	0.0994	0.0979	
8	0.0572	0.0572	0.0572	0.0572	0.0994	0.0786	
9	0.0225	0.0225	0.0225	0.0225	0.0321	0.0678	
10	0.0685	0.0685	0.0685	0.0685	0.0994	0.0720	
Cr	0.0800	0.0800	0.0800	0.0800	0.0183		

### A.3 Environmentally Friendly Results

Table A.5: Environmentally friendly case

Plan no.	Economic					Robustness			
	NPC	Initial Capital	Operating Cost	Excess Elec.	Diesel	PV	WT	Battery	
1	0.0139	0.3934	0.0136	0.2889	0.0397	0.1525	0.2250	0.1497	
2	0.2210	0.0292	0.1780	0.0210	0.1869	0.0467	0.0308	0.0487	
3	0.1951	0.0297	0.1780	0.0271	0.1869	0.0467	0.0366	0.0487	
4	0.1522	0.0292	0.1780	0.0142	0.1869	0.0467	0.0272	0.1497	
5	0.0927	0.0297	0.1179	0.0258	0.1154	0.1525	0.0353	0.0932	
6	0.0277	0.1290	0.0239	0.1123	0.0397	0.0833	0.2283	0.1316	
7	0.1342	0.0757	0.1179	0.0765	0.0683	0.0833	0.0984	0.0726	
8	0.0680	0.0787	0.0823	0.0765	0.0683	0.0833	0.0984	0.1316	
9	0.0273	0.1597	0.0280	0.2854	0.0397	0.1525	0.1257	0.1316	
10	0.0680	0.0459	0.0823	0.0725	0.0683	0.1525	0.0941	0.0427	
Cr	0.0292	0.0200	0.0498	0.0693	0.0052	0.0021	0.0489	0.0198	

Table A.6: Environmentally friendly case

Plan no.	Environmental				Technical		Priority
	CO2	SO2	NOx	PM	Ren. Frac.		
1	0.0120	0.0120	0.0120	0.0120	0.0131	0.0342	
2	0.2382	0.2382	0.2382	0.2382	0.1766	0.2003	
3	0.2382	0.2382	0.2382	0.2382	0.1766	0.1984	
4	0.1761	0.1761	0.1761	0.1761	0.1766	0.1660	
5	0.0972	0.0972	0.0972	0.0972	0.1026	0.0971	
6	0.0175	0.0175	0.0175	0.0175	0.0242	0.0304	
7	0.0725	0.0725	0.0725	0.0725	0.0994	0.0854	
8	0.0572	0.0572	0.0572	0.0572	0.0994	0.0735	
9	0.0225	0.0225	0.0225	0.0225	0.0321	0.0376	
10	0.0685	0.0685	0.0685	0.0685	0.0994	0.0770	
Cr	0.0800	0.0800	0.0800	0.0800	0.0183		

## A.4 Consistency Ratio

Table A.7: Consistency Ratio

Matrix	Cr [%]
NPC	2.92
Initial Capital	2.00
Operating Cost	4.98
Excess Elec.	6.93
Diesel	0.52
PV	0.21
WT	4.89
Battery	1.98
CO2	8.00
SO2	8.00
NOx	8.00
PM	8.00
Ren. Frac.	1.83
Sub category Environmental	0.00
Sub category Robustness	0.65
Sub category Economical	1.00
General criteria Environmental	3.52
General criteria Profit	1.14

## Appendix B

# Distribution Functions

For the statistics the open source SciPy [17] library for python has been used. In this appendix the distribution functions used from that library are explained.

### B.1 Empirical CDF

The empirical distribution functions is calculated by ordering all the measurements and calculating the cumulative probability of each.

$$EmpCDF(x) = \text{numberofobservations} \leq x / n \quad (B.1)$$

### B.2 Normal Distribution

$$f(x, loc, scale) = \frac{\exp(-\frac{1}{2}(\frac{x-loc}{scale})^2)}{scale\sqrt{2\pi}} \quad (B.2)$$

### B.3 Beta Distribution

$$f(x, loc, scale, a, b) = \frac{\Gamma(a+b)(\frac{x-loc}{scale})^{a-1}(1 - (\frac{x-loc}{scale}))^{b-1}}{scale\Gamma(a)\Gamma(b)} \quad (B.3)$$

### B.4 Weibull Distribution

$$f(x, loc, scale, c) = \frac{c(\frac{x-loc}{scale})^{c-1}\exp(-(\frac{x-loc}{scale})^c)}{scale} \quad (B.4)$$



## Appendix C

# K-means Clustering

The algorithm divides the samples into clusters, each of them described by the mean of the samples in the cluster. The means are called cluster centroids. The K-means algorithm clusters data of samples in  $n$  groups of equal variance minimizing Within-cluster sum-of-squares criterion [18], as seen in C.1.

$$\sum_{i=0}^n \min_{\mu_j \in C} (||x_i - \mu_j||^2) \quad (C.1)$$

The algorithm first chooses initial centroids, choosing a number of samples from the dataset. In the next step it assigns all the samples to the nearest centroid. Finally it generates new centroids by taking the mean value of all of the assigned samples to each previous centroid. The different between the previous and actual centroid is calculated and the algorithm will run until this error is lower than a certain value.